ORNL/SUB--93-SM036/1

ornl

OAK RIDGE NATIONAL LABORATORY

LOCKHEED MARTIN

ORNL/SUB/93-SM036/1

Cost-Effective Method for Determining the Grindability of Ceramics

Final Report

Changsheng Guo and Ronald H. Chand

Ceramic Technology Project

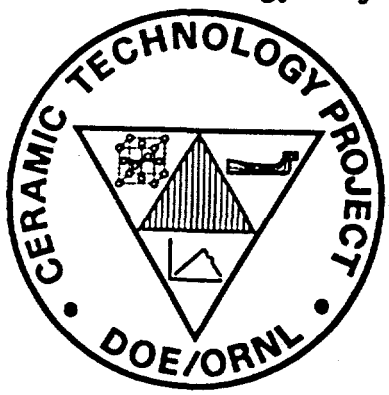

MANAGED AND OPERATED BY
LOCKHEED MARTIN ENERGY RESEARCH CORPORATION
FOR THE UNITED STATES
DEPARTMENT OF ENERGY

ORNL-27 (3-96)

DISCLAIMER

ORNL/SUB/93-SM036/1

Cost-Effective Method for Determining the Grindability of Ceramics

Final Report

Changsheng Guo and Ronald H. Chand

Chand Kare Technical Ceramics
2 Coppage Drive
Worcester, MA 01603

Date Published: February 1997

Funded by
Office of Heavy Vehicle Technologies
Office of Transportation Technologies
Energy Efficiency and Renewable Energy
U.S. Department of Energy

Prepared by the
OAK RIDGE NATIONAL LABORATORY
Managed by
Lockheed Martin Energy Research Corporation
for the
U.S. Department of Energy
under Contract No. DE-AC05-96OR22464

Table of Contents

COST-EFFECTIVE METHOD FOR DETERMINING THE GRINDABILITY OF CERAMICS

Changsheng Guo
Ronald H. Chand

Chand Kare Technical Ceramics, Inc.
2 Coppage Drive
Worcester, MA 01603-1252

1 Summary

The objective of this program was to develop a cost-effective method to determine the grindability of ceramics leading to cost-effective methods for machining such ceramics. In this first phase of activity, Chand Kare Technical Ceramics directed its efforts towards development of a definition for ceramic grindability, design of grindability-test experiments, and development of a ceramics-grindability test system (CGTS). The grindability study also included the establishment of the correlation between the grindability and conventional grinding practices. The above goals were achieved. A definition based on material removal rate under controlled force grinding was developed. Three prototype CGTSs were developed and tested; suitable design was identified. Based on this, a fully automatic CGTS was developed and is ready for delivery to Oak Ridge National Laboratory. Comprehensive grindability tests for various commercially available engineering ceramics were conducted. Experimental results indicated that ceramics have significantly different grindabilities even though their mechanical properties were not significantly different. This implies that grindability of ceramics can be greatly improved. Further study is needed to establish correlations between microstructure and grindability. Therefore, grindability should be evaluated during the development of new ceramics or improvement of existing ones.

In this report, the development of the ceramic-grindability definition, the development of CGTS, extensive grindability results, and the preliminary correlation between grindability and mechanical properties (such as flexural strength, hardness, elastic modulus, and fracture toughness) were summarized.

2 Introduction

Ceramic materials such as silicon nitride, silicon carbide, aluminum oxide, and zirconia have great potential as structural materials because of their lower densities, superior wear resistance, and high-temperature characteristics over commonly used metal alloys (Liao et al 1990; Moriwaki et al, 1989; Tonshoff et al 1989; Hu and

Chandra, 1993)[1], but their acceptance in the marketplace is still limited. This is partly due to the fabrication processes available for converting these materials into usable components. A major concern is the high-machining cost of ceramic components (Kovach et al, 1993; Ota and Miyahara, 1993) because of the poor grindability of ceramics.

Currently in industries, the choice of machine and process parameters such as wheel speed, workspeed, and depth of cut are is always made empirically by the operators or by some "experts" in the organization. Each operator, depending upon requirements for a particular component, grades the grinding process as satisfactory or requiring improvements by trial and error. The process is evaluated as efficient or inefficient strictly according to the market price. Therefore, a scientific approach is needed to provide guidelines for selecting proper process parameters. Furthermore, in order to reduce the overall machining cost of ceramics, ceramics with not only superior mechanical properties but also good grindability should be developed. Study of grindability of ceramics becomes necessary because it can provide a fundamental understanding of the grinding behavior of a particular ceramic material.

Grindability of ceramics should be related to mechanical and thermal properties and microstructure of ceramics. There are a few papers dealing with grindability of ceramics (Kondo et al, 1994; Moriwaki et al, 1989; Subramanian, 1985; Roth and Tonshoff, 1993); however, no scientific definitions have been developed. Besides, a cost-effective methodology is needed for measuring grindability. In the literature reviewed, ceramics is only compared in terms of the magnitude of grinding forces. But, grinding force strongly depends on the mode of grinding (ductile flow or brittle fracture). Usually, grinding force and power consumption are higher for ductile-flow grinding than for brittle-fracture grinding. Therefore, grinding force is not a parameter depending solely on a material property.

In this research effort, grindability of ceramics is considered as a material property. Grindability of ceramics can provide valuable information for "design for manufacturability." Ceramic manufacturers can use grindability as a criteria to evaluate newly developed ceramics. By comparing the grindability of a newly-developed ceramic with that of a ceramic of well established machining parameters, machining parameters for the newly-developed ceramic can also be established.

3 Definition of Grindability

Grindability definition was considered from several aspects (productivity, cost and part quality). The advantages and disadvantages of each possible definition was discussed. A most suitable definition was chosen based on the basic requirements of

---

[1] References are listed at the end of the report in alphabetic order.

grindability.

Grindability or machinability is defined as a complex property of a material, which controls the ease or difficulty with which the material may be machined to the size, shape, and surface finish required commercially. Unlike other material properties such as hardness, toughness, and strength which are well defined and procedures for experimentally determining the values of these mechanical properties are standardized, grindability itself is a vague concept; in fact, there is no commonly recognized definition. If one material is said to be easier to grind than another, it can mean different things for different engineers with different interests. The meaning usually depends on the purpose of the research. It also tends to reflect the immediate interest of the user. People who are concerned with surface-finish problems tend to think in terms of 'finishability'; others may consider that the term can be used to indicate how fast a material can be removed; others may consider it to be a measure of the tool life or even cost. Machinability still tends to remain a term which means 'All things to all men' (Mills and Redford, 1983). The objective of the present research was to cost-effectively determine the grindability of ceramic materials. In the following, we discussed grindability from various aspects in terms of productivity, part quality, and cost. The merits and disadvantages of each possibility in defining grindability were discussed. Based on the discussion, a workable definition was chosen.

3.1 Basic Requirements for Grindability Definition

Before we started to discuss the definition of grindability, it was necessary to consider the basic requirements which served as guidelines for choosing the various options. It should be remembered that we were looking for a cost-effective way. It was desirable that the testing procedure required only a minimum of time, material, and labor. Therefore, it had to satisfy the following requirements: easy to obtain experimentally, cost effective to determine, and sensitive to material properties. Each of them was considered separately.

3.1.1 Easy to obtain experimentally

The grindability of a material needs to be obtained experimentally. It should be defined in such a way that it can be obtained very easily. The experimental set-up should be simple. Test specimen preparation should be easy, preferably MOR bars used for flexural-strength tests. The experiment itself should be easy to conduct. The measurement of parameters needed to find the grindability should also bé easy. The calculation after the measurements should be very simple. The experiment should also be designed to eliminate the operators' influence.

3.1.2 Cost effective to obtain

Cost effectiveness is a very important aspect in evaluating grindability. Of

course cost is closely related to how easily the grindability can be experimentally obtained. The definition should satisfy the requirement that the experiment for determining the grindability of a ceramic can be done very quickly. The experiment should be so designed that no special training is needed for conducting it. Also, the abrasive-tool and specimen consumption should be small, and specimen preparation should be easy.

3.1.3 Sensitive to material properties

One of the purposes for conducting a grindability test is to rank the ceramic materials in terms of their easiness to grind. The definition should be able to reveal small differences in grindability. Therefore the definition should be sensitive to material properties. The definition should be such that it will reveal the difference in material properties instead of other grinding parameters such as workspeed and depth of cut.

3.2 Various Possibilities of Defining Grindability

In metal cutting, attempts to measure machinability are usually based upon determinations of tool wear, chip behavior, energy consumption, or rate of material removal. Grindability can also be addressed from various aspects, namely productivity, part quality and cost. For each aspect, it also can be defined in terms of different parameters. In this section, we looked at each of these aspects, and discussed the merits and disadvantages of all the possible definitions. After evaluating each definition, using the basic requirements proposed above, the most suitable one was chosen.

3.2.1 In terms of productivity

First we looked at how to define grindability in terms of productivity. Volumetric material removal rate z_w (volume of material removed per unit time per unit width of grinding) was used as a measure of how fast the material can be removed. In grinding of metallic materials using conventional aluminum oxide wheels, this parameter is usually used to characterize a grinding process and compare grinding wheels, grinding fluids, and work materials. It is also used as a criteria to choose suitable grinding parameters such as wheel speed, workspeed, depth of cut, and dressing conditions. Here the material removal rate was used to discuss grindability of ceramic materials.

In terms of how the in-feed is given or accomplished, grinding operations can be divided into two categories: controlled force grinding and controlled in-feed grinding. In controlled force grinding, the normal grinding force is controlled to a predetermined value, and the rate at which the material is removed depends on the material being ground. In controlled in-feed grinding, the in-feed (depth of cut) is kept constant and the normal force varies with work material. We considered both types of grinding and discussed its appropriateness for testing grindability.

3.2.1.1 Controlled force grinding

We looked at controlled force grinding in which the normal grinding force was kept constant by using a special grinder, such as the one shown in Figure 1. The rate of downfeed achieved by grinding the material under test using an abrasive tool of predetermined form can be taken as a measure of the grindability of the material. For this controlled force grinding, the specimen can be held in two ways: horizontally, as in Figure 1(a), or longitudinally, as in Figure 1(b). If it is held horizontally as in Figure 1(a), the specimen can be ground with or without table traverse motion. Without table traverse motion, the pressure between the contact wheel and the specimen varies because of the contact length between the specimen and the contact wheel increases as the contact wheel cuts into the specimen, as shown in Figure 2(a). The grinding conditions vary during the test. There are two additional aspects which need to be considered as regards table traverse motion: First, how fast the traverse should be, and secondly, how to control the reverse at both ends of the specimen, which both pose difficulties for testing.

If the specimen is held longitudinally as in Figure 1(b), no traverse motion is needed and also the grinding condition can be maintained unchanged during the test if the specimen is preformed to conform with the size of the contact wheel as shown in Figure 2(b). Also, a platen support under the belt can be used to eliminate the need of preforming the test specimen. Therefore, holding the specimen longitudinally seems to be superior to holding it horizontally.

It is very simple to use controlled force grinding to determine grindability. Applying a predetermined normal force and grinding the material for a specified period time, more material will be removed if the ceramics is easier to grind, and less will be removed if it is difficult to grind. The amount of material removed will distinguish the grindability of each material. The mathematical definition of grindability, in terms of material removal rate under controlled force grinding and the proposed experimental method for determining a material's grindability, will be discussed later.

3.2.1.2 Controlled in-feed grinding

Most of the practical grinding operations are performed under controlled in-feed grinding in which the downfeed (depth of cut) is controlled to a predetermined value (depth of cut 'a') during a grinding pass as in Figure 3. Under this condition and with other grinding conditions kept constant, the grinding forces and power needed to remove the given layer of material depends on the property of the material being ground. Higher forces and power will be experienced if the material is difficult to grind, and lower forces and power will be experienced if the material is easy to grind. The magnitude of the forces and power (or specific energy defined as energy consumption per unit volume of material removal) can be used to distinguish the grindability of different materials.

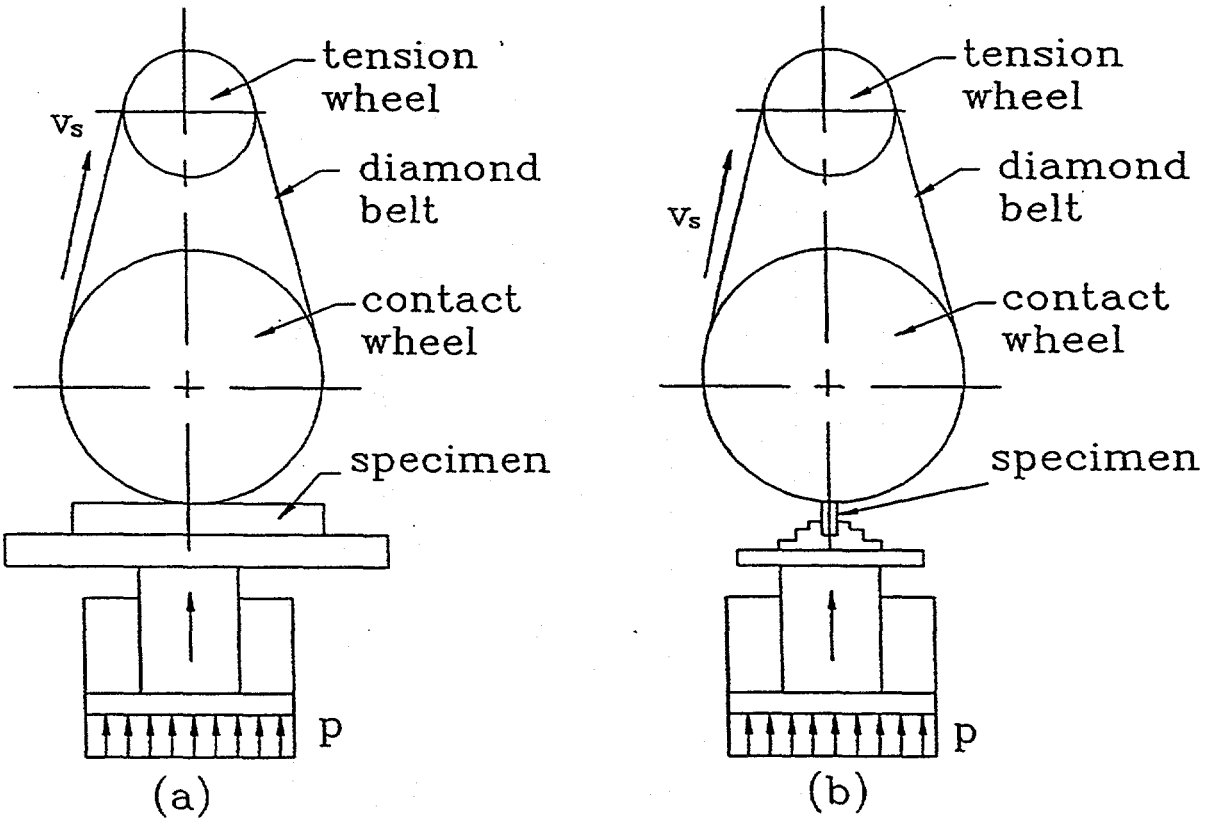

Figure 1. Illustration of controlled force grinding.

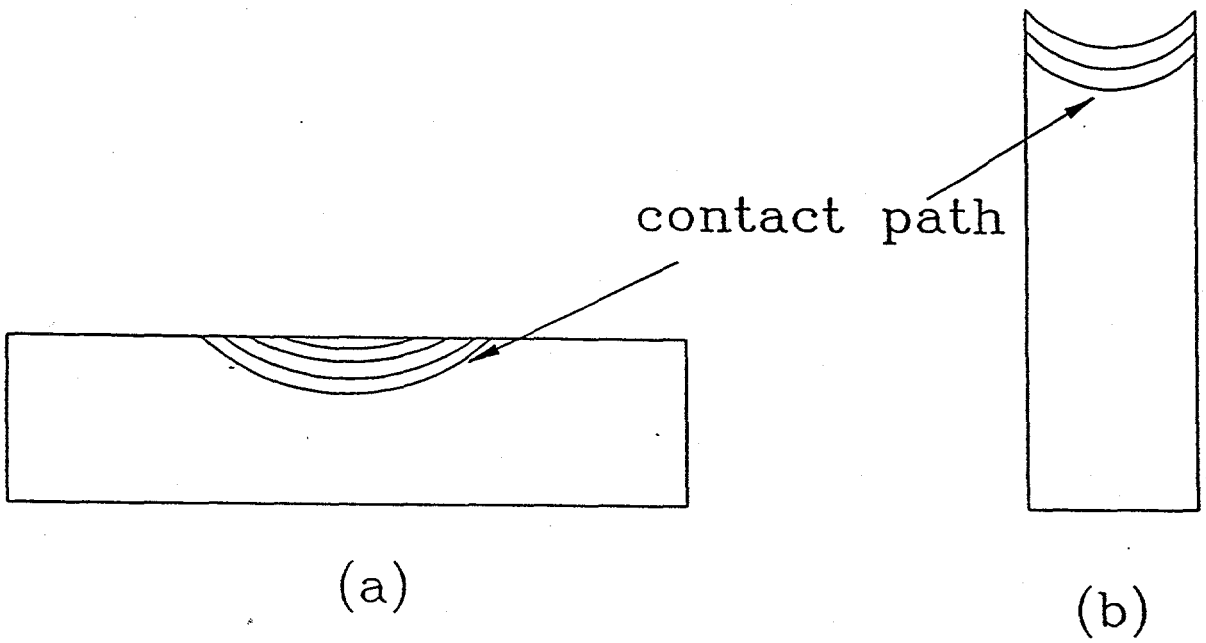

Figure 2. Variation of contact lengths (a) holding specimen horizontally, (b) holding specimen longitudinally.

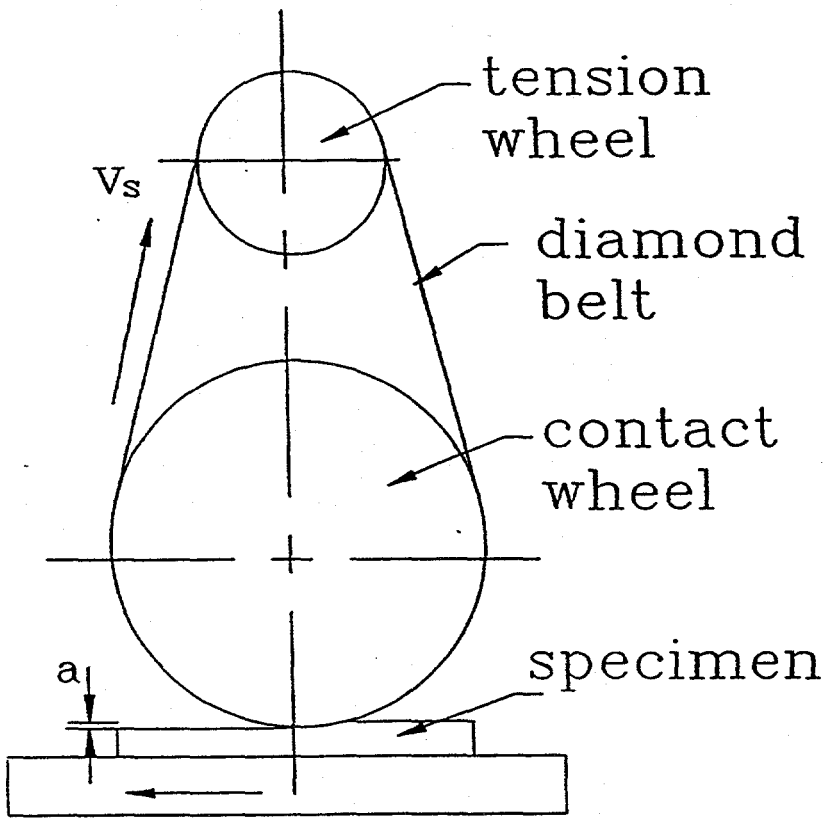

Figure 3. Illustration of controlled in-feed grinding.

One of the shortcomings of using controlled in-feed grinding is that a force dynamometer is needed. A reliable one may be costly. Another problem is that the forces and power (specific energy) strongly depend on the mode of grinding, ductile or brittle. Usually, much smaller forces and power are experienced under brittle mode than under ductile mode. For ceramic materials, whether the grinding is under ductile or brittle mode depends more on the grinding conditions than on the material properties. Most of the time, the grinding is conducted under a combination of both brittle and ductile modes. Furthermore, it is also difficult to choose an appropriate grinding condition (depth of cut, workspeed) under which all the ceramic materials can be tested.

3.2.2 In terms of quality

When part quality is a problem, the grindability can also be discussed in terms of quality. However quality itself is a concept which needs to be clarified. Part quality can be addressed from various aspects. First of all, **size and geometry accuracy** is one aspect of the quality. When considering size and geometry accuracy from the view point of grindability, it means whether it is easy to obtain certain accuracy requirement for a part of certain material. Definitely, achieving certain size and geometric accuracy depends more on the machine accuracy and the part geometry itself than on the material properties. For grinding of ceramic materials, it should be relatively easier to achieve certain accuracy than for metallic materials because of the much higher elasticity E (Young's modulus) of ceramic materials. Secondly, **surface integrity**, which includes surface roughness, residual stresses and burn marks, is another important aspect of quality. For ceramic grinding, residual stress is usually compressive, workpiece burn is rarely a problem because of much lower grinding temperature due to the much higher thermal conductivity of diamond abrasives (Zhu, Guo, Malkin and Sunderland, 1995) and the higher temperature resistance of ceramic materials. Surface finish is usually difficult to obtain because of the brittle characteristics of ceramic materials. However, surface finish also depends more on the grinding mode than on material properties.

Part quality is definitely material related. It is easier to achieve certain quality requirement for some materials than for others. However, machining quality is more related to the grinding machine used, grinding parameters chosen, and the company's practice rather than to material properties. Also, it will not be cost effective to quantitatively characterize quality for the purpose of grindability. Part quality may not be very sensitive to material properties. It also posts higher requirements for grindability testing. Our conclusion was that quality was not suitable for defining grindability in a cost-effective manner.

3.2.3 In terms of cost

Cost in terms of dollar values strongly depends on a company's situation such

as management and labor cost. For the purpose of studying grindability, cost can be discussed in terms of machining time, power consumption, and wheel consumption. Definitely, cost is closely related to productivity, but wheel cost can be a big portion of the overall machining cost for ceramic grinding. This can be characterized by considering how much ceramic material can be removed by consuming unit volume of diamond wheel. Therefore, grinding ratio should be a good parameter to use for defining grindability in terms of cost. This grinding ratio, also called G-ratio, is defined as the ratio of volumetric material removal rate to the volumetric wheel wear rate, or

$$G \equiv \frac{Z_w}{Z_s} \tag{1}$$

where z_w is the volumetric material removal rate per unit width of grinding (mm^3/mm second) and z_s is the volumetric wheel wear rate per unit width of grinding (mm^3/mm second).

G-ratio is a valuable parameter for evaluating various grinding wheels, grinding fluids and choosing optimum grinding conditions for grinding of metallic materials with conventional aluminum oxide wheels. It can also be used to compare and rank the grindability of ceramic materials. If G-ratio is high, material is considered to be easy to grind, and otherwise it is considered to be difficult to grind. There are two difficulties using G-ratio as a measure of ceramic grindability. First, it is very difficult to measure the volumetric wear rate of a diamond wheel because of its much higher-wear resistance, which posts difficulty for testing. Secondly, it is very time consuming to conduct tests to measure G-ratios even for conventional abrasive wheels. A significant amount of grinding has to be conducted to achieve a measurable amount of wheel wear for diamond wheels. Therefore, it is not cost effective to use G-ratio to define grindability for ceramics.

Summarizing the above discussion, we can conclude that grinding forces, power (or specific energies) obtained for controlled in-feed grinding and surface finish depends more on the mode of grinding (brittle or ductile) than on the material itself. The mode of grinding depends more on the grinding condition than on the material. Therefore, these parameters are not suitable for defining grindability for evaluating material. From the cost view point, G-ratio should be used. But it is not a workable definition either. Therefore, normalized volumetric material removal rate obtained under controlled force grinding, which measures the rate of in-feed achieved per unit force/per unit belt speed, should be used to define the grindability of ceramics.

3.3 Mathematical Definition of Grindability

It is our conclusion that normalized volumetric material removal rate obtained under controlled force grinding should be used to define the grindability of ceramics. It should be noted that grindability is a unique material property. Therefore, the

influence of other factors on material removal rate should be excluded from the definition. Under controlled force grinding, material removal rate should be a function of normal grinding force per unit width of grinding F_n, wheel speed (or belt speed) v_s, material properties, and wheel (or belt) characteristics. If ϕ_c is a parameter which accounts for the influence of ceramic material property on material removal rate, and ϕ_d is a parameter which accounts for the influence of diamond wheel (or belt) characteristics on material removal rate, the material removal rate z_w (volumetric material removal per unit time per unit width of grinding) can be expressed as:

$$z_w = f(v_s, F_n, \phi_c, \phi_d) \tag{2}$$

If same kind of diamond belt is used for all the grindability tests, the influence of diamond belt on material removal rate can be excluded from equation (2). This is similar to hardness tests in which some predetermined indenters should be used in order to obtain comparable results. Therefore, the material removal rate per unit normal grinding force is defined as the material removal parameter, or

$$\Lambda_w = \frac{\partial z_w}{\partial F_n} \tag{3}$$

Under controlled force grinding, material removal parameter Λ_w increases with wheel speed v_s. In order to find a parameter which depends only on material property, we define

$$\lambda = \frac{\partial \Lambda_w}{\partial v_s} = \frac{\partial}{\partial v_s}\left(\frac{\partial z_w}{\partial F_n}\right) \tag{4}$$

which is the volumetric material removal rate per unit wheel speed under unit normal grinding force.

For grinding of metallic materials with conventional aluminum oxide wheels, it has been found that the material removal rate is proportional to the normal force if the dominant material removal mechanism is cutting instead of plowing, as schematically illustrated in Figure 4(a). Therefore the material removal parameter Λ_w for a given wheel speed is the slope of the corresponding line and does not depend on the normal grinding force. Under this condition, the material removal parameter is only related to the material property and wheel speed (or belt speed). Research under controlled force grinding has indicated that material removal rate is approximately proportional to the wheel speed v_s. These linear relationships still hold true for ceramic grinding, as seen in Figures 6 and 7. Those results were obtained using the second version of the prototype CGTS (see Figure 22). The material numbers in these two figures are listed in Tables 1 and 5. Therefore, we have a parameter which is only related to the material property, or

$$\lambda_w = \frac{z_w}{v_s F_n} = g(\phi_c) \tag{5}$$

which is the slope of the line in Figure 4(b). This parameter λ_w has a physical meaning; represents the equivalent cross-sectional area of a ribbon-like strip of material being removed from the workpiece under unit normal force. This parameter can be used to distinguish the grindability of various ceramic materials because it only depends on material property. For easier-to-grind material, parameter λ_w will be bigger, and for difficult-to-grind material, it will be smaller. In the next section, we discuss how to experimentally evaluate this normalized material parameter. After testing all the available ceramic materials, a result similar to what is given in Figure 5 will be obtained, with large λ_w value corresponding to easy-to-grind materials, and smaller λ_w values corresponding to difficult-to-grind materials.

As a practical matter, it is necessary to choose an appropriate diamond belt to conduct all the grinding tests in order to obtain comparable testing results. This requirement may be difficult to satisfy because the diamond belt selected for some ceramic materials may not suitable for others. Analogous to Rockwell hardness testing in which different indentors (ball or cone) are used for materials of different hardness, different diamond belts may also be used to account for various ceramic materials. If so, the grindability of ceramic materials may need to be measured using different scales such as *grindability scale A, B or C* etc analogous to the Rockwell hardness definition.

After the belt is chosen, the appropriate normal force range and belt speed need to be determined. The belt speed commonly used in practice is about 30 m/s. It is desirable that all the tests be conducted under the same range of normal grinding force in order to obtain comparable results. But different range of normal force may need to be applied in order to successfully grind all the available materials. For materials which are easy to grind, smaller normal force should be used, and for materials which are difficulty to grind, larger normal force should be used. Under this condition, we can also define different grindability scales analogous Rockwell hardness scale A and C in which different loads are applied using the same indentor. If the material removal rate increases proportionally with the normal force as in Figure 4(a), extrapolation technique can be used to obtain comparable result at the standard condition. Therefore, ceramic grindability is defined as the normalized material removal rate, or

$$G_c = \lambda_w = \frac{z_w}{F_n v_s} \tag{6}$$

which has the same unit as the wear coefficient (or specific wear rate) in triobology studies.

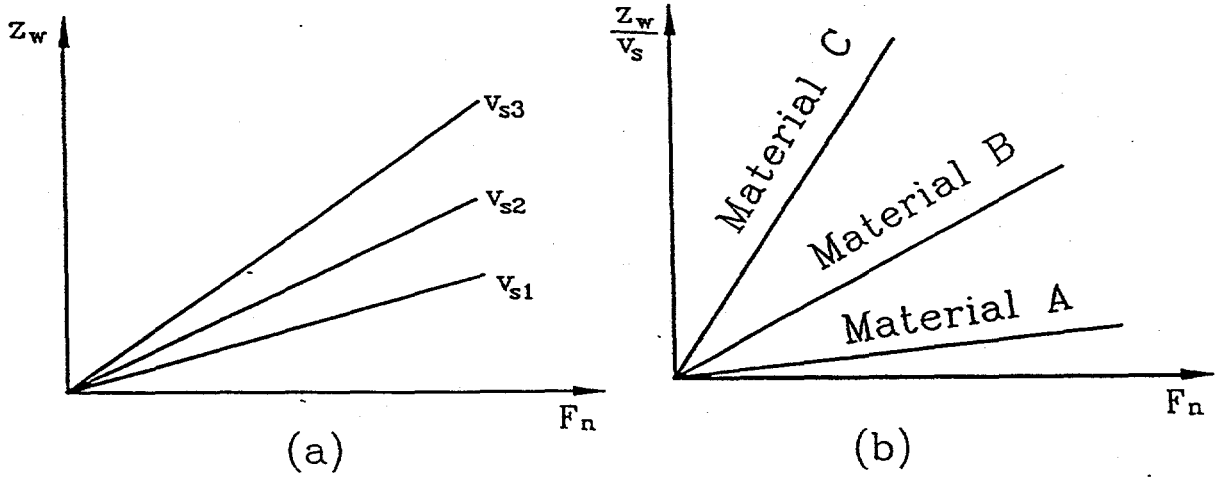

Figure 4. Empirical relationship between normal force and material removal rate.

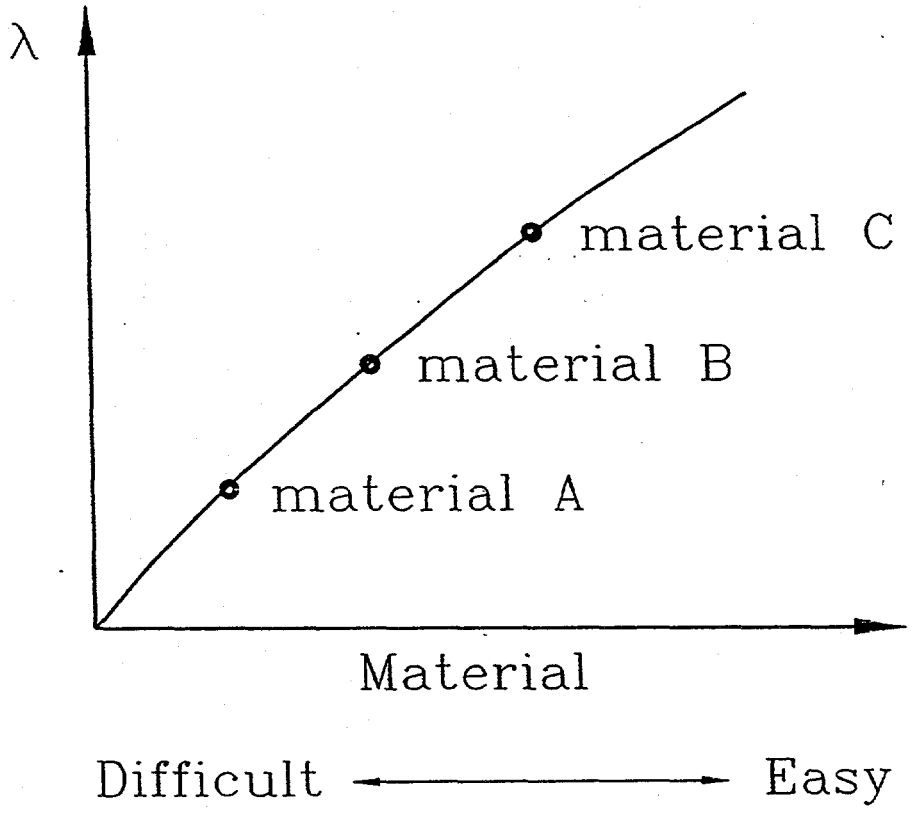

Figure 5. Normalized material removal parameter versus different materials.

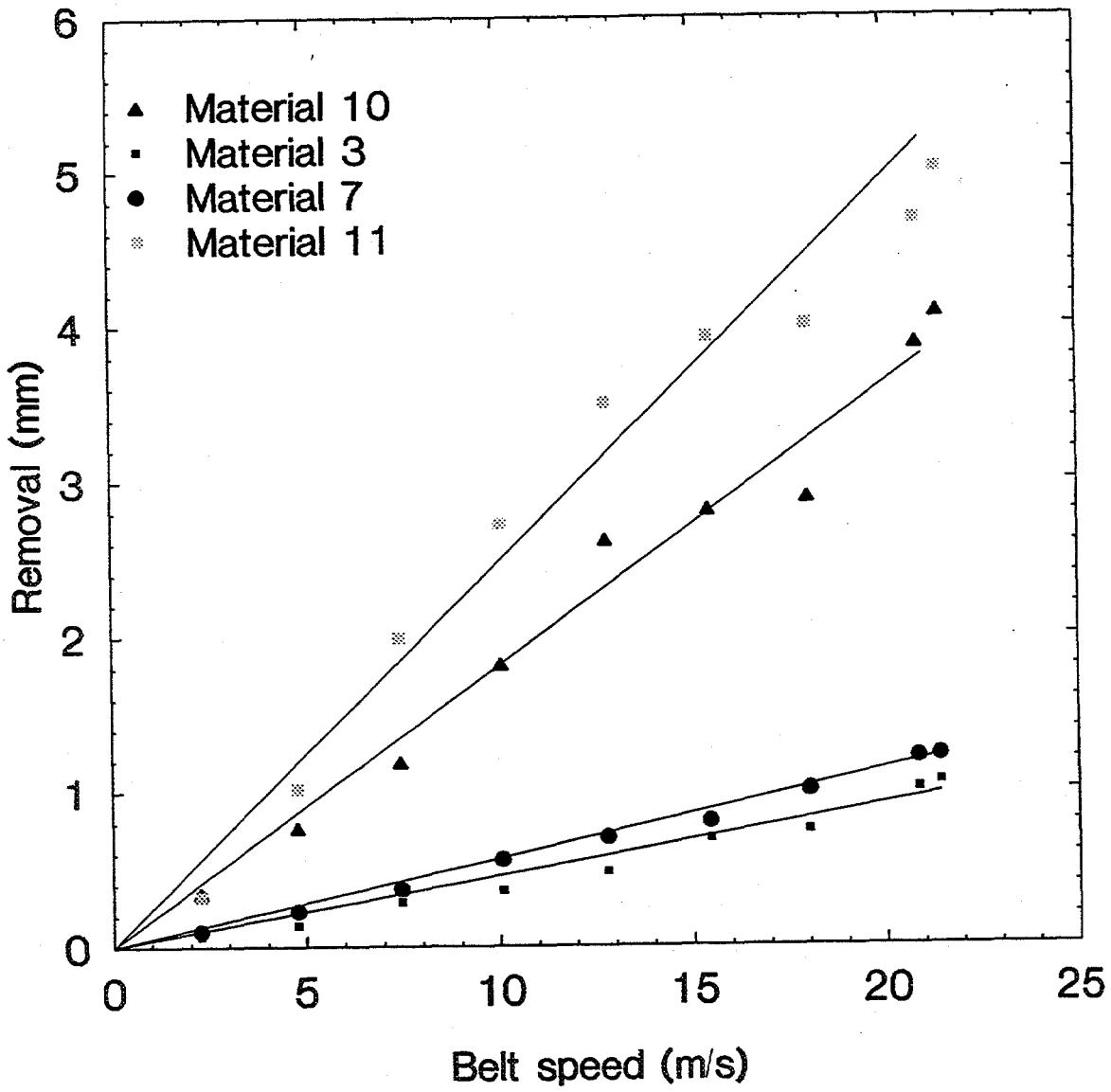

Figure 6. Removal versus belt speed.

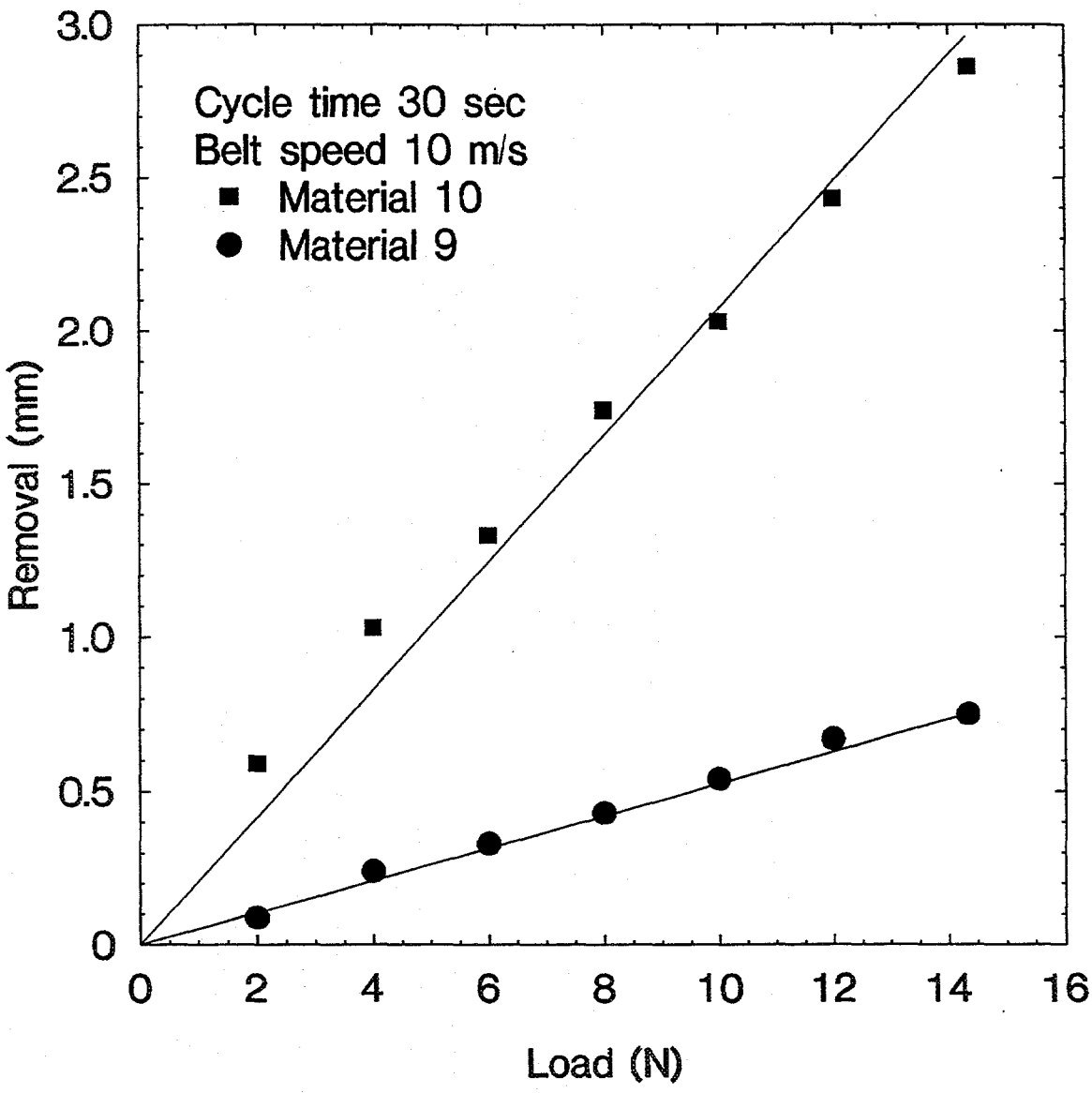

Figure 7. Removal versus normal force.

For the purpose of ranking various ceramic materials in terms of a dimensionless number, a reference material should be chosen. The reference material is chosen to be of reasonable grindability and of the same basic type as the test materials but, importantly, it should be chosen for the consistency of its grinding characteristics. For the reference material chosen, some grinding tests should be conducted to determine its λ_w value. If the grindability of the reference material is specified as 10, the grindability of any material can be expressed as:

$$G_{c1} = \frac{\lambda_w}{\lambda_r} 10 = 10 \frac{z_w}{v_s F_n} \frac{1}{\lambda_r} \tag{7}$$

It should be noted that the ranking varies if the property of the reference material varies. Therefore, defining grindability as in equation (7) is not recommended. In the following study, definition in equation (6) is used.

3.4 Multiple Tests

In order to reduce experimental error and obtain more accurate result, multiple tests should be used to evaluate parameter λ_w in equation (5). For test number i, normal force F_{ni} is applied and the specimen is ground for a period time of T. The accumulative volume of material removal per unit width of grinding is Q_{wi}. The average material removal rate can be calculated as:

$$z_{wi} = \frac{Q_{wi}}{T} \tag{8}$$

The material removal parameter Λ_{wi} can be calculated by

$$\Lambda_{wi} = \frac{z_{wi}}{F_{ni}} \tag{9}$$

and the normalized parameter λ_{wi} can be calculated by

$$\lambda_{wi} = \frac{\Lambda_{wi}}{v_s} \tag{10}$$

After n tests for each material, we have the following data matrix which can be used to calculate the average value of the normalized parameter λ_w for the tested material by

$$\lambda_w = \frac{1}{n} \sum_{i=1}^{n} \lambda_{wi} \tag{11}$$

Test Data Matrix

F_n(N/mm)	F_{n1}	F_{n2}	F_{n3}	F_{n4}	F_{n5}	.....	F_{nn}
Q_w(mm^3/mm)	Q_{w1}	Q_{w2}	Q_{w3}	Q_{w4}	Q_{w5}	.....	Q_{wn}
z_w(mm^3/mms)	z_{w1}	z_{w2}	z_{w3}	z_{w4}	z_{w5}	.....	z_{wn}
Λ_w	Λ_{w1}	Λ_{w2}	Λ_{w3}	Λ_{w4}	Λ_{w5}	.....	Λ_{wn}
λ_w	λ_{w1}	λ_{w2}	λ_{w3}	λ_{w4}	λ_{w5}	.....	λ_{wn}

4 Selection of Abrasive Tools for Grindability Tests

It is proposed to use diamond belts instead of diamond wheels to conduct grindability tests in order to eliminate the influence of wheel truing and dressing. Structurally, there are two types of diamond belts available. In one structure, diamond grits are deposited on the base material in a form of a series of diamond clusters as seen in Figure 8. We call it cluster-type belt. Extensive investigation about this type belt has revealed that it is not suitable to grindability test application. First of all, this type of belt was designed for polishing which means that the diamond grits are very fine. The coarsest available grit size is 30 microns which is not suitable for material removal as required in grindability test. The cluster-type belt should give more consistent results due to its structural consistency. This kind of belt should be further examined in the grindability standardization.

For the second type of belt, the diamond grits are randomly deposited on the base material (similar to sand papers). The belt manufacturer can supply belt with very coarse grit size (up to 100 mesh size) which is suitable for grinding with much higher material removal rate. This belt was chosen for grindability testing.

In order to test the grinding capability of the chosen belt, a preliminary test rig was developed. The test rig was mounted on a milling machine. An aluminum wheel was mounted on the spindle (where the milling cutter used to be mounted) and was used to drive the diamond belt. Another wheel was vertically mounted on the work table to support the belt and apply tension to the belt. The belt tension was adjusted by moving the work table. The belt speed was varied by changing the spindle speed. Various ceramic bars were forced against the belt manually while the belt was running at different speeds. Preliminary tests have shown that the selected belt is capable of grinding various commercially available ceramic materials.

5 Development of the CGTS

As discussed in the previous chapter, controlled force grinding with coated

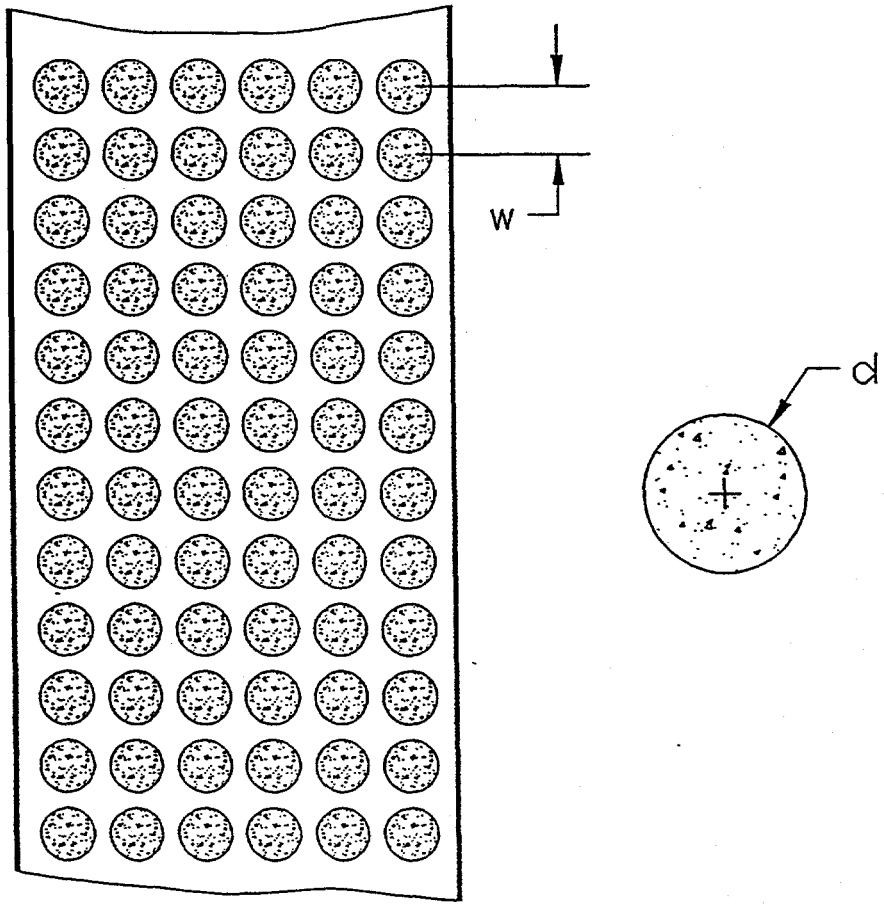

Figure 8. Schematic of cluster-type diamond belt surface structure.

diamond belt was chosen to test grindability. Theoretically speaking, there are several ways to achieve controlled force grinding: pneumatic cylinder, hydraulic cylinder, torque control motor and ball screw mechanism, pulley with weight, and dead weight. Each of the options was reviewed. With pneumatic cylinder, load cannot be maintained to a constant value if pressure fluctuations exist in the air line. Also, the availability of pressurized air may impose limitation for use of the grindability test system. If hydraulic cylinder is chosen, a hydraulic system is needed for the test machine which can make the machine complex. One of the limitations of torque control motor is that the torque output varies during one motor revolution. This variation will be more evident when the motor is running at low speeds. In our application, the in-feed is very small, especially with hard-to-grind materials, which requires that the motor run at very low speeds. The pulley with weight or dead weight option should be the simplest and most reliable method.

Under controlled force grinding, there are two ways to accomplish in-feed. With the first option, the specimen is forced to the belt under certain load as shown in Figure 9. The grinding continues until the predetermined time limit is reached. The accumulated material removal divided by the time leads to the volumetric material removal rate. With the second option, the grinding continues until a predetermined amount of material is removed. Dividing the amount of material removal by the time spent to remove this material leads to the volumetric removal rate. The problem with the second option is that it may take very long time to grind away the given amount of material, which may lead to a significant wear of belt. The belt's grinding performance may vary significantly because of severe belt wear. In our design, the first option was used.

Based on the above idea, three prototype CGTSs were developed and tested during the two-year project period. In the following, each of them was examined and the experimental results obtained were discussed.

5.1 Prototype CGTS - version #1

An illustrative sketch of the first prototype CGTS is given in Figures 10 and 11 to show the mechanisms of its operation. The test machine consists of a diamond-belt driving, adjusting, and tension unit, a specimen-positioning, holding, and indexing unit, a controlled-force application unit, a fast-feed and fast-retract unit, a coolant-supply unit, a timing unit, and a machine base. Belt dimensions chosen were: 30-inches long and 2-inches wide. The belt speed is around 4,500 feet/min (22.86 m/sec). The belt was driven by an electric motor of 1-horse power. A stationary platen was placed beneath the belt to overcome the grinding force. The specimen was forced to the platen portion of the belt under a controlled force. After grinding a predetermined period of time, the specimen was retracted quickly. For the next test, the specimen was indexed across the belt width to utilize a new portion of the belt surface, as seen in Figure 11.

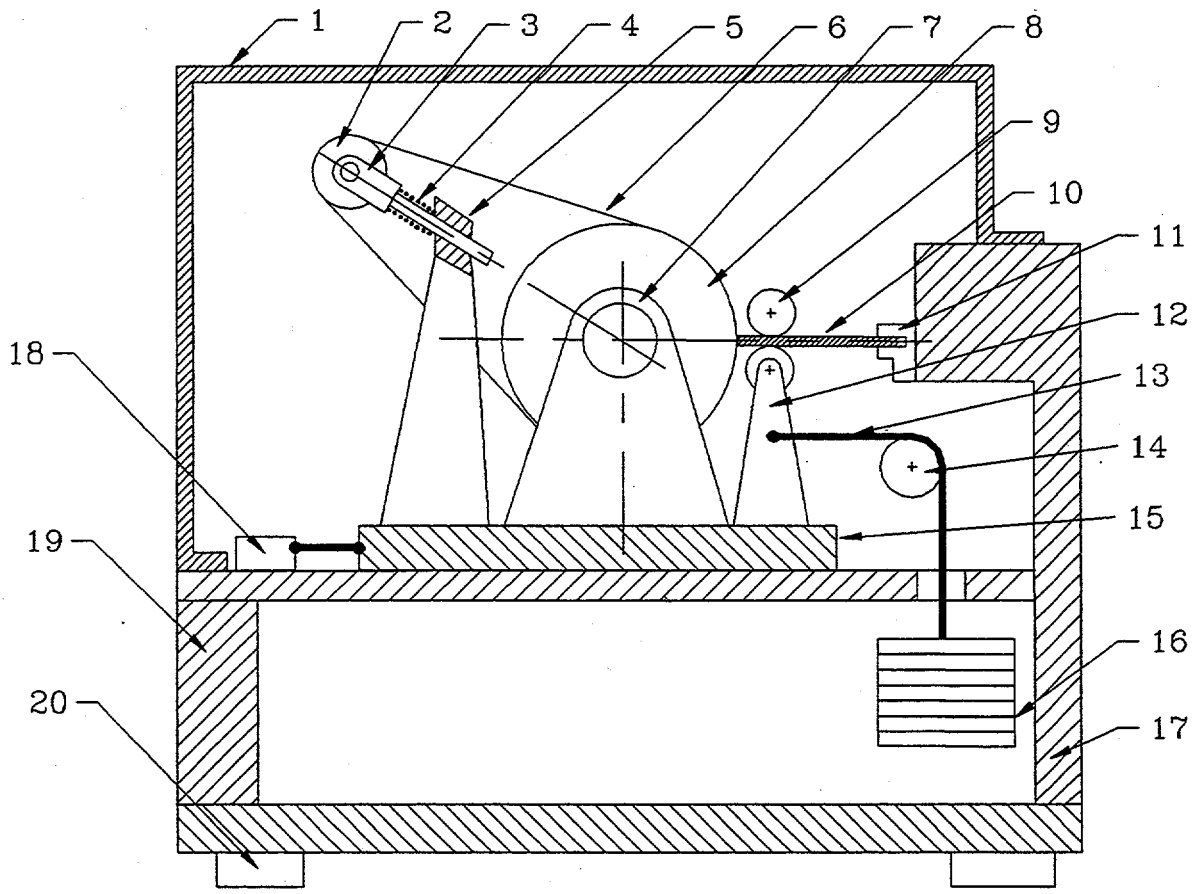

Figure 9. Schematic illustration of controlled force grinding with predetermined cycle time.

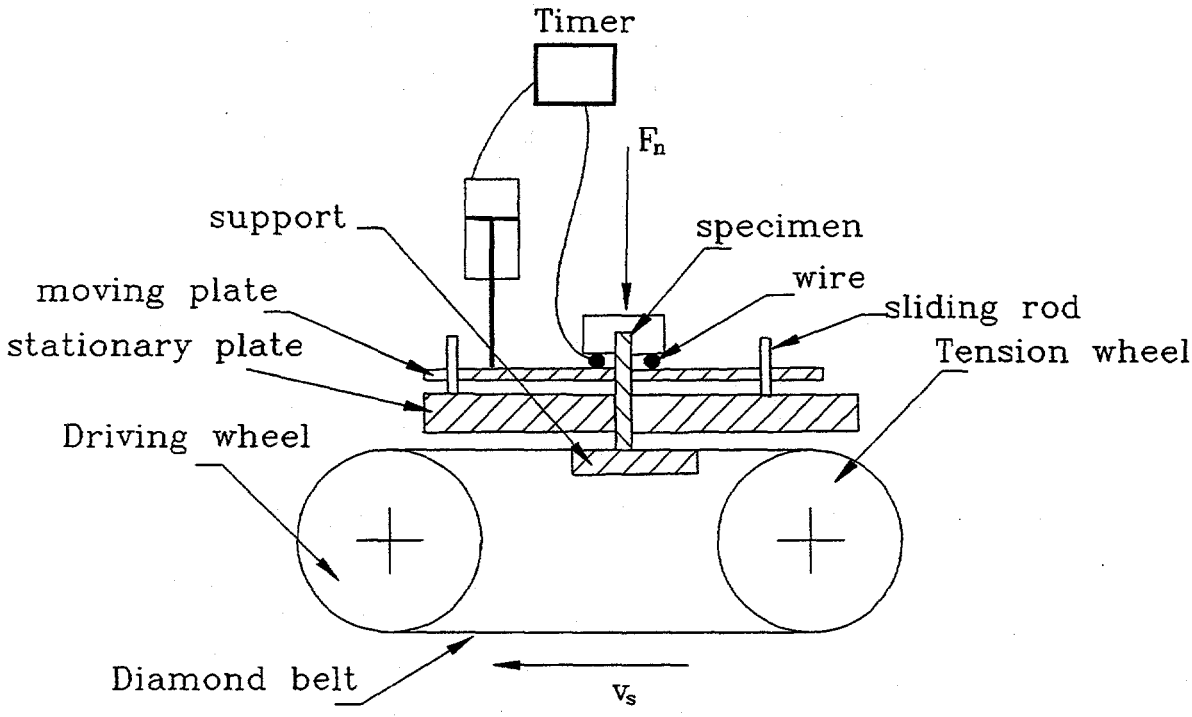

Figure 10. A sketch of the first prototype of the CGTS (version #1).

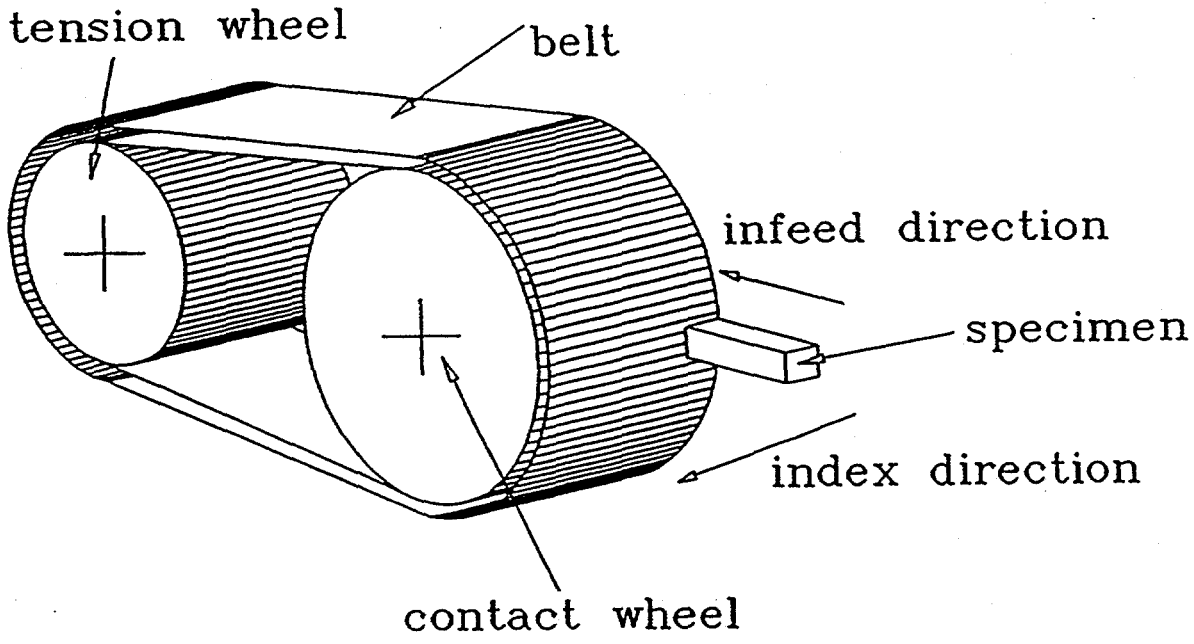

Figure 11. Illustration of the interaction between specimen and diamond belt during grinding.

The belt tension was adjusted using a preloaded spring with a mechanism for quick belt change over. A mechanism is also designed to adjust parallelness between the center of the driving wheel and the center of the idle wheel. The purpose of this adjustment was to maintain a newly installed belt to the center of the contact wheel. The fast feed speed of the specimen toward the belt was controlled with an air cylinder. A coolant supply system was incorporated with the test machine to accomplish wet grinding operation. A timing system was also incorporated with the test machine to account the actual grinding time. A desired grinding time can be programmed into the timer. Controlled force was accomplished by adding weights.

The operation of the test machine was as follows (see Figure 10): after a specimen of known length was mounted and the machine is started, the air cylinder lowered the moving plate at the preadjusted speed. As soon as the specimen contacted the belt (grinding begins), the circuit was broken and the timer started counting down from the programmed cycle time. When the cycle time was over, the air cylinder quickly retracted the specimen. This completed one test. The specimen was then removed and measured for stock removal.

An overview of the test machine is given in Figure 12. A view of the system without the base is given in Figure 13.

5.1.1 Test specimens

A standard MOR bar (3-mm by 4-mm cross section, 50-mm long) was chosen as the specimen design for grindability testing of ceramics. For the first set of tests, ten MOR bars from each material were manufactured.

List of materials used in the preliminary tests

Silicon Nitride: GS44	Allied Signal Ceramic Components
Silicon Nitride: GN10	Allied Signal Ceramic Components
Silicon Carbide: Hexoloy SA	Carborundum
Silicon Carbide: CVD	Morton Advanced Materials
Aluminum Oxide: WESGO 99.8	WESGO
Aluminum Oxide: Coors AD 99.8	COORS
Silicon Carbide	Norton Company
Silicon Nitride	Norton Company
Ziconia	Norton Company

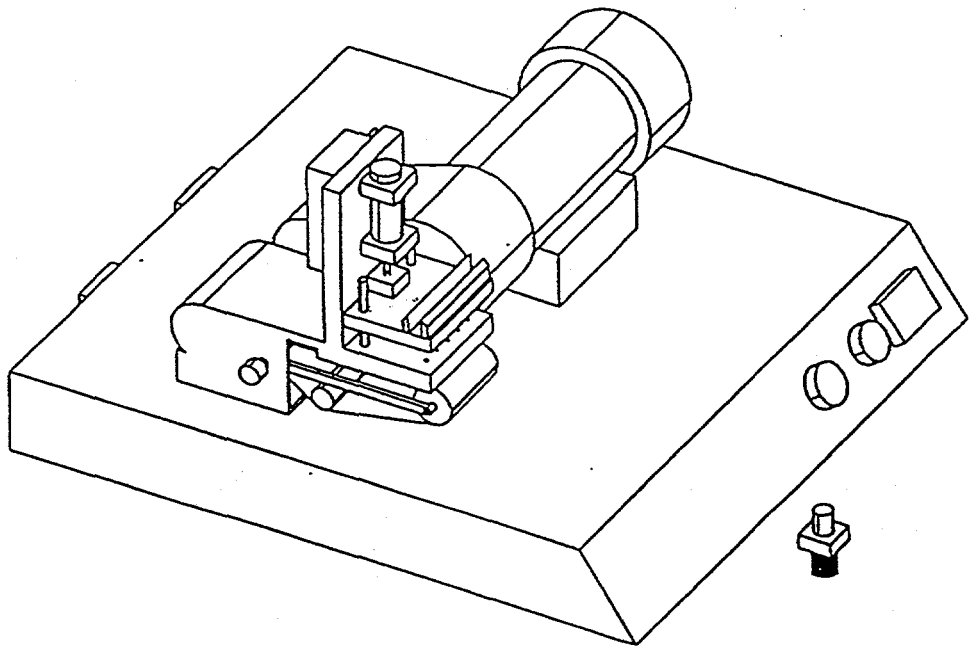

Figure 12. An overview of the test machine.

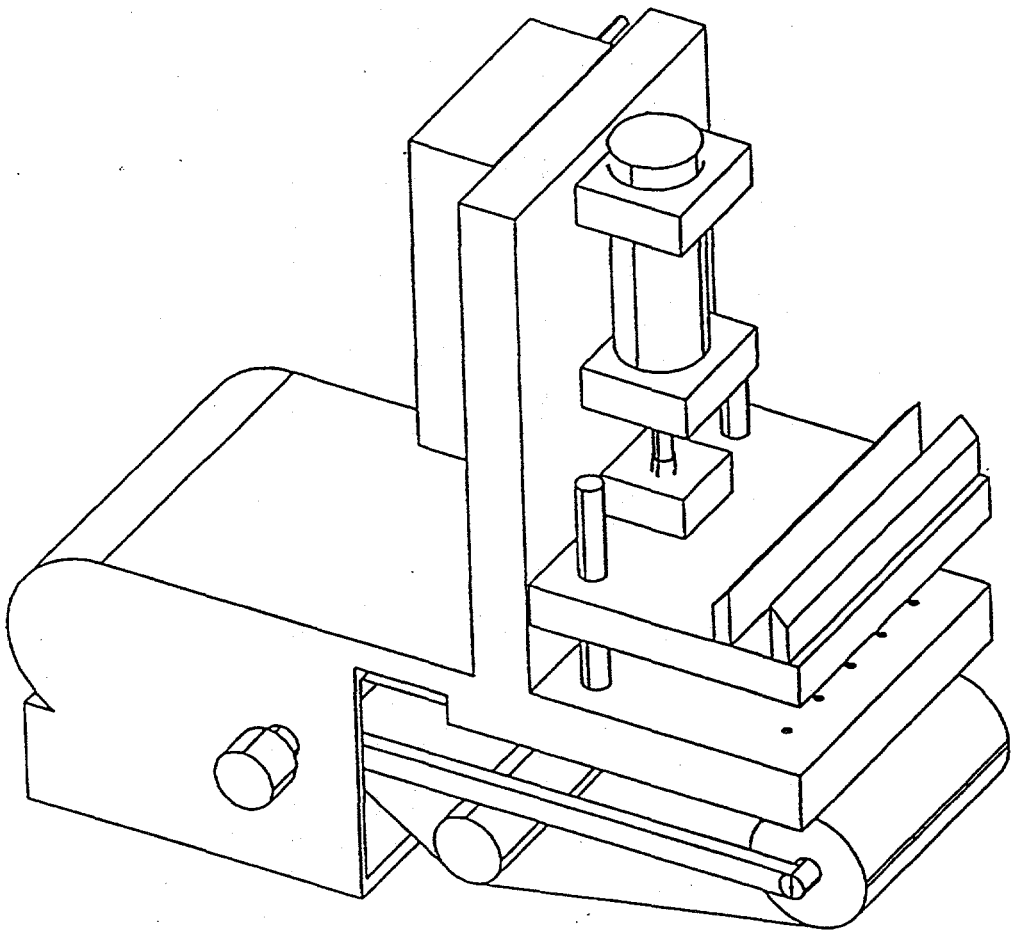

Figure 13. View of the test machine without the base.

5.1.2 Initial grindability tests

In the original design, the specimen was mounted on a slide which was supposed to move up and down freely. But some initial tests showed that the variation of the friction drag of the slide had significant influence on stock removal. Three different MOR bars were ground for 15 seconds under a load of 450 grams with both a coarse belt (100 grit size) and a fine belt (220 grit size). The results are summarized in Table 1. From the results of the initial test, it can be seen that the normalized in-feed rate was very different for the three materials tested.

Table 1. Initial test result

Coarse belt (100 grit size)				
Material	Initial length	Final length	Amount removed	Normalized in-feed rate (mm/sec)
1	1.969	1.933	0.036	0.166
2	1.851	1.643	0.207	0.954
3	1.997	1.720	0.277	1.277
Fine belt (220 grit size)				
Material	Initial length	Final length	Amount removed	Normalized in-feed rate (mm/sec)
1	1.933	1.919	0.014	0.065
2	1.643	1.560	0.083	0.382
3	1.720	1.603	0.117	0.539

5.1.3 Improved CGTS

In order to further improve repeatability and consistency of the measurements, modifications to the test machine were made. After each modification, some tests were conducted to qualify the improvement. Modifications were done in the following aspects.

A Grinding Support

The support piece used to support the belt and specimen is shown in Figure 14. In the original design, a flat carbide plate was used, as shown in Figure 14(a). During experiments, it was found that the specimen was bouncing due to the thickness variation of the belt near the joint. In order to eliminate this bouncing movement, a softer material (Nylon) was used to replace the carbide plate. No improvement was observed in reducing the bouncing, but the nylon plate was worn very quickly. Then an adjustable roller support, as shown in Figure 14(b), was made to replace the flat support. The distance between the two rolls can be adjusted to find the optimum separation. The bouncing the specimen was reduced. However, the results showed variations due to the difference in sagging of the belt when grinding in middle of the belt and near the edge of the belt. The conclusion was that the original design of a carbide plate seems to be the best choice.

B Variable Speed Drive

In the original design, the belt speed was fixed at 4,500 SFPM at the suggestion of the belt manufacturer. In order to explore grinding under various speeds, a variable speed motor was used to replace the fixed RPM motor. The specimen bouncing was also reduced significantly by reducing the belt speed.

C Specimen Holder

A new specimen holder, as shown in Figure 15, was manufactured to replace the original holder, as shown in Figure 16. In the original design, the MOR bar was put into the holder and fixed in place using two set screws. The MOR bar served as a guide which slid freely within the holes in the fixed plate. The rectangle MOR bar did not fit very well within the hole. Also, the portion of the bar protruding out from the holder varied from test to test. Because of the limitation of the original design, only a few experiments could be conducted on each specimen. The new design, as shown in Figure 15, eliminated the above problems. A clamping stud with a lock nut was used to adjust the length of the specimen that protruded out from the specimen holder. The stud also transferred the grinding force to the specimen holder. Also, both the holder and the holes were hardened and ground. Two fitting clearances of 0.001 and 0.0015 inches were used in the experiment. It should be noted that sliding friction still exists.

D Belts

In order to reduce the specimen bouncing, a belt with a 67° slice joint, as shown in Figure 17(b), was purchased to replace the original belt, as shown in Figure 17(a) which had a 90° slice joint. This new belt used a joint called filmlock. The belt manufacturer claimed no thickness variation near the joint. The original belt uses a

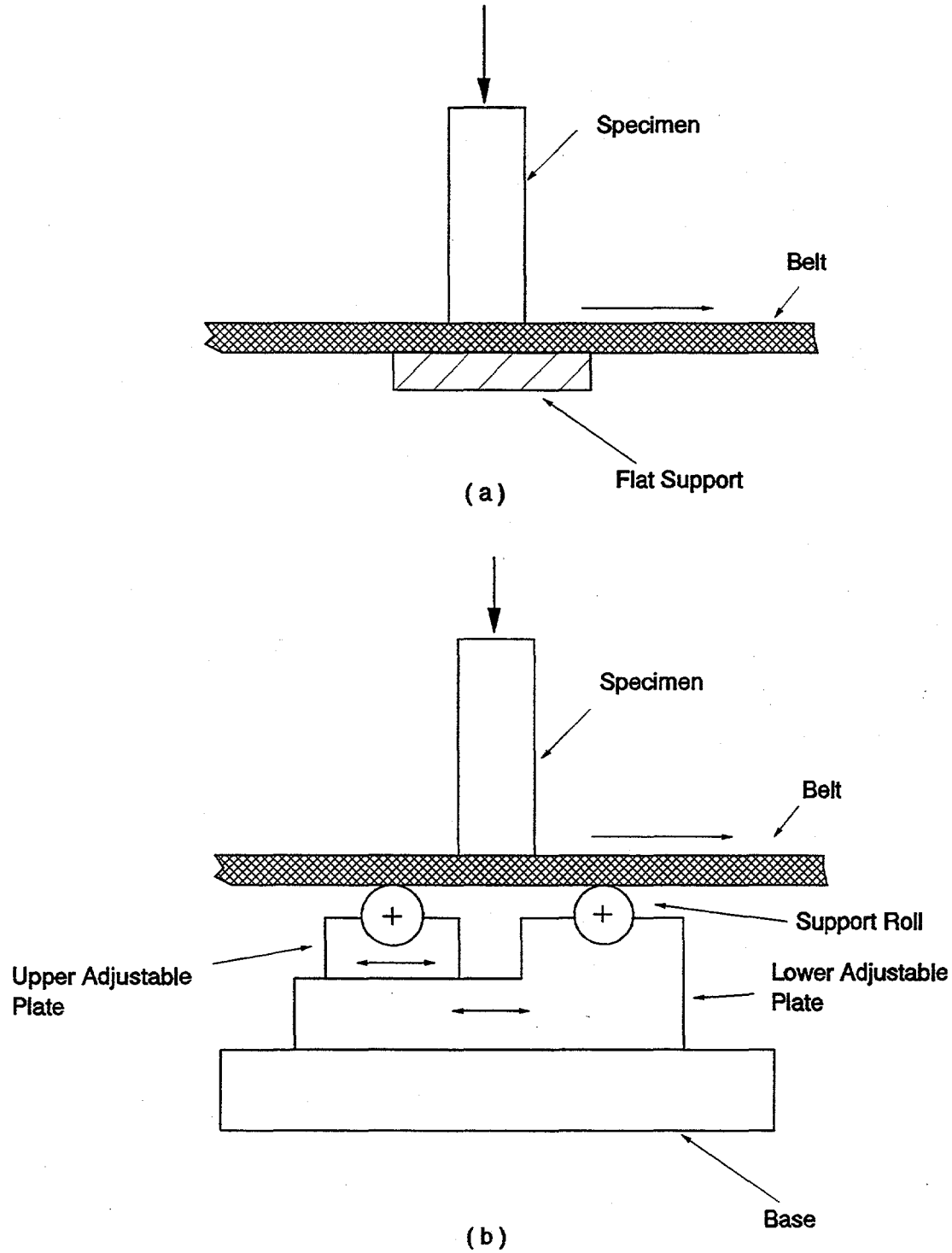

Figure 14. Two kinds of supports.

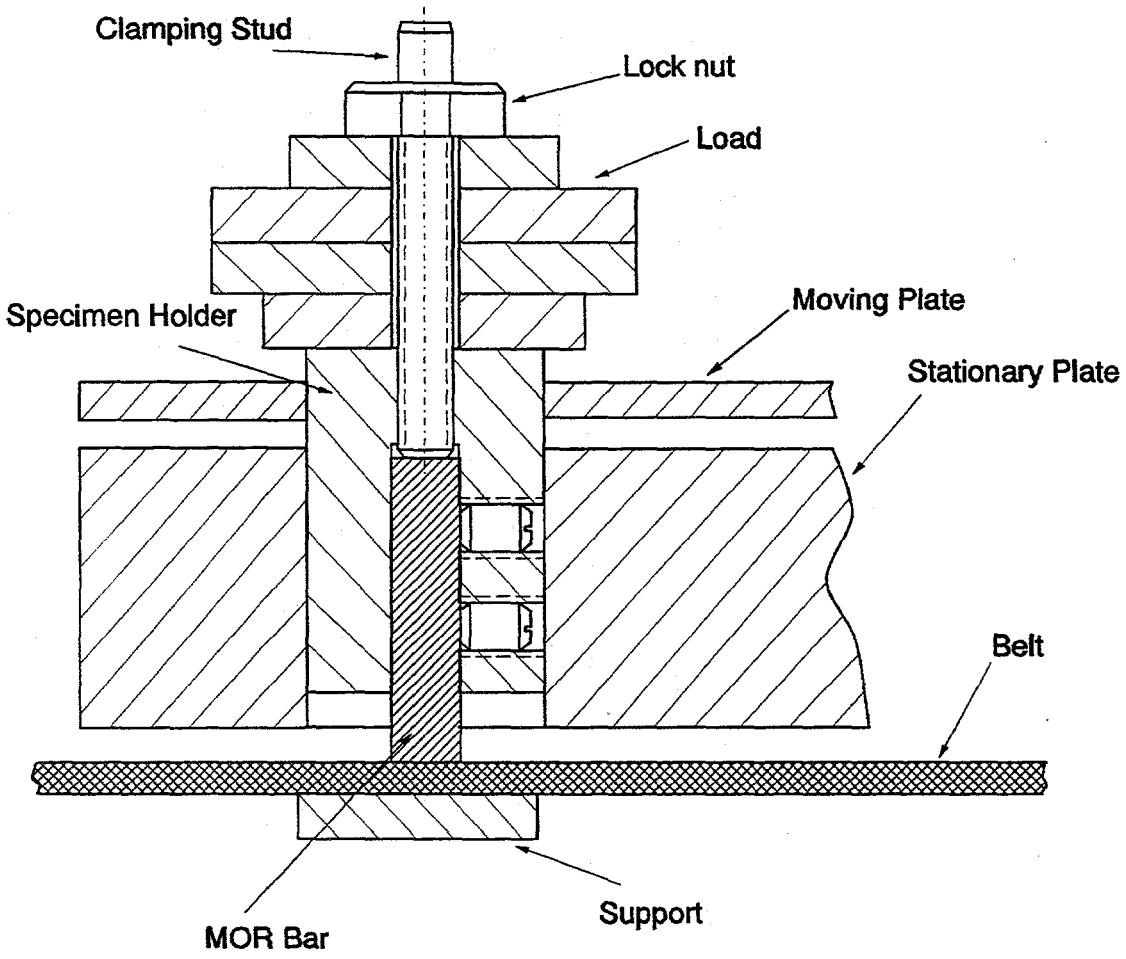

Figure 15. Improved specimen guiding and holding unit.

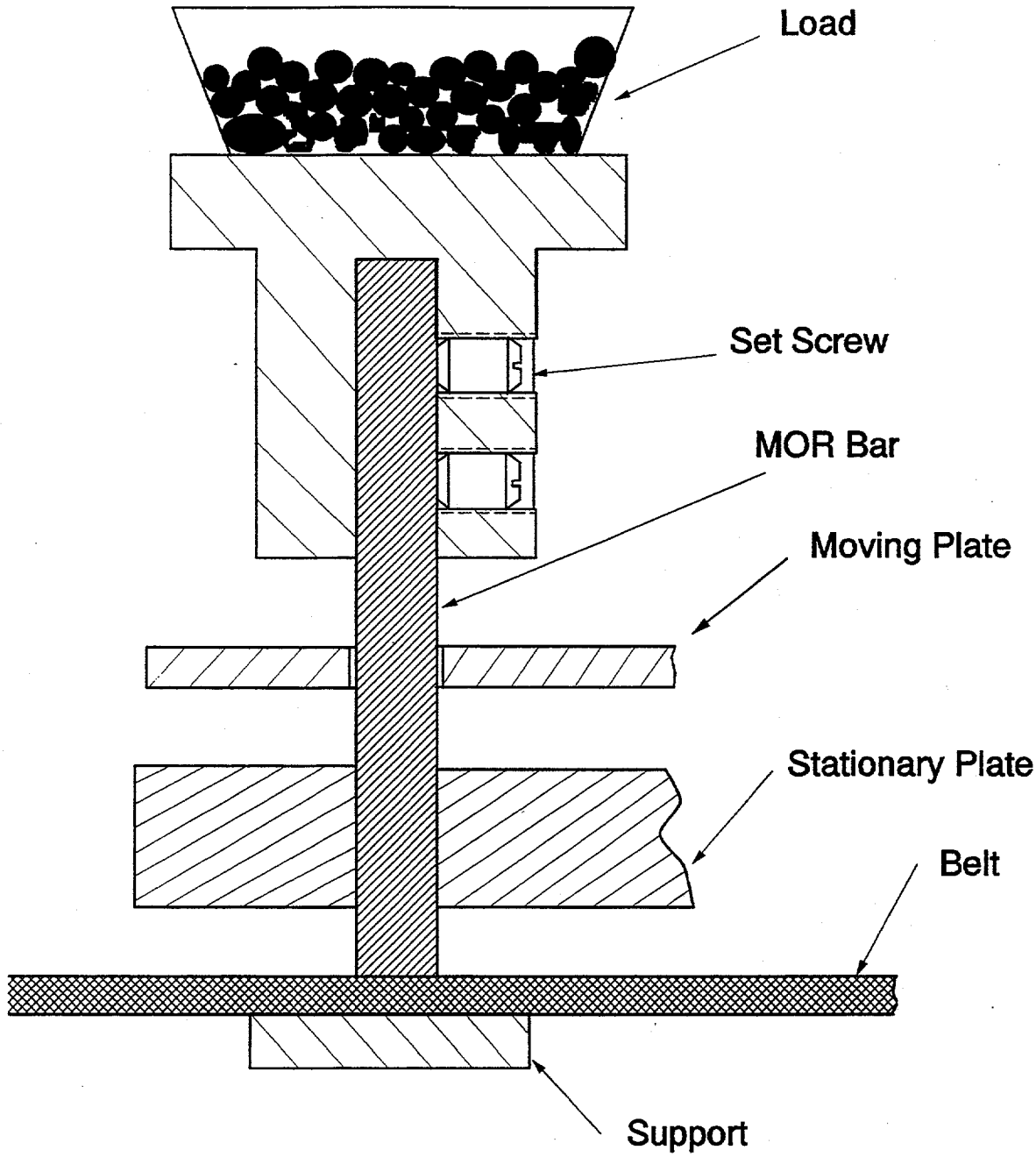

Figure 16. Original specimen guiding and holding unit.

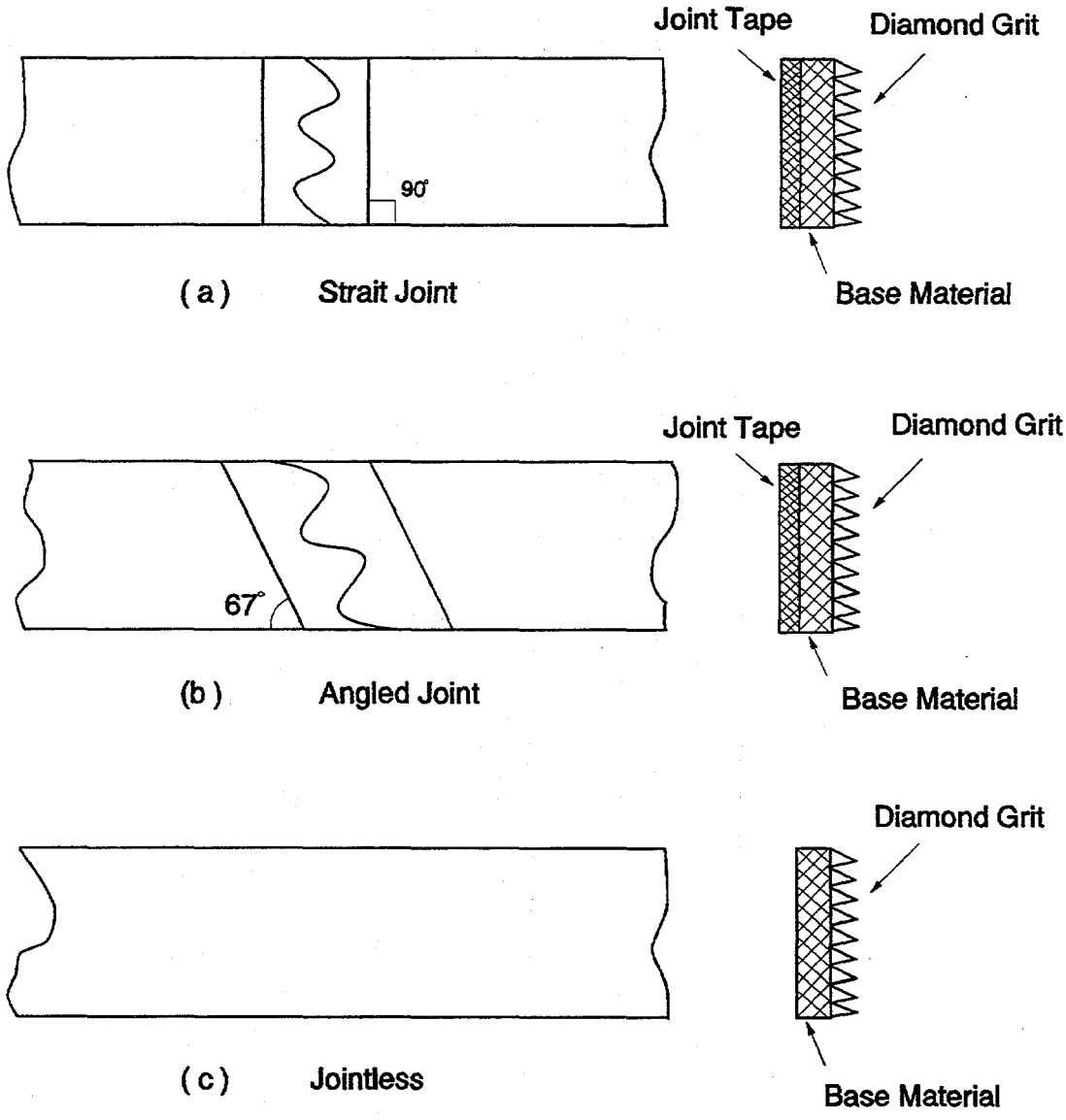

Figure 17. Various types of belt joints.

fabriclock which had about 0.003-inches thickness variation near the joint. Experiments indicated that the bouncing was greatly reduced. Also, it should be noted that belts without a joint, as shown in Figure 17(c), will be commercially available soon.

5.1.4 Preliminary grindability tests with the improved CGTS

After the modification of the test machine, more tests were conducted. Test conditions were as follows:

Belt speed: 22.86 m/s (4500 SFPM)
Load: 1000 grams
Specimen: 3 × 4 mm MOR bar
Wet grinding: Q = 0.5 gal/min
Cycle time: 30 seconds

For the preliminary test, five ceramic materials were tested. Some results of stock removal are given in Figure 18. The average removal rates are shown in Figure 19. It can be seen that 0.227 inches were removed for WESGO aluminum oxide, 0.189 inches for Carborundum Hexoloy SiC, 0.147 inches for Morton CVD SiC, 0.043 inches for Allied Signal silicon nitride GS44, and only 0.041 inches for Allied Signal silicon nitride GN10. If WESGO aluminum oxide is chosen as reference material, the ranking of the tested materials will appear as shown in Figure 20. From this preliminary test, it can be seen that silicon nitrides, silicon carbides, and aluminum oxides have very different grindabilities.

5.2 Prototype CGTS - version #2

In order to eliminate the influence of sliding friction on test results, the original sliding structure was replaced with a pivot and lever mechanism, as shown in Figure 21. The air cylinder is still used for gap elimination and fast retraction of the specimen. The distance from the pivot point to the specimen (grinding point) was 12 inches. From the previous experiments, it was found that the material removal is about 0.200 inches for the softest material (aluminum oxide), which corresponded to an angle of less than 1 degree. As compared with the original sliding mechanism, the friction influence should be virtually eliminated with this pivot-lever system due to the very small rolling friction of the ball bearing. Some experiments were conducted using this improved test machine shown in Figure 22. It can be seen that the results for the 7 tests were very consistent with an error of less than 4%.

5.3 Prototype CGTS - version #3

Extensive tests were conducted using the second prototype of the CGTS (see next section for results). The results indicated that repeatability of less than 10% can

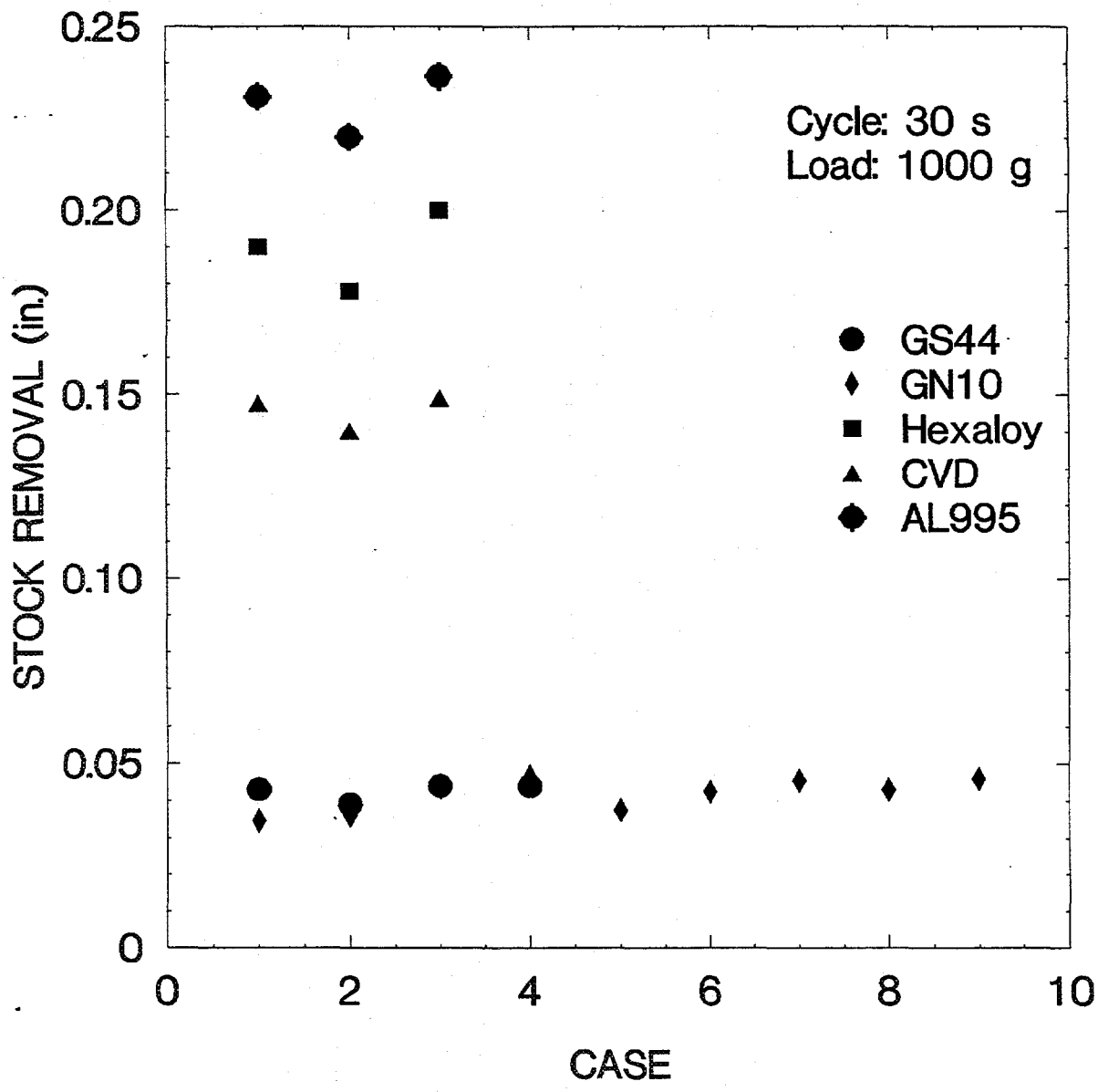

Figure 18. Stock removal for various materials tested.

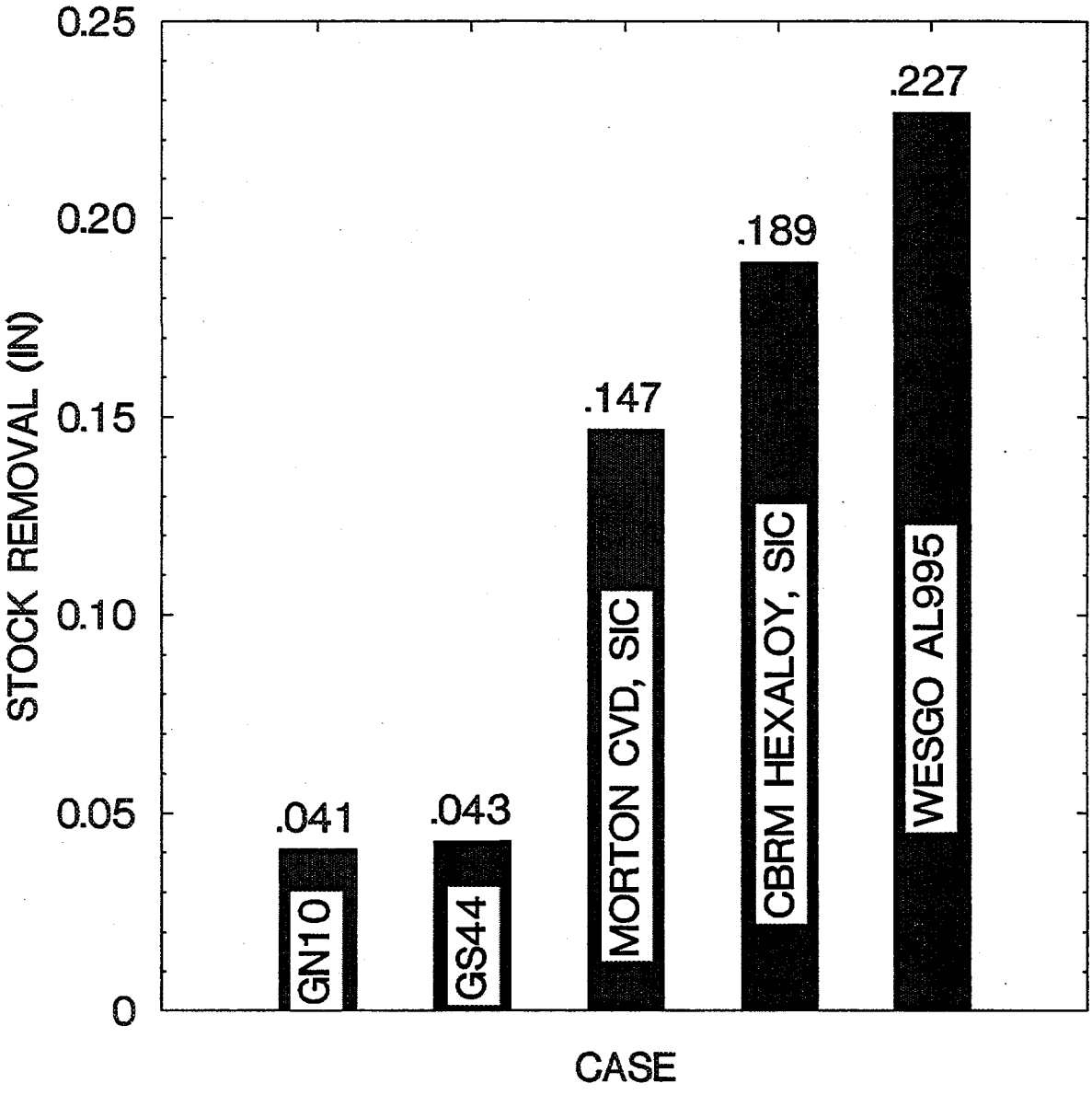

Figure 19. Average stock removal for various materials tested.

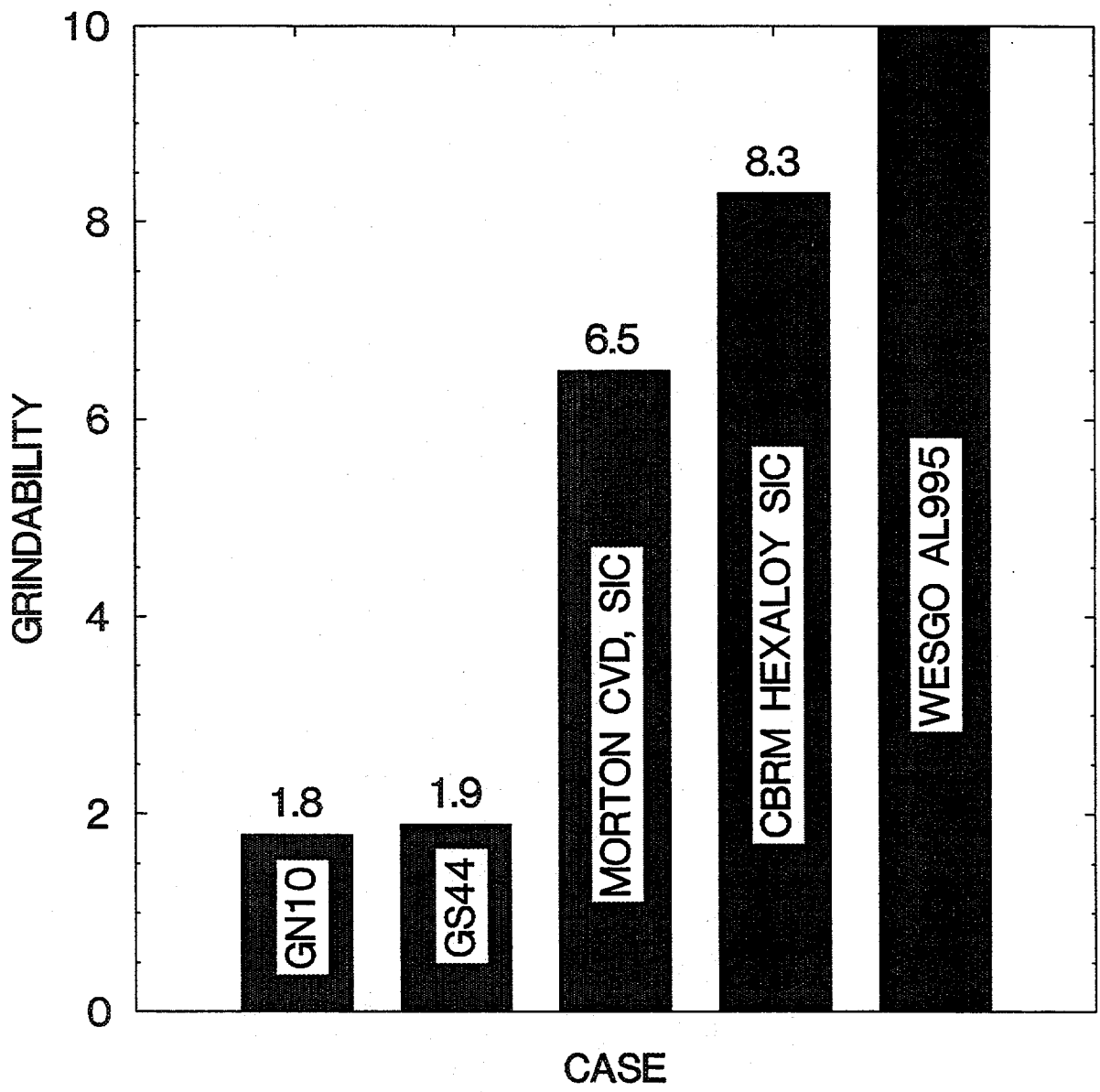

Figure 20. Grindability for various materials tested.

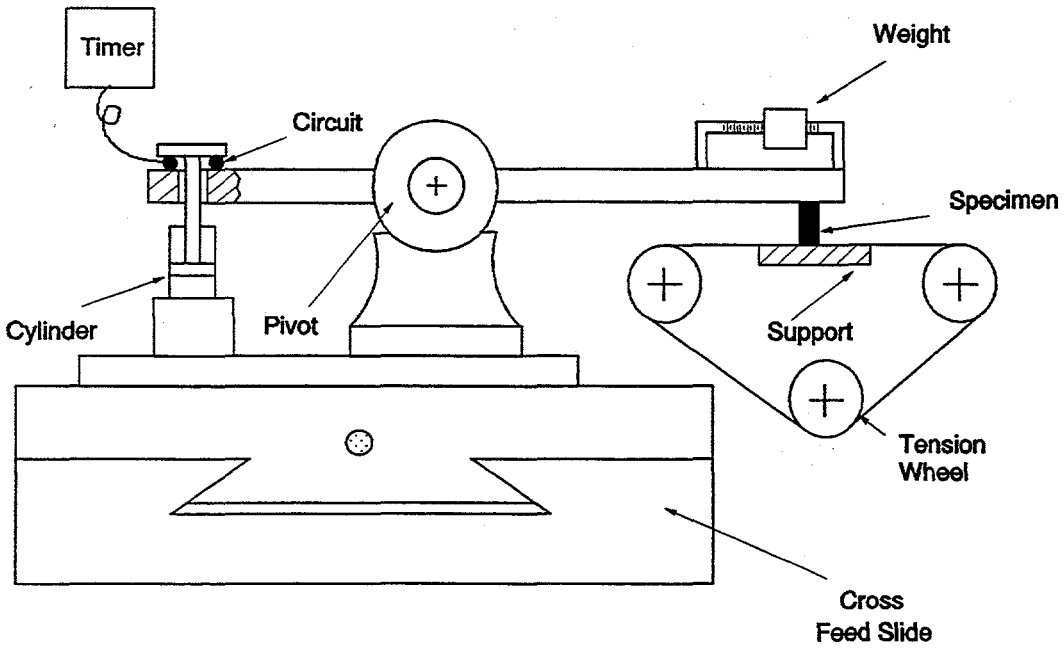

Figure 21. The pivot-lever design (version #2).

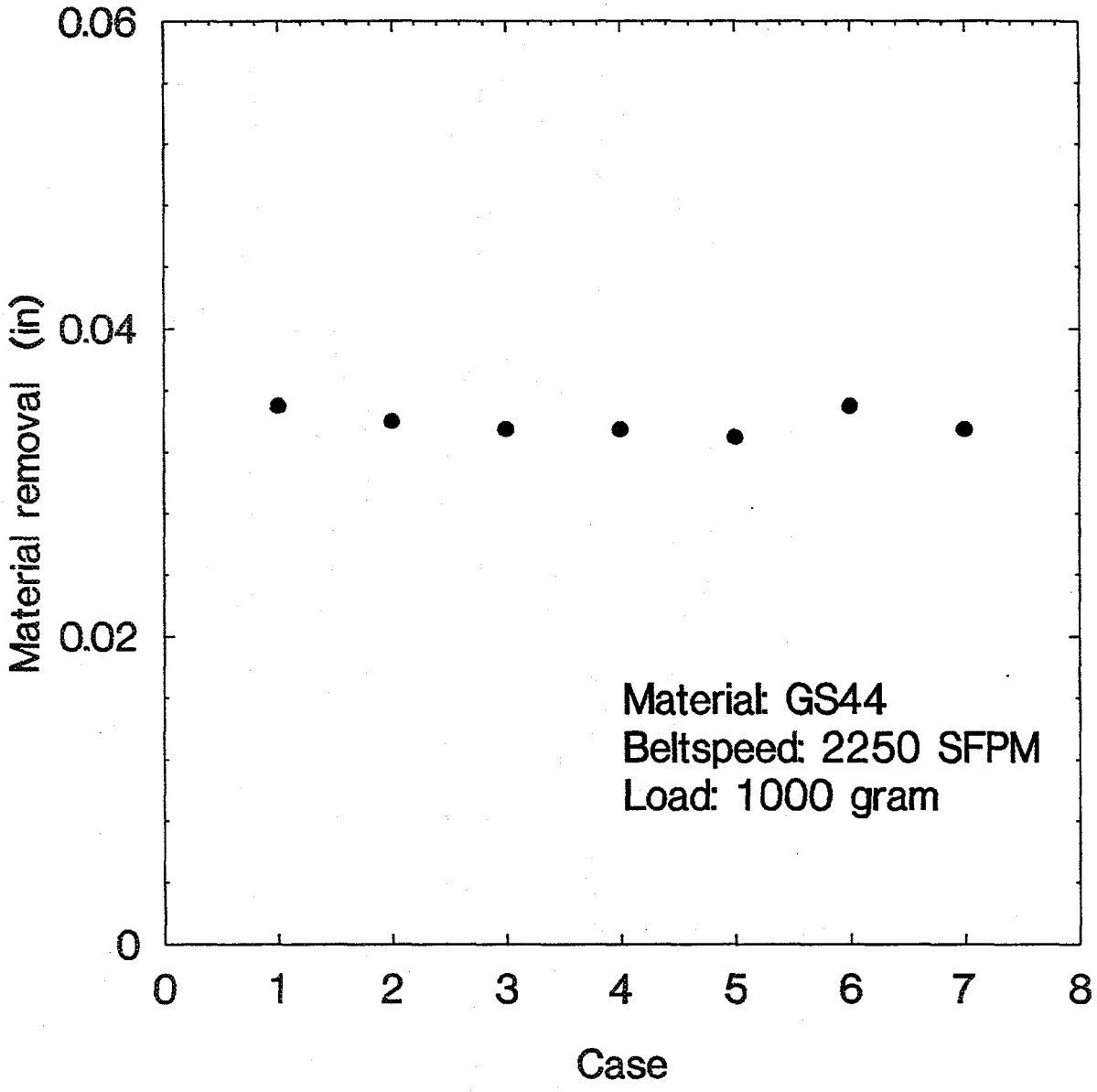

Figure 22. Test results for GS44 with the modified test machine.

be maintained. It was decided to develop the final CGTS based on this design. The air cylinder was replaced with a linear actuator in the final design. The normal force was applied by using weight, which was driven by a linear actuator to change the grinding force. Figures 23 and 24 show the final ceramic grindability test system, Figure 25 is a schematic illustration, and Figure 26 is an isometric sketch, which has the following features:

- Fully computerized to eliminate operators influence.
- Grinding with diamond belt to eliminate influence of wheel dressing.
- Standard MOR bars as test specimen for cost-effectiveness.
- Computer controlled force and speed adjustment for various ceramics.
- In-process gaging of removal rate with analogue and digital read out.

6 Grindability Test

Comprehensive grindability tests were conducted on 12 ceramic materials (seven types of silicon nitride, two types of zirconia, two types of silicon carbide and one type of aluminum oxide) as listed in Table 2 under the grinding conditions given in the last row of Table 2. Before the final characterization of the 12 materials listed in Table 2, some preliminary tests were conducted to choose the optimum belt speed and normal grinding force.

6.1 Belt Wear Test

For the first set of experiments, the variation of material removing capability of the chosen diamond belt was investigated. Material 9 (silicon nitride G) and material 11 (silicon carbide B) were used (refer to Table 2 for material numbers). For each material, all the tests were conducted at the same belt location (the location across the belt width, as shown in Figure 11). The results are given in Figure 27. As expected, during 30-second grinding period the amount of removal reduced with time. These results indicated that the removal rate can vary significantly with grinding time. Therefore, only a short period of grinding should be used at each belt location to minimize the influence of belt wear on the grindability measurement.

6.2 Influence of Belt Speed

For the second set of experiments, the influence of belt speed on material removal was investigated. Materials 8 (silicon nitride F) and 11 (silicon carbide B) were tested. The belt speed was varied from 2 to 21 m/s. Each test was conducted at a new belt location. Results are given in Figure 6. It can be seen that material removal was proportional to belt speed under a constant normal force. The material removal can be simply normalized by the belt speed to eliminate the influence of belt speed. The deviation of results from the linear relationship at higher belt speeds may be due to the vibration of the system.

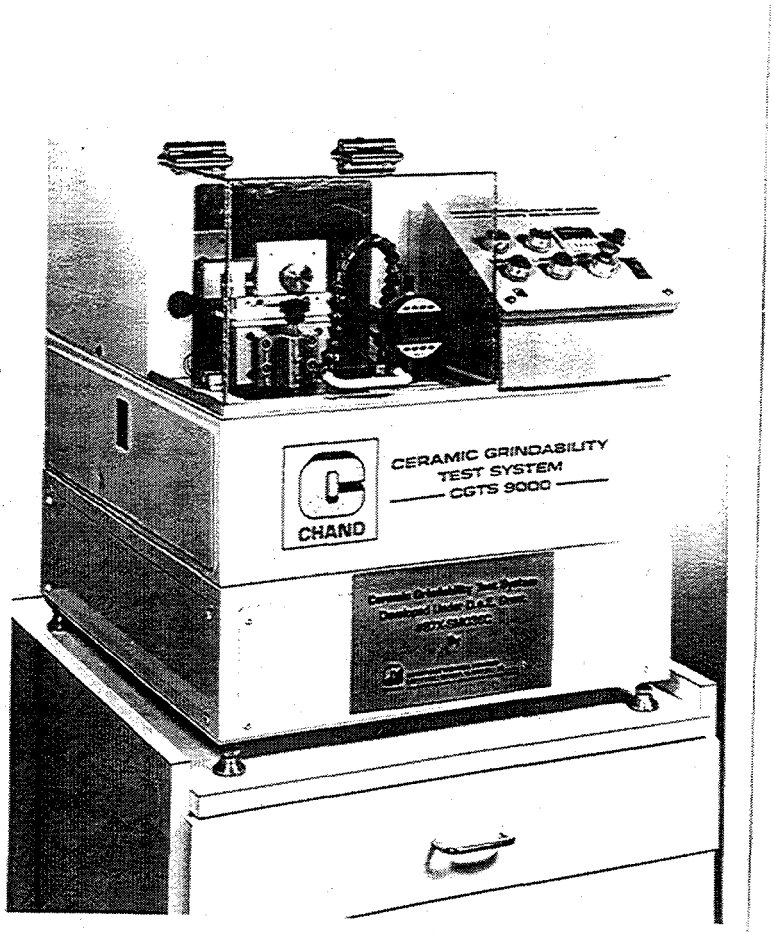

Figure 23. Photograph of the final CGTS.

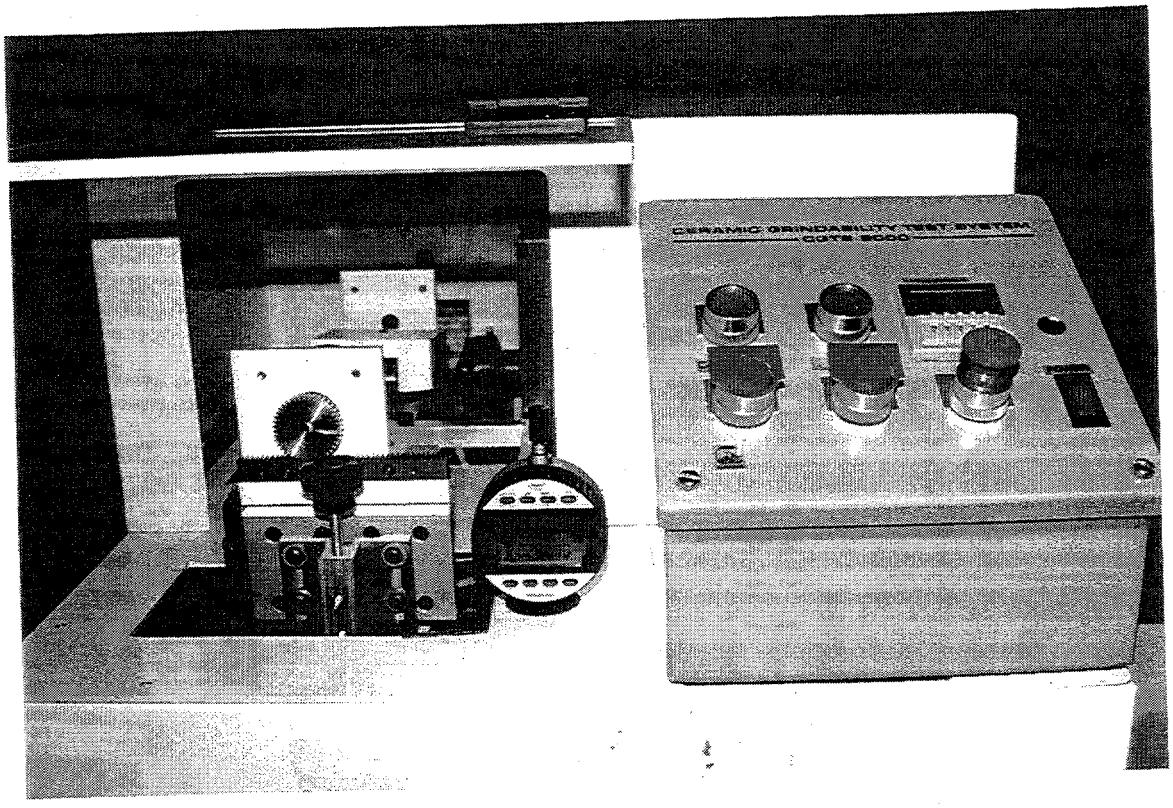

Figure 24. Photograph of part of the CGTS.

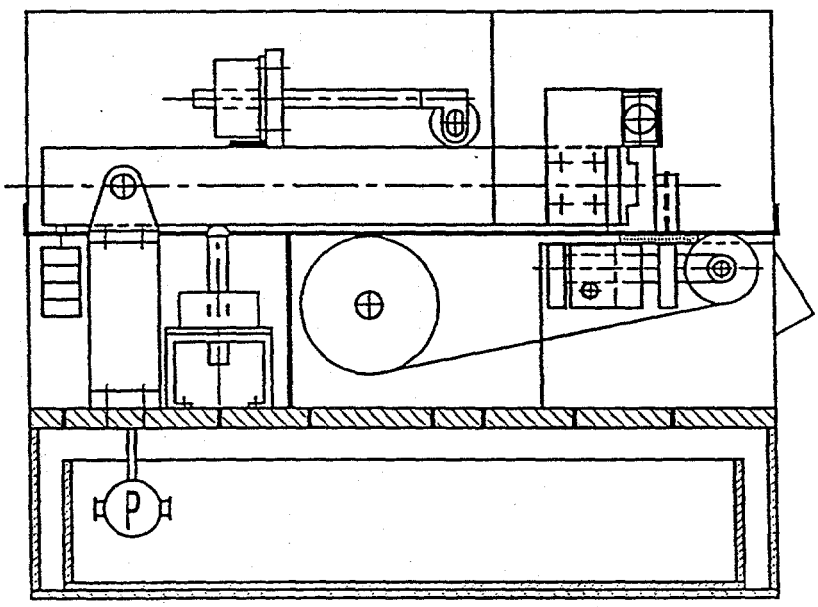

Figure 25. Schematic illustration of the final CGTS.

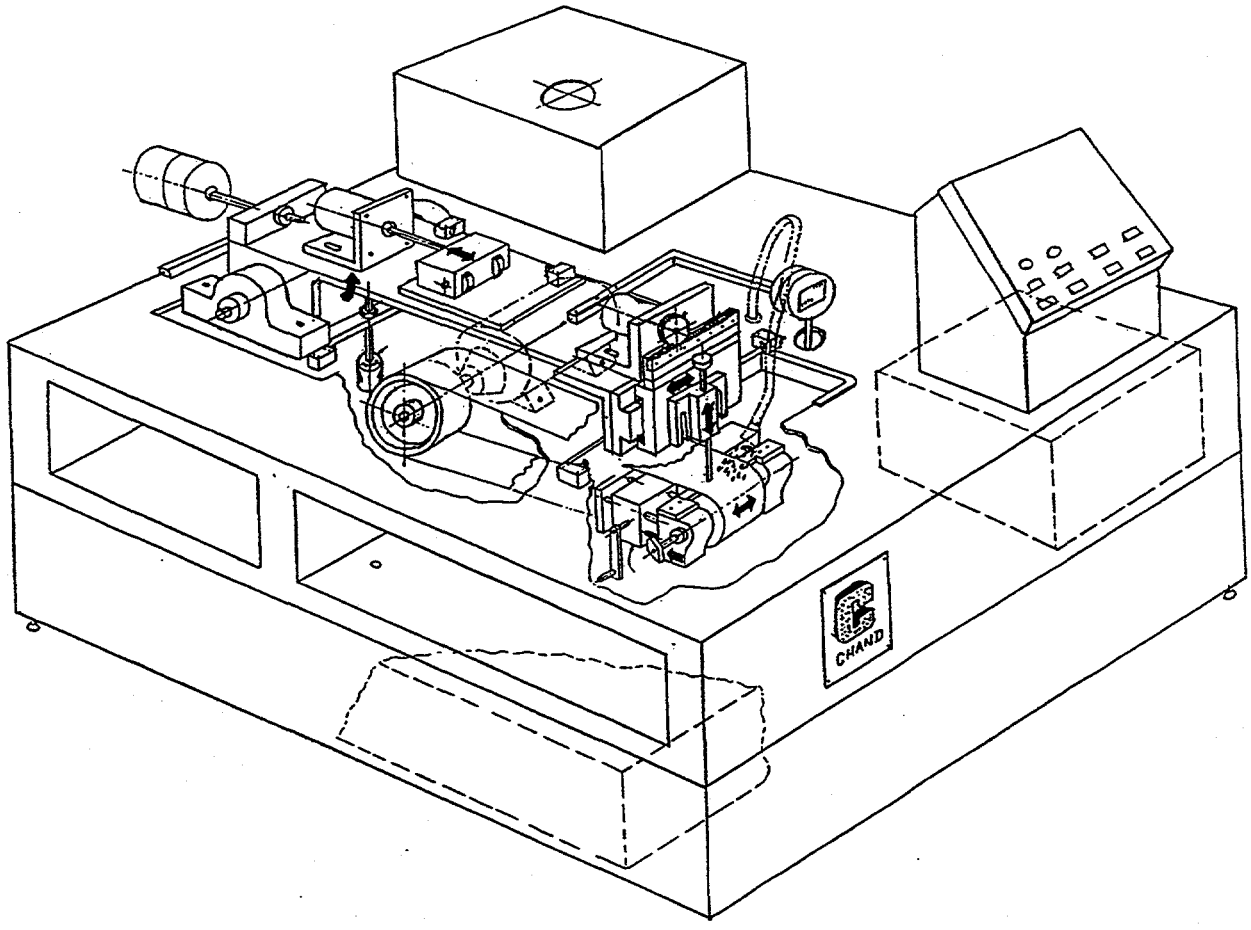

Figure 26. Isometric sketch of the final CGTS.

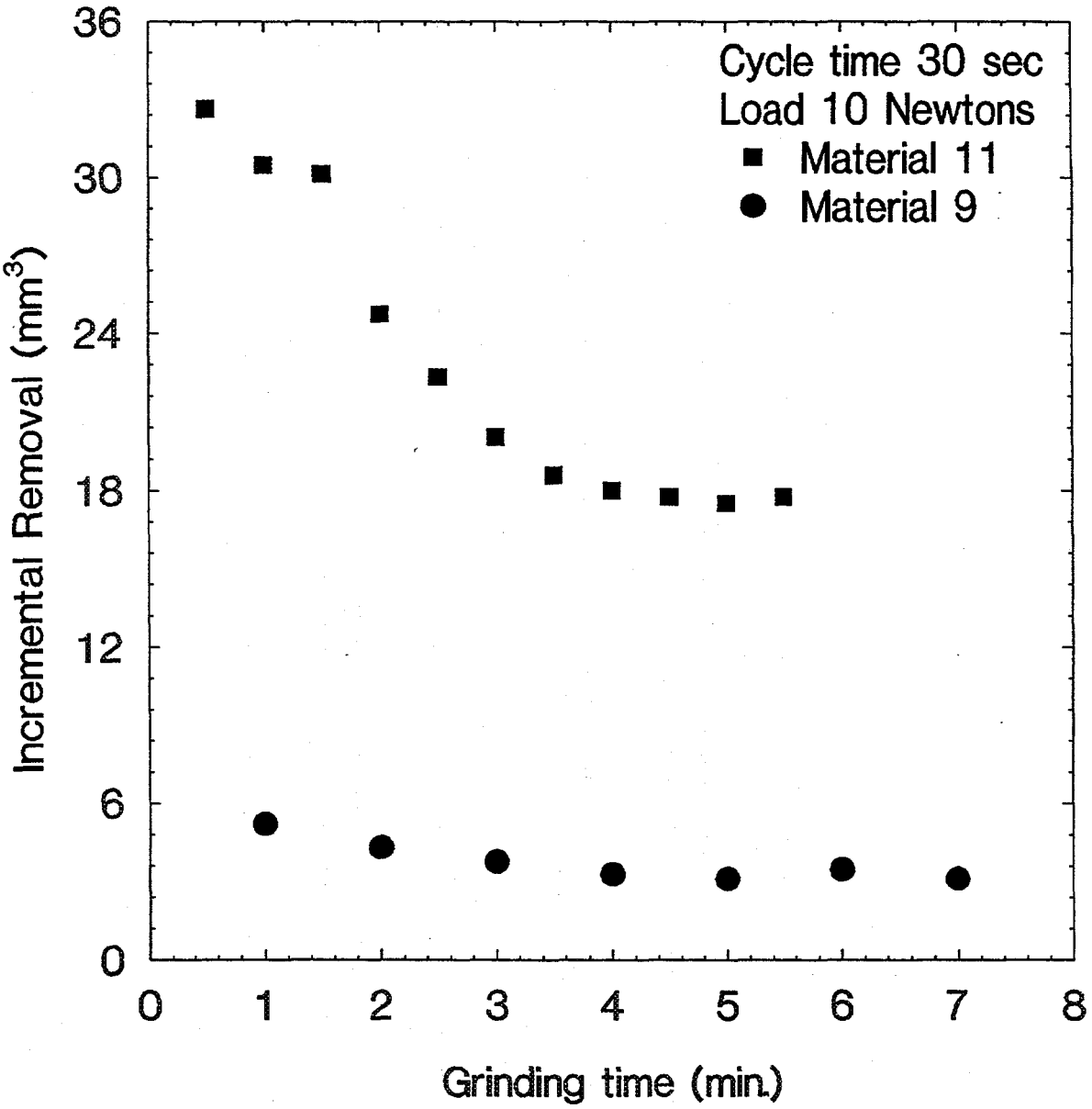

Figure 27. Removal versus grinding time.

Table 2. Material summary

	Material	Hardness HV	Weibull modulus	Flex Strength (MPa)	Fracture toughness
1	Si_3N_4, A	1860		590	5.70
2	Si_3N_4, B	1500		620	6.60
3	Si_3N_4, C	1500		620	6.60
4	ZrO_2, A	1200		630	8-12
5	ZrO_2, B	1200		630	8-12
6	Si_3N_4, D	1500		620	6.60
7	Si_3N_4, E	1500		620	6.60
8	Si_3N_4, F	1460	20-35	1050	8.25
9	Si_3N_4, G	1670	12-22	983	6.50
10	SiC, A	2500		595	2.70
11	SiC, B	2800	10	460	4.60
12	Al_2O_3	1360		310	

Grinding condition

Normal load:	10 Newtons
Belt:	220 mesh diamond belt, 762 × 50.8 mm, 3M
Belt speed:	v_s = 10 m/s
Specimen dimension:	Standard MOR bar 3 × 4 mm
Cycle time:	30 and 60 seconds

6.3 Influence of Normal Force

For the third set of experiments, the influence of normal grinding force on material removal was investigated. Materials 9 (silicon nitride G) and 10 (silicon carbide A) were used for this test. The normal load was varied from 2 to 14 Newtons at a belt speed of 10 m/s. Once again, each test was conducted at a new belt location. Results are given in Figure 7. It can be seen that the material removal was proportional to the normal force.

6.4 Grindability of Some Ceramics

Based on the above tests and suggestions from the belt manufacturer, a belt speed of 10 m/s and normal load of 10 Newtons were chosen for the final characterization. Two sets of tests were conducted for the 12 ceramics. For the first set, 11 grinding tests were conducted for each of the 12 materials with five tests at belt location 1, three tests at location 2, and the rest at location 3. It can be seen that the amount of material removal for each material group is significantly different. For a 30-second grinding period, the removal is about 4-5 mm for aluminum oxide, about 2 mm for silicon carbide, approximately 1 mm for zirconia, and only 0.4-0.6 mm for silicon nitride. Comparison of ceramics belonging to the same group such as silicon nitride can provide more useful information. For this purpose, the seven silicon nitrides were further compared. The seven materials tested belonged to three groups in terms of material removal. Material 1 had the highest removal, Materials 2, 3 and 9 had the lowest, and Materials 6, 7 and 8 were in the middle. ANOVA analysis was conducted in order to compare the seven materials. The over all F-value is 43.84 and the p-value is 0, which means that the seven materials are significantly different. In order to test the difference among materials statistically, a T-test was conducted for all the pair combinations of the seven materials. Results are given in Table 3. For a significant level of $p = 0.05$, Materials 6 and 7 have no significant difference, Materials 7 and 8 have no significant difference, and Materials 2 and 9 have no significant difference. Actually, Materials 6 and 7 are from two batches of the same material, and Materials 2 and 3 are from two batches of another material.

In order to eliminate the influence of belt wear on the results as shown in Figure 27 and to detect differences among the seven silicon nitride materials, another set of tests was conducted in which only one test was conducted at each belt location. For each material, 10 tests were conducted. By comparing the results of the two characterizations, it was seen that the mean values of material removal for the second set are higher than the first set as listed in Table 4. This is expected because each test was conducted at a new belt location in the second set of tests, as compared with the first set in which multiple tests were conducted at each location. Grindabilities of the tested ceramics were obtained from the definition. Results are given in the 4th and 7th columns of Table 4. A plot of grindability is given in Figure 28.

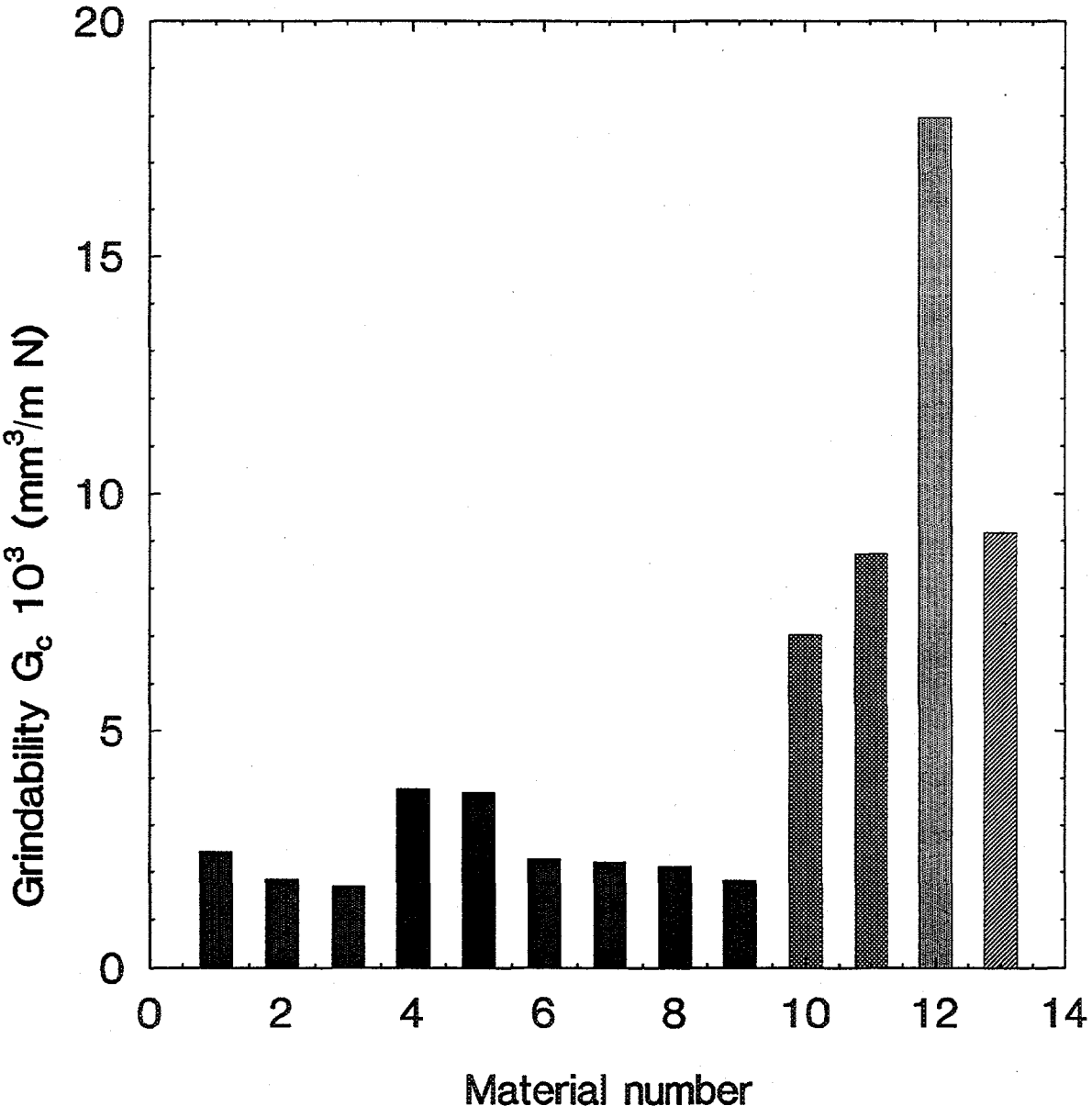

Figure 28. Comparison of material removal for various ceramics.

Table 3. T-test Result (p-value)

Material		1	2	3	6	7	8	9
1	test 1		0	0	0.005	0	0	0
	test 2		0	0	0.004	**0.076**	0.003	0
2	test 1			0	0	0	0.001	**0.077**
	test 2			0.007	0	0	0.001	**0.611**
3	test 1				0	0	0	0.002
	test 2				0	0	0	0.034
6	test 1					**0.056**	0.007	0
	test 2					**0.212**	**0.052**	0
7	test 1						**0.450**	0
	test 2						**0.225**	0
8	test 1							0
	test 2							0

Table 4. Mean and standard deviation of material removal

Material	Test 1			Test 2		
	Mean	Std. Dev.	C_G 10^{-4} mm^3/m N	Mean	Std. Dev.	C_G 10^{-4} mm^3/m N
1	0.596	0.073	24.3	0.618	0.014	25.2
2	0.454	0.027	18.5	0.508	0.029	20.7
3	0.418	0.029	17.1	0.423	0.041	17.3
4	0.929	0.045	37.9			
5	0.906	0.038	37.0			
6	0.561	0.050	22.9	0.571	0.046	23.3
7	0.545	0.056	22.2	0.556	0.041	22.7
8	0.520	0.055	21.2	0.540	0.040	22.0
9	0.447	0.031	18.2	0.478	0.043	19.5
10	1.721	0.276	70.2			
11	2.148	0.308	87.7			
12	4.441	0.590	181.3			

6.5 Additional Grindability Tests

Grindability tests were conducted for five additional ceramics (Materials 13 to 18 in Table 5). For Materials 14 to 18, a batch of MOR bars were manufactured and their flexural strengths were measured. Some samples from the same batch used to measure the flexural strength were used to measure their grindability. The measured grindabilities are listed in the last collum of Table 5 together with the results for the 12 ceramics tested previously.

In Figure 29, grindabilities of various ceramics are plotted. The grindabilities of the silicon nitride ceramics tested are plotted in Figure 30. It can be seen that the easiest material tested (Material 12, aluminum oxide) has a grindability more than 26 times of the most difficult material tested (Material 15, silicon nitride - I). If silicon nitride ceramics are compared, the easiest material tested (Material 18, silicon nitride - L) has a grindability about 5 times of the most difficult material tested (Material 15, silicon nitride - I). However, their mechanical properties are similar. This indicates that grindability of ceramics can be greatly improved through 'design for grindability' in the ceramic development stage. Therefore, it is necessary to understand the correlation between grindability and microstructure in order to identify the driving force of grindability. This is beyond the scope of phase one work. In the next section, some preliminary correlations between grindability and mechanical property will be discussed.

7 Grindability and Mechanical Properties

7.1 Correlation between Grindability and Flexural Strength

Extensive grindability tests were conducted for various ceramics. Some of those tested ceramics had very similar mechanical properties, and others had very different ones (see Table 5). Therefore, we wanted to know whether correlations exist between grindability and mechanical properties, such as hardness, flexural strength, and fracture toughness. Grindability is plotted versus flexural strength in Figure 31 for all the ceramics tested. These results seem to indicate that grindability generally decreases with flexural strength. However, more tests are needed to further prove this. In Figure 32, only silicon nitride ceramics are compared. From this graph, it is hard to accept the above suggestion.

7.2 Correlation between Grindability and Hardness

Any correlation between grindability and hardness would be also of interest to both ceramic manufacturers and ceramic machining factories. Grindabilities are plotted versus hardness (Vickers scale) in Figure 33 for all the ceramics tested. No simple correlation could be found between grindability and hardness. Silicon carbide ceramics tested were much harder than the silicon nitride ceramics tested. But silicon carbide ceramics generally had higher grindabilities than silicon nitride ceramics. This may be

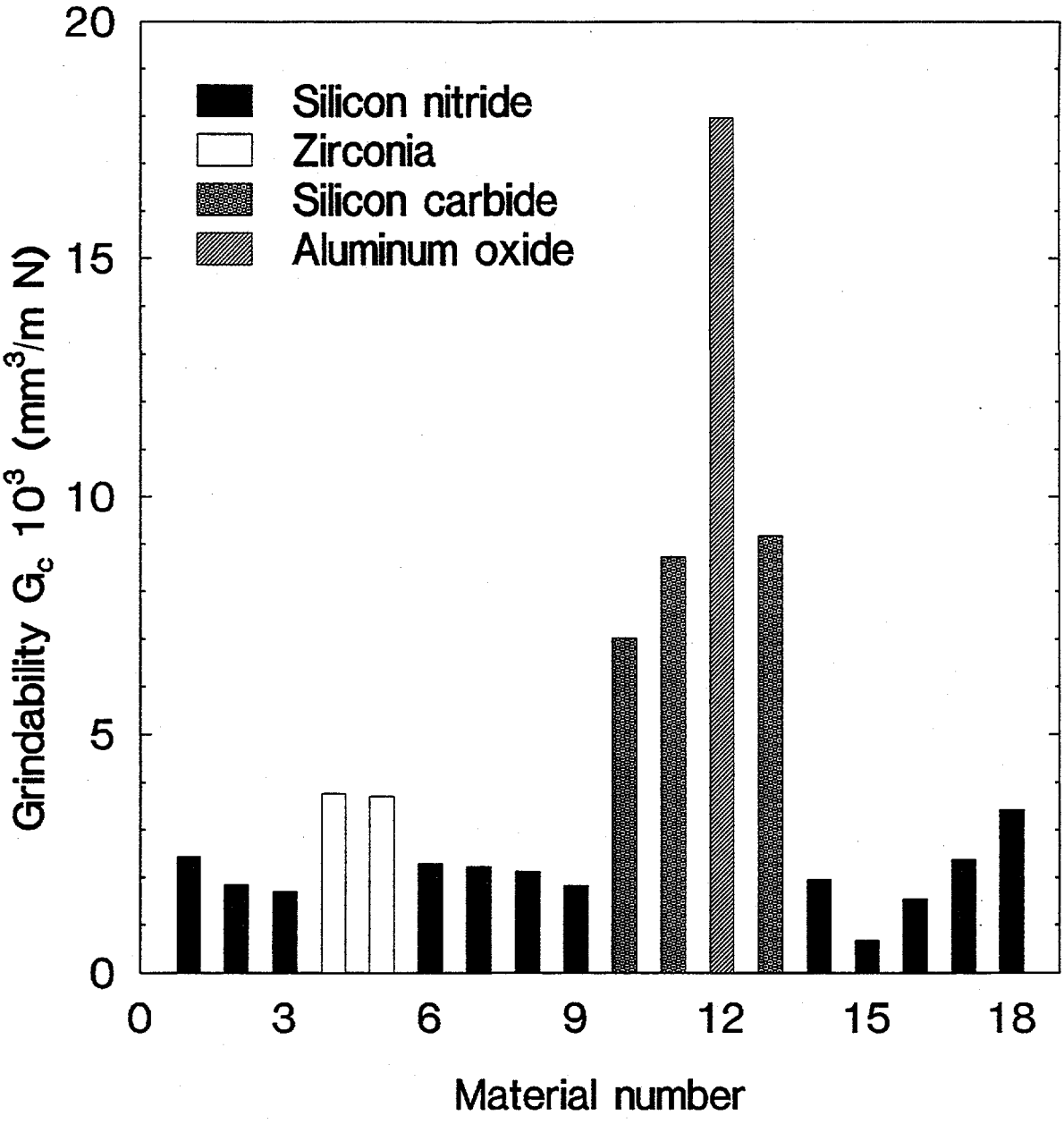

Figure 29. Grindabilities of various ceramics.

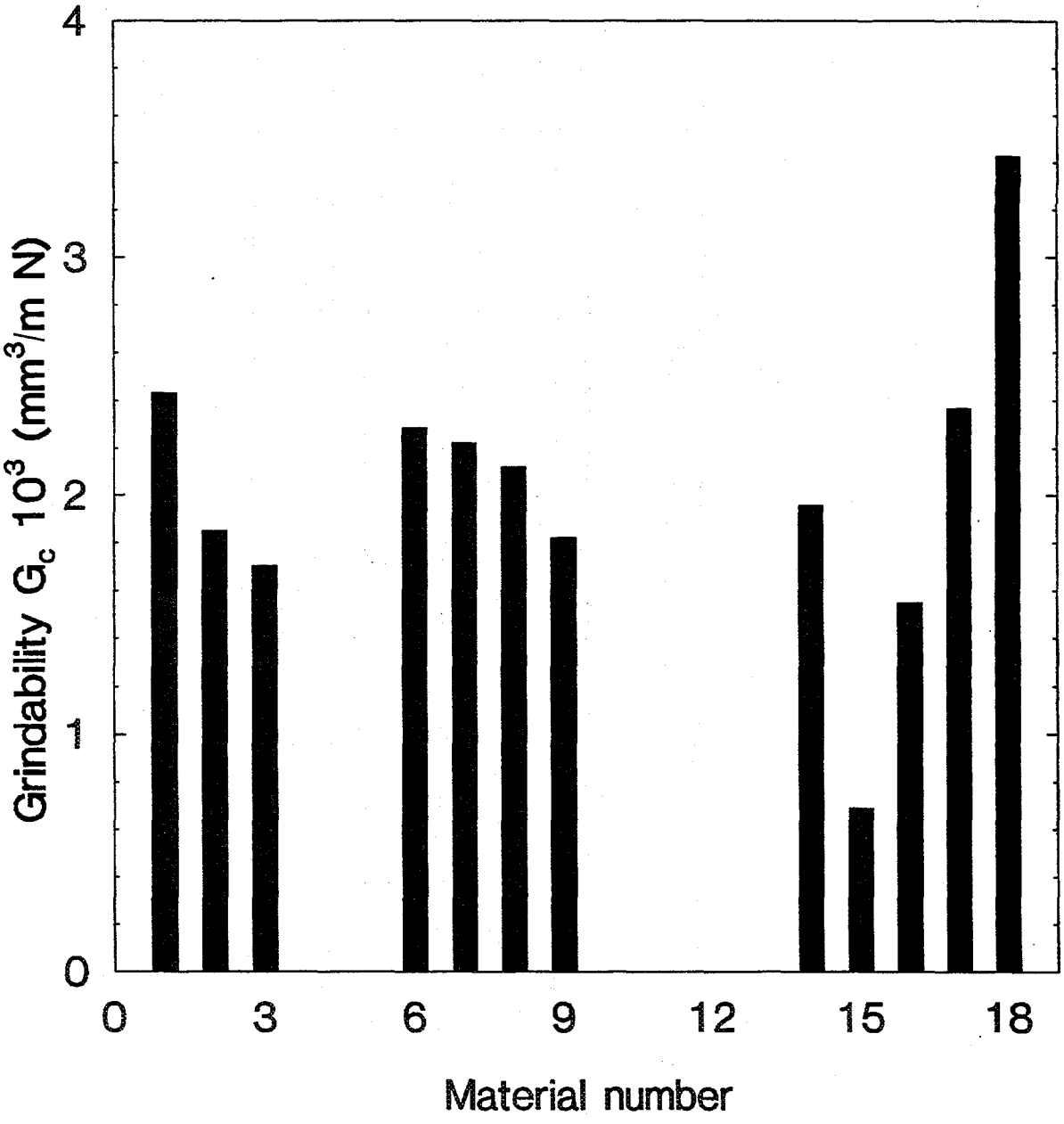

Figure 30. Grindability of silicon nitride ceramics.

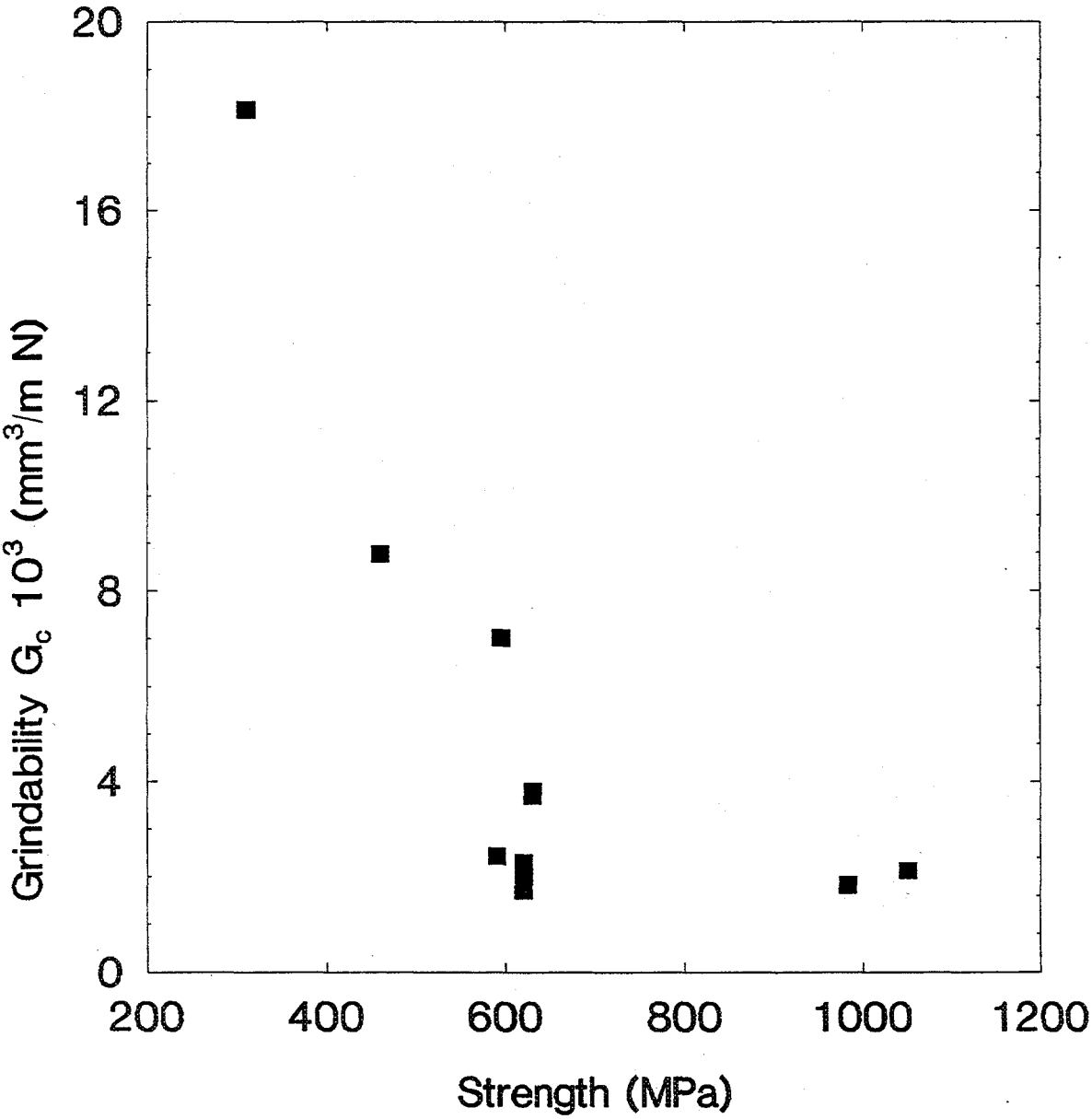

Figure 31. Grindability and flexural strength.

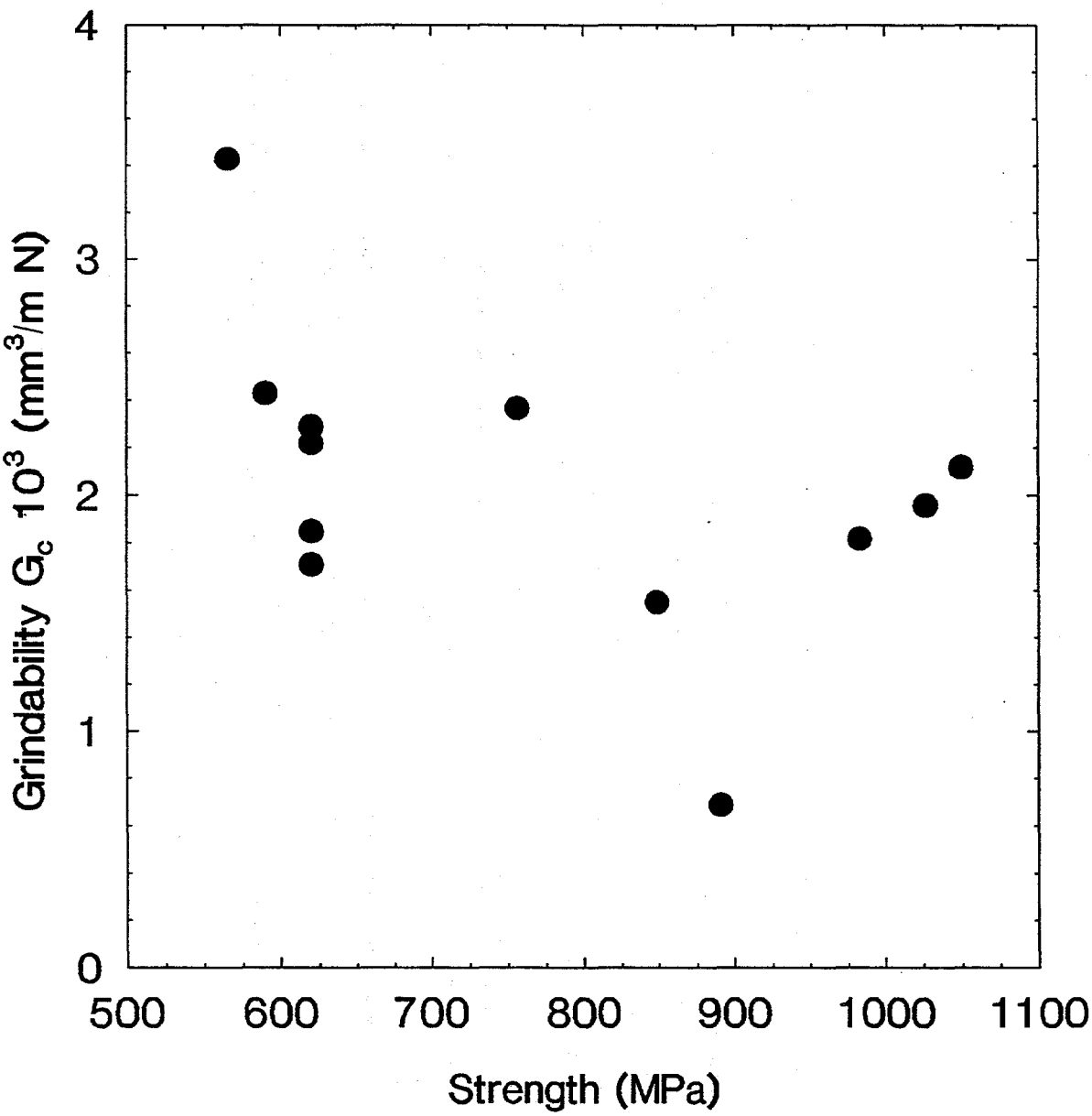

Figure 32. Grindability and strength (silicon nitride).

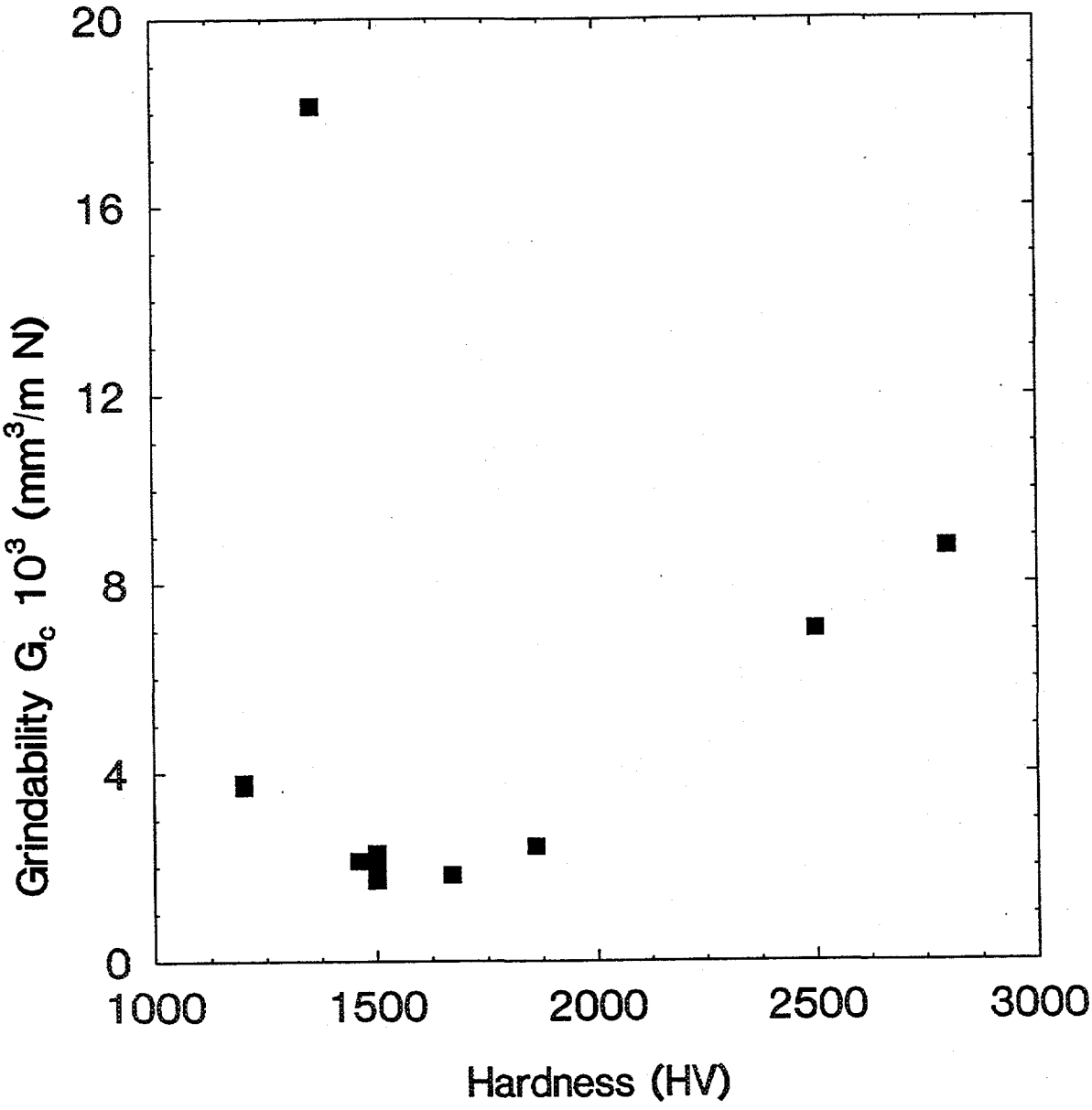

Figure 33. Grindability and hardness.

due to their lower flexural strength and low fracture toughness. The results for silicon nitride are given in Figure 34.

7.3 Correlation between Grindability and Fracture Toughness

Fracture toughness is an important mechanical properties of ceramics which measures the crack-growth resistance of a ceramic. It was expected that grindability would correlate better with fracture toughness. However, there seems no simple correlation between grindability and fracture toughness, as indicated in Figures 35 and 36.

7.4 Grindability and Elasticity, Poisson's Ratio

Elastic modulus is usually used to correlate with specific wear rate in triobological studies of ceramics. Plots are given of grindability versus elasticity (Figure 37) and grindability versus poisson's ratio (Figure 38) for the silicon nitride ceramics tested.

A more interesting plot is given in Figure 39, which shows that ceramics of exactly same mechanical properties have significantly different grindabilities. Similarly, ceramics of very different mechanical properties have very similar grindabilities. More research is needed to understand the main influencing factors of grindability. One possibility is to correlate grindability with microstructure of ceramics.

Based on the grindability tests conducted for various ceramics, there seems no simple correlation between grindability and mechanical properties, such as flexural strength, hardness, elasticity, and fracture toughness. Grindability is a comprehensive parameter which cannot be replaced by any other mechanical properties commonly evaluated. It should be evaluated together with hardness, flexural strength, fracture toughness and other mechanical properties during the material development stage. It should be noted that the mechanical properties of Materials 1 to 13 listed in Table 5 are published by the material manufacturers. It may not represent the test specimen used in the grindability tests. Those parameters should be measured as for Materials 14 through 18.

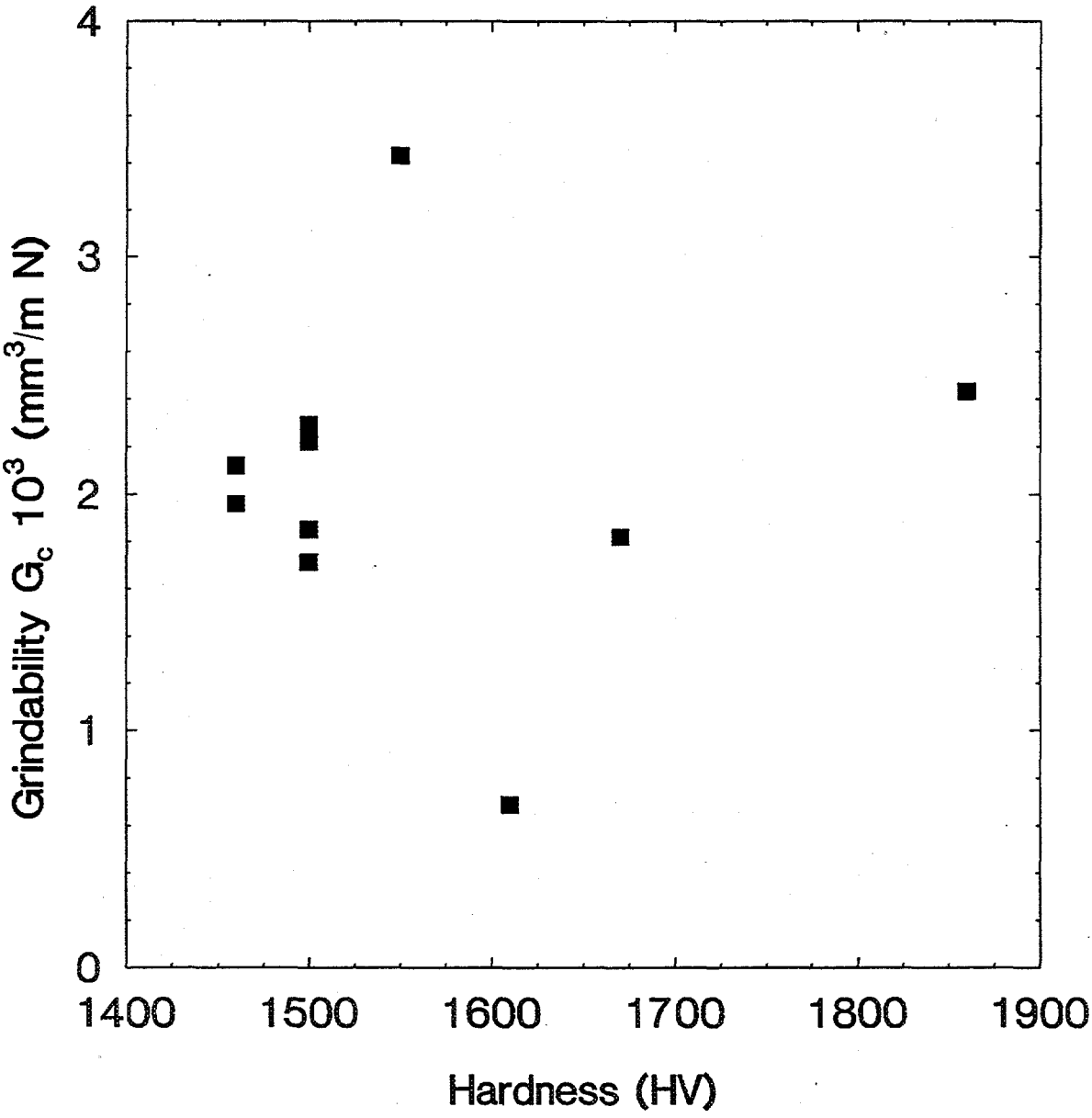

Figure 34. Grindability and hardness (silicon nitride).

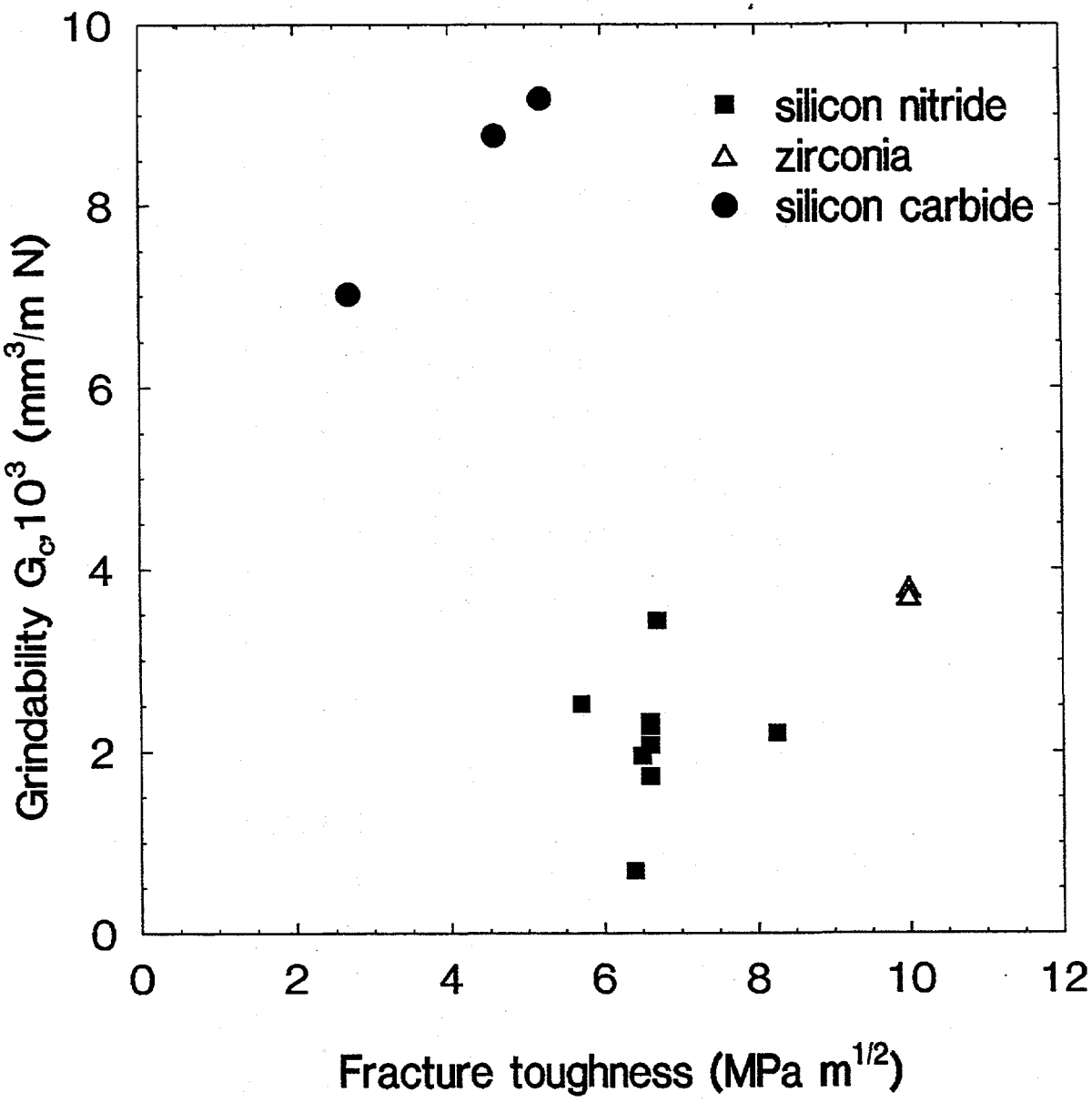

Figure 35. Grindability and fracture toughness.

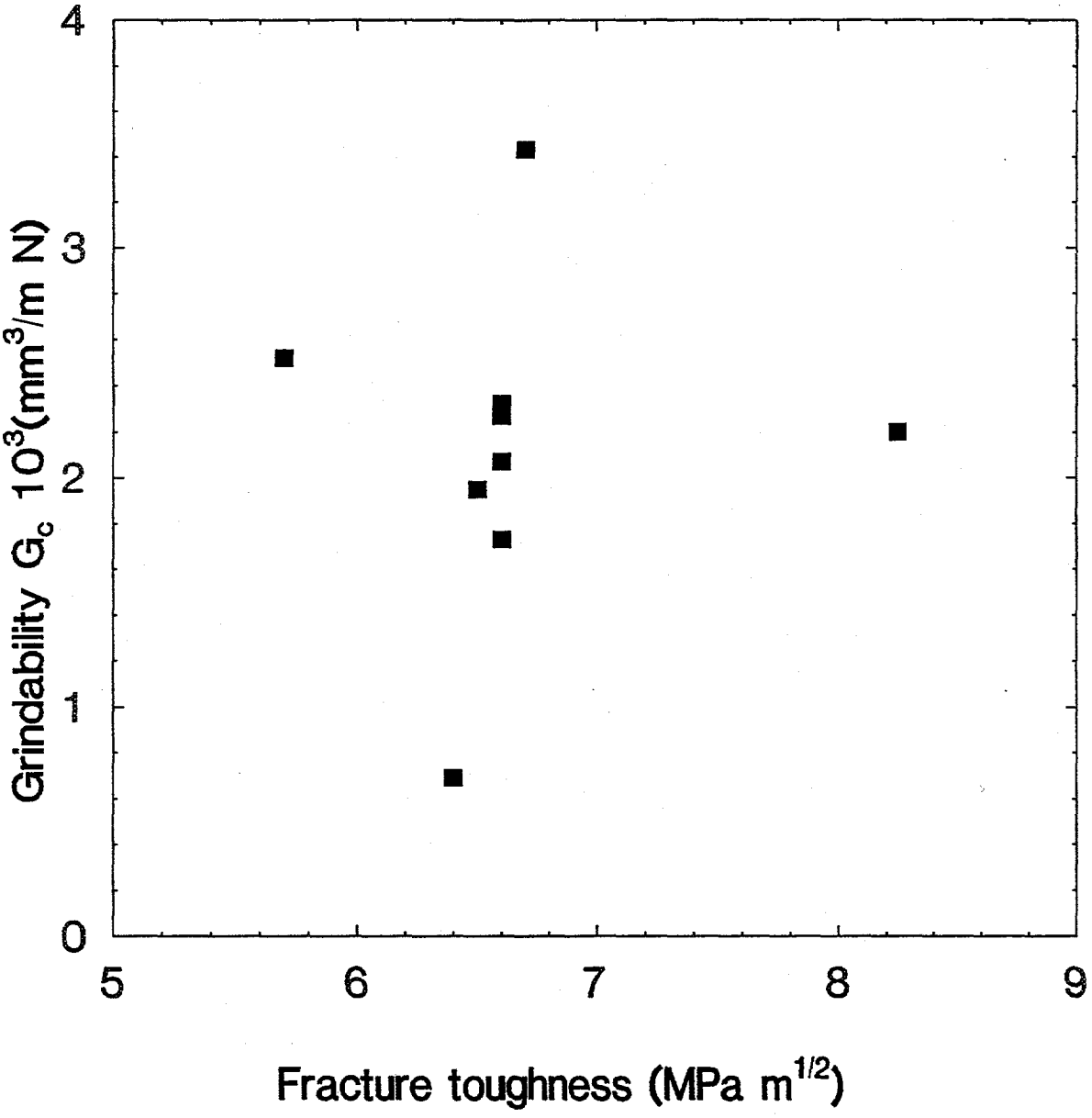

Figure 36. Grindability and fracture toughness (silicon nitride).

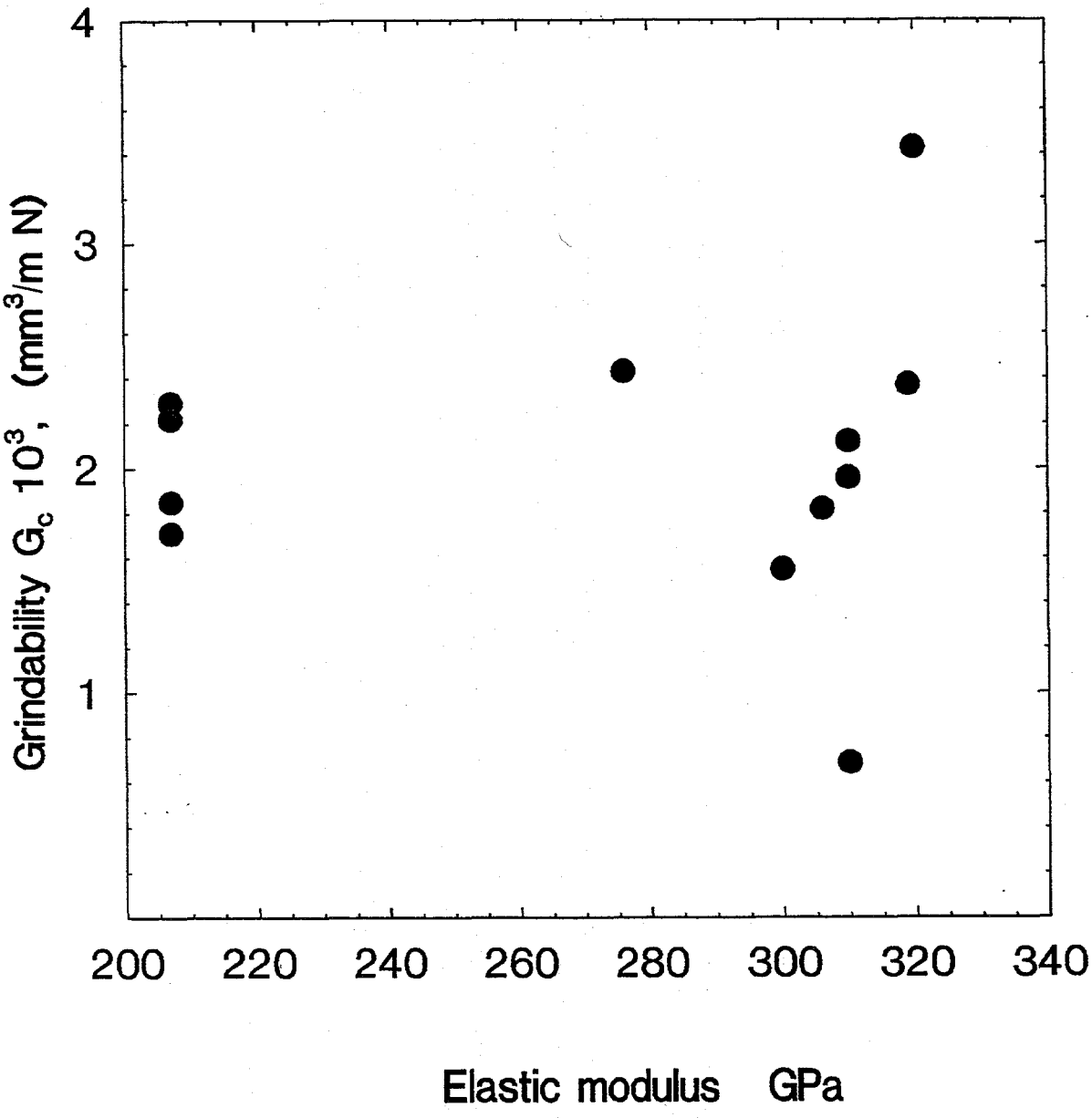

Figure 37. Elastic modulus and grindability.

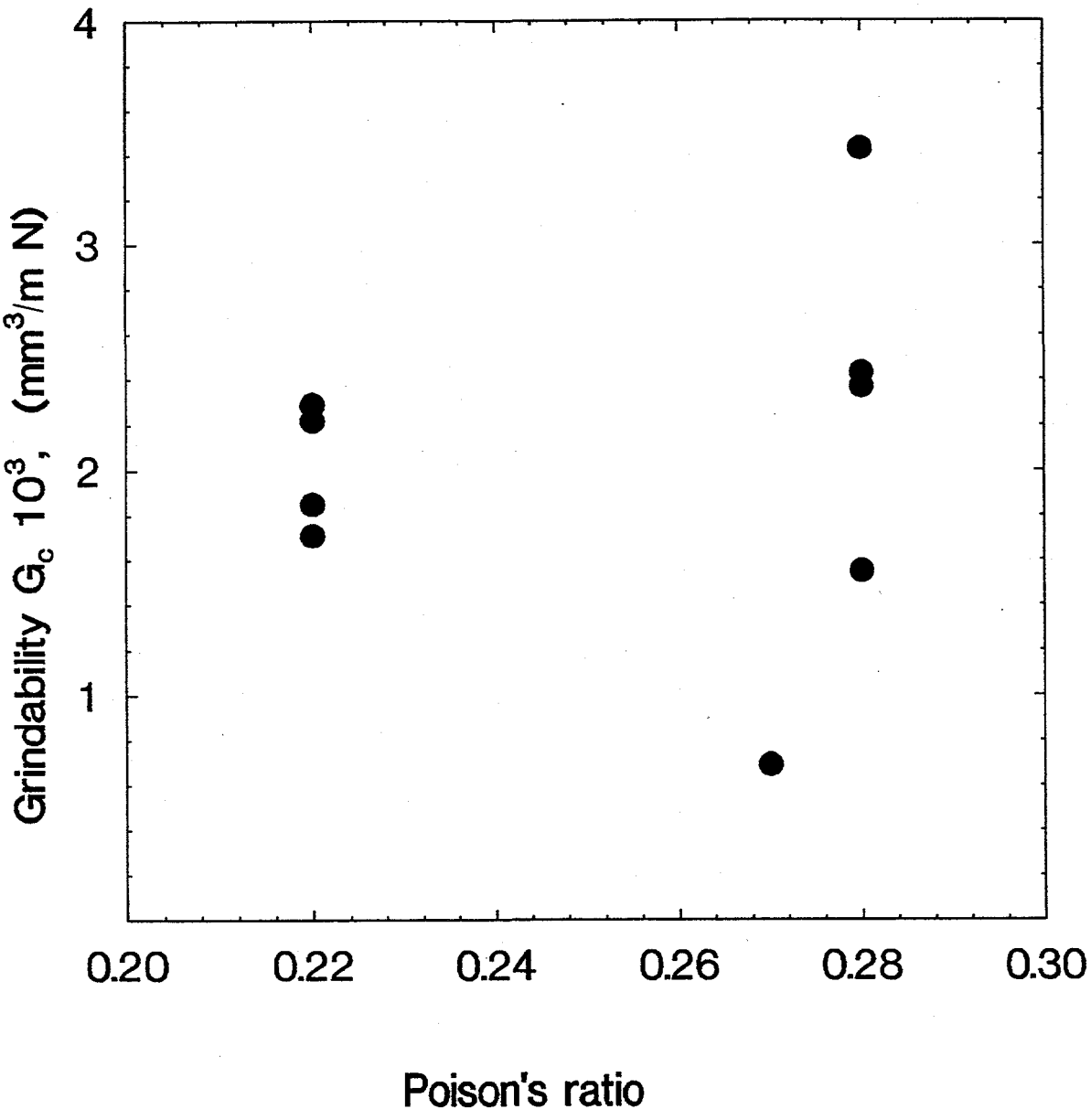

Figure 38. Poison's ratio and grindability.

Table 5. Summary of materials tested

Number	Material	Hardness HV	Strength (MPa)	E GPa	Poisson ratio	Fracture toughness	G_c (10^{-4} mm^3/m N)
1	Si_3N_4 - A	1860	590	276	0.28	5.70	24.3
2	Si_3N_4 - B	1500	620	172-241	0.22	6.60	18.5
3	Si_3N_4 - C	1500	620	172-241	0.22	6.60	17.1
4	ZrO_2 - A	1200	630	207-241	0.31	8-12	37.9
5	ZrO_2 - B	1200	630	207-241	0.31	8-12	37.0
6	Si_3N_4 - D	1500	620	172-241	0.22	6.60	22.9
7	Si_3N_4 - E	1500	620	172-241	0.22	6.60	22.2
8	Si_3N_4 - F	1460	1050	310	-	8.25	21.2
9	Si_3N_4 - G	1670	983	306	-	6.50	18.2
10	SiC - A	2500	595	466	0.21	2.70	70.2
11	SiC - B	2800	460	410	0.14	4.60	87.7
12	Al_2O_3	1360	310	-	-	-	181.3
13	SiC - C	1550	655	455	0.14	5.2	91.8
14	Si_3N_4 - H	1460	1027	310	-	8.25	19.6
15	Si_3N_4 - I	1610	891	310	0.27	6.4	6.9
16	Si_3N_4 - J	1420	849	300	0.28	6.7	15.5
17	Si_3N_4 - K	1540	756	319	0.28	6.9	23.7
18	Si_3N_4 - L	1550	566	320	0.28	6-7.5	34.3

7.5 Grindability and Microstructure

In the previous section, correlation between grindability and mechanical properties (hardness, flexural strength and fracture toughness) were studied. No simple correlation was found between grindability and mechanical properties for the 18 ceramics tested. More ceramic materials need to be tested in order to further support the preliminary conclusion. In order to find out factors determining the ceramic grindability, microstructure of some of the ceramics tested were studied. The as-ground surfaces were observed under a scanning electron microscope. Those surfaces were also observed after they were etched for one hour in a hydrofluoric solution (49% HF).

In Figures 40, SEM micrographs of the as-ground surfaces of Materials 4, 8, 10, 12 are given. It can be seen that the material was removed by both ductile flow (plastic deformation) and brittle fracture. However, the percentage of brittle fracture depends on the material. Materials 10 (silicon carbide) and 12 (aluminum oxide) show much higher brittle fracture than Material 8 (silicon nitride).

In Figure 41, SEM micrographs of the as-ground surfaces of 4 silicon nitride ceramics are given. Once again, it can be seen that the material was removed by both ductile flow and brittle fracture. The percentage of brittle fracture is different for different ceramics. More work is needed in this area.

8 Correlation Study

8.1 Correlation between Grindability and Practical Grinding Practices

Ceramics of higher grindabilities could be ground faster than those of lower grindabilities. However, conventional grinding machine and diamond wheels can only offer very limited material removal rates. The allowable material removal rates are often limited by the available spindle horse power the grinder and chip-storage capability of diamond wheels. Improved diamond wheels and grinding machines of higher spindle horse power are needed to grind at higher removal rates for ceramics of higher grindabilities.

In order to investigate correlation between grindability and practical grinding practices, five ceramics of known grindabilities were ground under practical grinding conditions with a resin bonded diamond wheel on an instrumented surface grinder. Grinding force components and spindle power consumption were measured. The grinding tests were conducted under the following conditions: wheel speed $v_s = 30$ m/s, work speed $v_w = 200$ mm/s, depth of cut $a = 0.0127$ mm, diamond wheel: SD400B100, wheel diameter $d_s = 304$ mm. The results are summarized in Table 6.

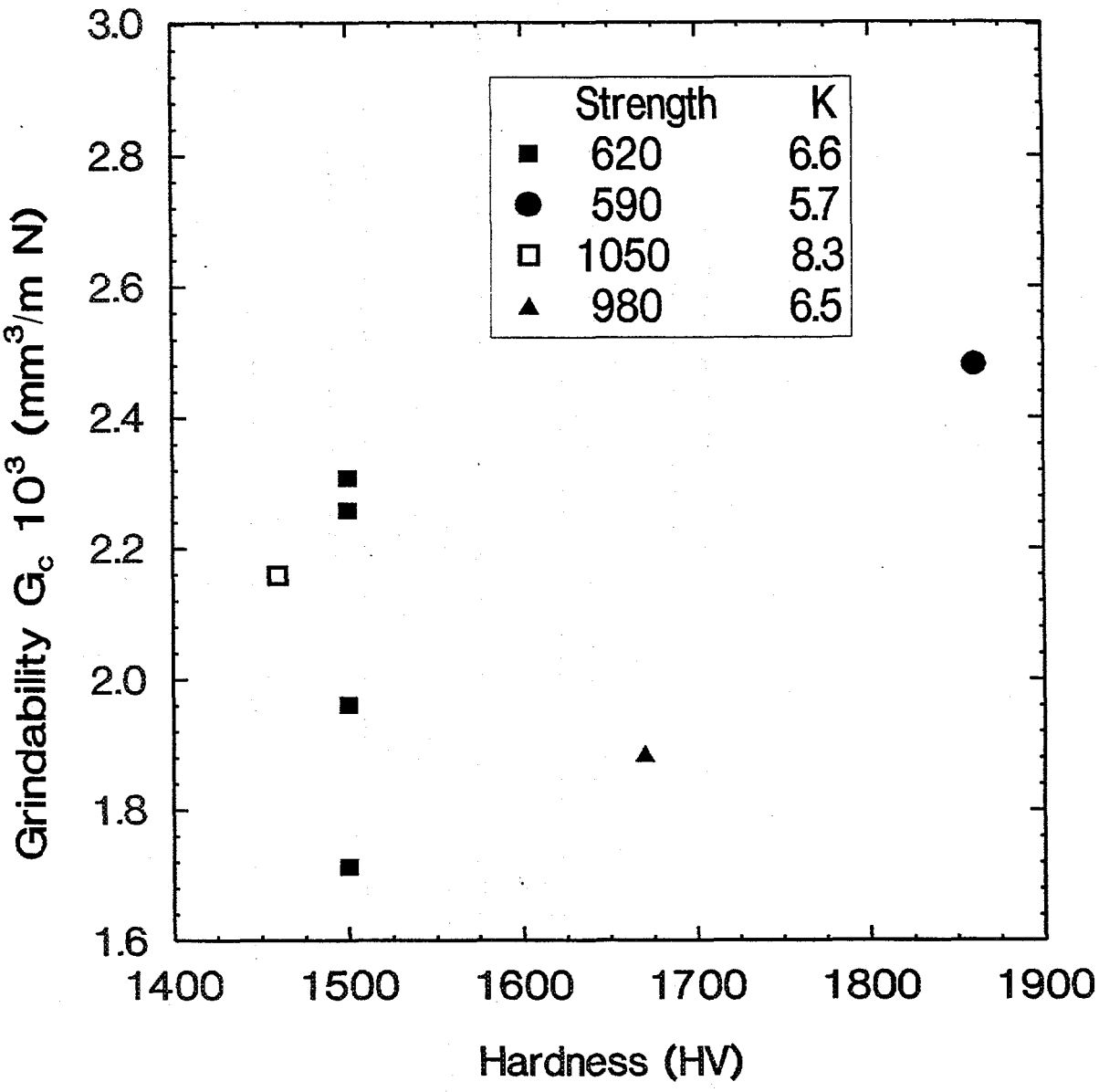

Figure 39. Grindability and material property.

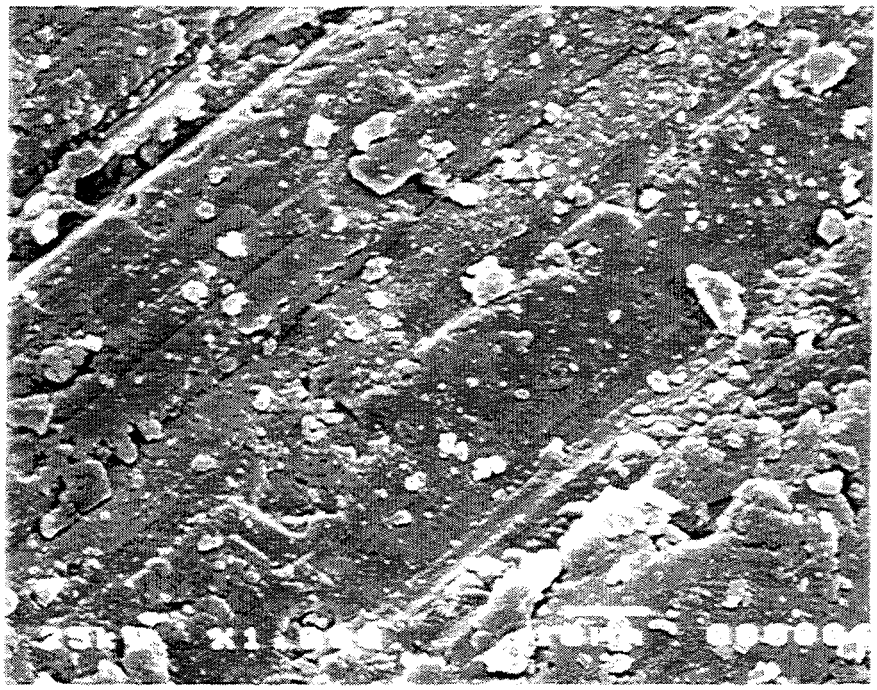

(a) Material 4

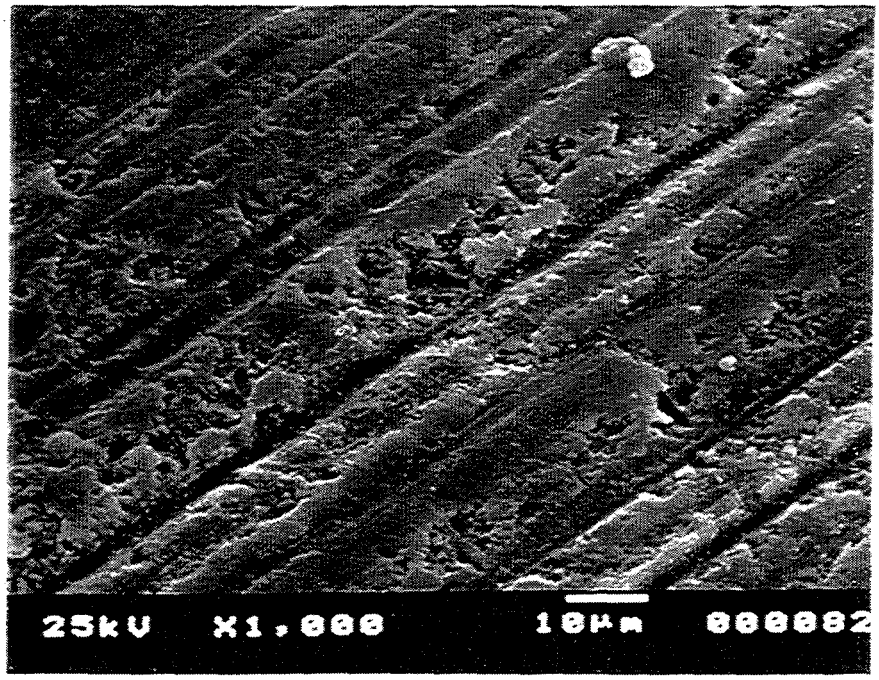

(b) Material 8

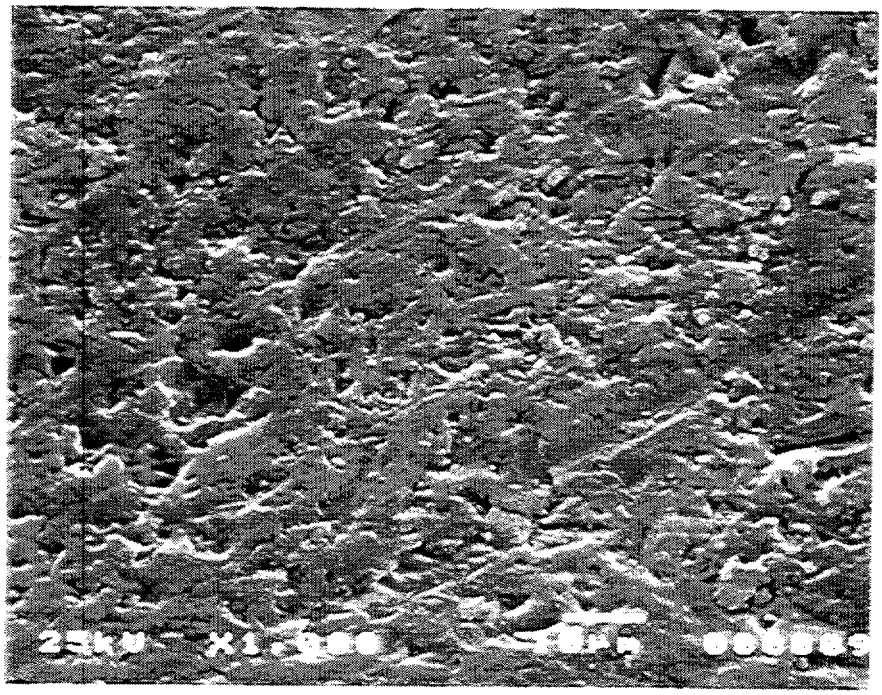

(c) Material 10

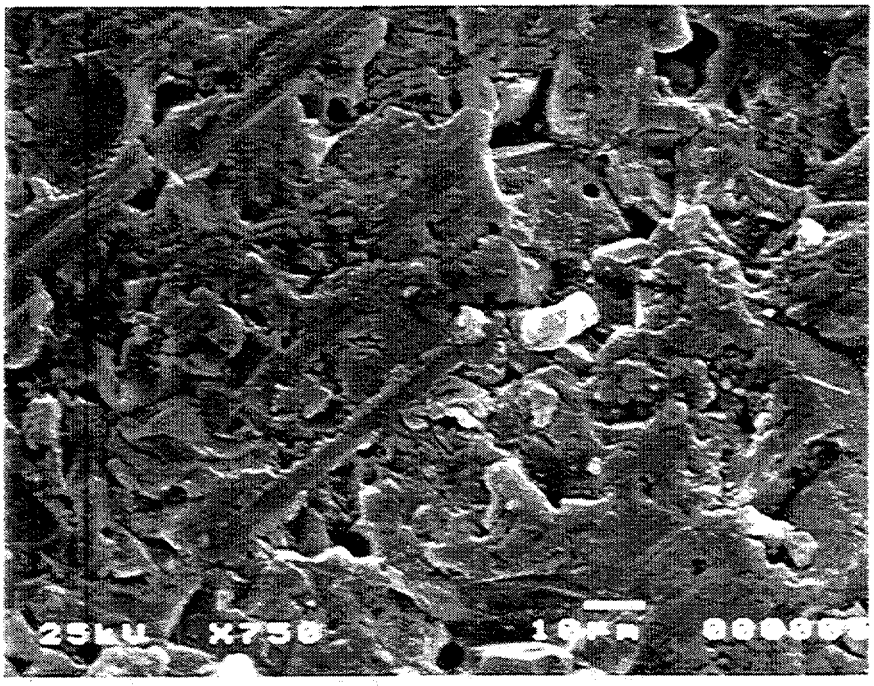

(d) Material 12

Figure 40. SEM micrographs of the as-ground surfaces of some ceramics.

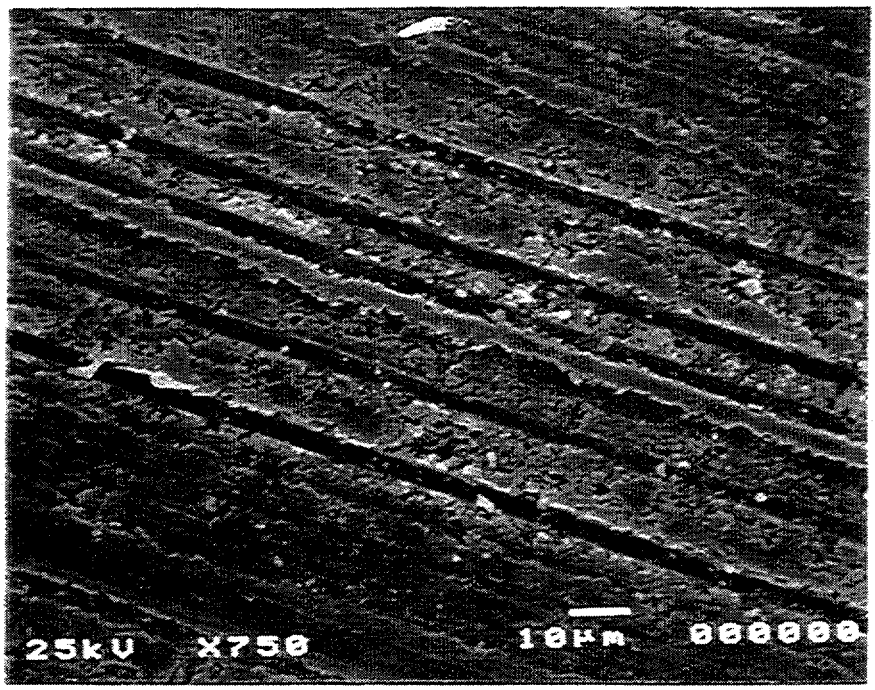

(a) Material 8

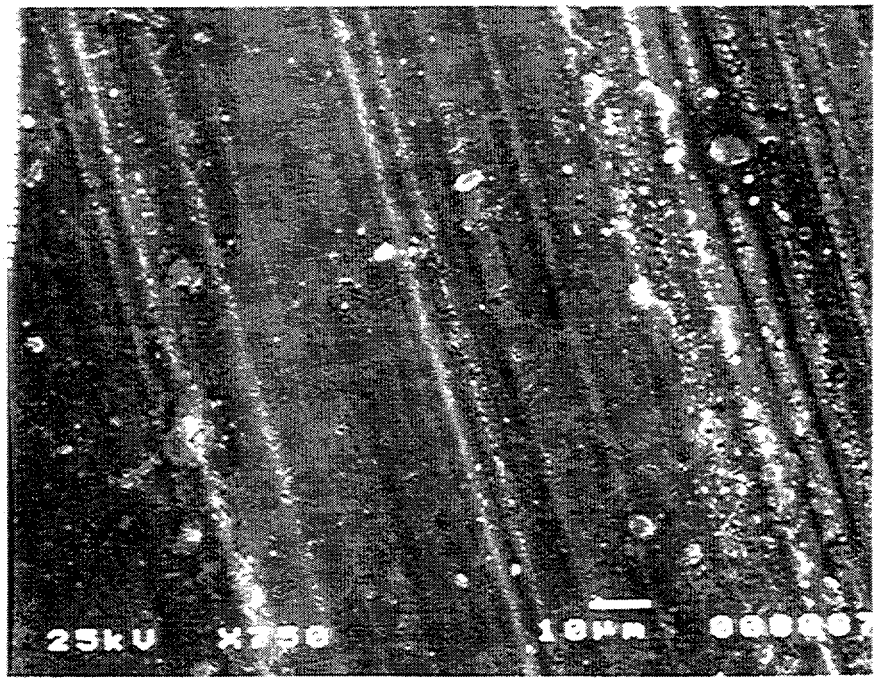

(b) Material 14

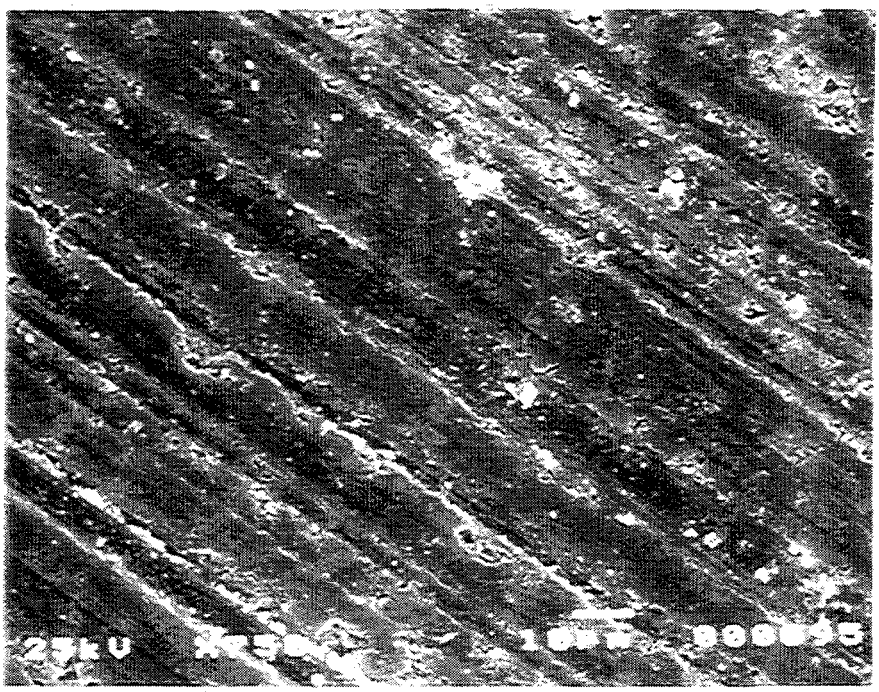

(c) Material 17

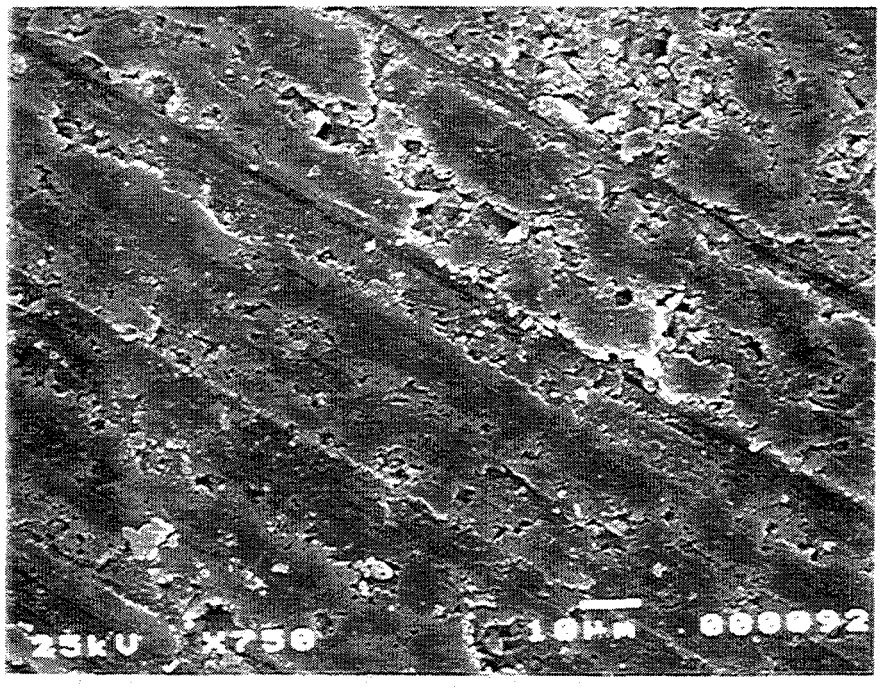

(d) Material 18

Figure 41. SEM micrographs of the as-ground surfaces of some silicon nitride ceramics.

Table 6 Correlation results

Material	Fn (N/mm)	Ft (N/mm)	u (J/mm^3)	$G_c \times 10^4$ ($mm^3/N\ m$)
1	5.2	1.3	15.7	181.3
2	8.2	1.8	20.8	91.8
3	7.6	2.1	24.5	87.7
4	18.8	2.3	34.7	21.2
5	21.2	3.5	44	18.2

Table 7

a (mm)	0.0127	0.0254	0.0508	0.0762
a (in)	0.0005	0.001	0.002	0.003
u_m (J/mm^3)	18.1	24.3	32.8	35.6
Fn_m (N/mm)	10.1	71.2	151.1	191.7
Ft_m (N/mm)	3.8	12.2	26.9	22.0
Note			Loud noise	Loud noise

It can be seen that grindability results do correlate well with practical grinding practices in terms of grinding forces and specific energy under the same removal rate, i.e., higher force and specific energy are needed for grinding ceramics of lower grindabilities. The grindability results suggest that Material 1 can be ground much faster than Material 5. In order to prove this, another set of tests was conducted on Material 1 with higher depths of cut. Results are given in Table 7. The results were also plotted in Figures 42 and 43. It can be seen that the normal grinding forces increase significantly with depth of cut. The specific energy usually decreases with the increase of depth of cut due to the so-called "size effect." However, it increases with depth of cut in this example, which shows that the wheel was severely loaded. The increase in specific energy with depth of cut was caused by the limited chip-storage space of the diamond wheel used. At higher depths of cut, larger chip-storage-spaces are needed to carry material being removed. The chip-storage capability of the diamond wheel limited the allowable material removal rate even though the material

has very high grindability. Under some other circumstances, workpiece may limit the allowable removal rate because excessive force may cause workpiece of certain geometry to break.

Ceramics of higher grindabilities can be ground faster, however, grinding wheel, grinding machine, and job requirements may limit the allowable removal rate to much smaller values.

8.2 Establishing Formulation between Grindability and Grinding Parameters

The purpose of establishing correlations between grindability and practical grinding practices was to select, improve, and optimize grinding parameters based on ceramic grindability. The difficulty lies in the varieties of diamond wheels used in ceramic machining industry.

Experiments conducted for grinding one silicon nitride ceramic with a resin bonded diamond wheel indicated that the normal grinding force correlated well with a scratched-surface parameter as shown in Figures 44. It can be seen that there exist two distinct regions. It was believed that ductile regime grinding was dominant in the firs region and brittle fracture in the second one. For any ceramic, the following relationship exist (Malkin et al, 1995):

$$\frac{F_n}{b} = p_d(c,w)\left(\frac{v_w}{v_s}\right)^{1/2} a^{3/4} d_e^{1/4} + h_d \qquad (12)$$

for the first region and

$$\frac{F_n}{b} = p_b(c,w)\left(\frac{v_w}{v_s}\right)^{1/2} a^{3/4} d_e^{1/4} + h_b \qquad (13)$$

for the second region. Where v_w is the work speed, v_s is the wheel speed, a is the depth of cut, d_e is the equivalent wheel diameter which is calculated as:

$$d_e = \frac{d_s d_w}{d_s \pm d_w} \qquad (14)$$

where d_s is the wheel diameter, d_w is the work diameter, The '+' is for external grinding and '-' is for internal grinding. For surface grinding, $d_e = d_w$. The parameters $p_d(c, w)$ and $p_b(c, w)$ in equations (12) and (13) depend on the diamond wheel used, the ceramic being ground, and fluid applied. Parameter $p_d(c, w)$ represents ductile-dominant grinding and parameter $p_b(c, w)$ represents brittle-fracture-dominant grinding. Equations (12) and (13) can be rewritten as follows:

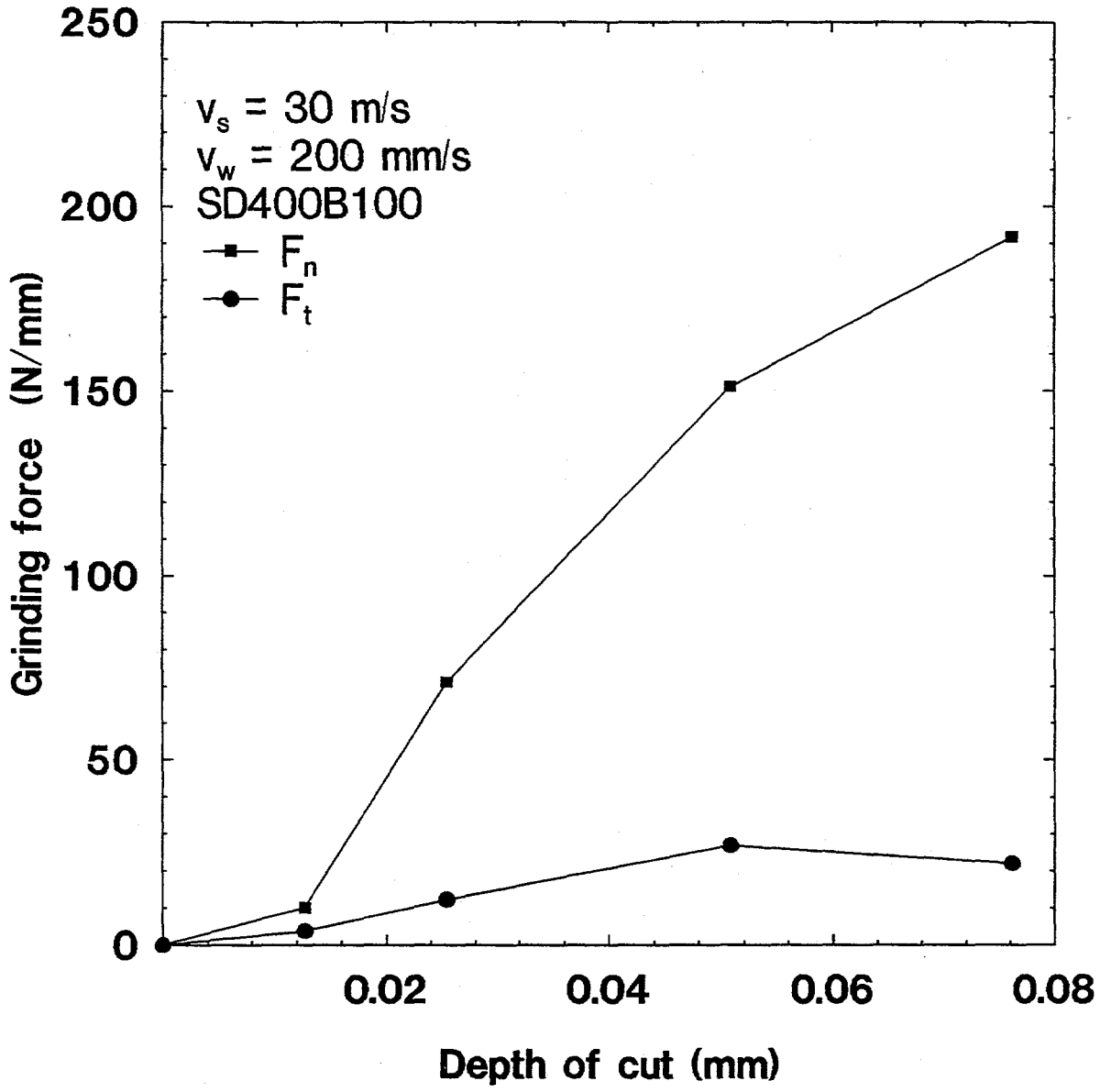

Figure 42. Grinding force versus depth of cut.

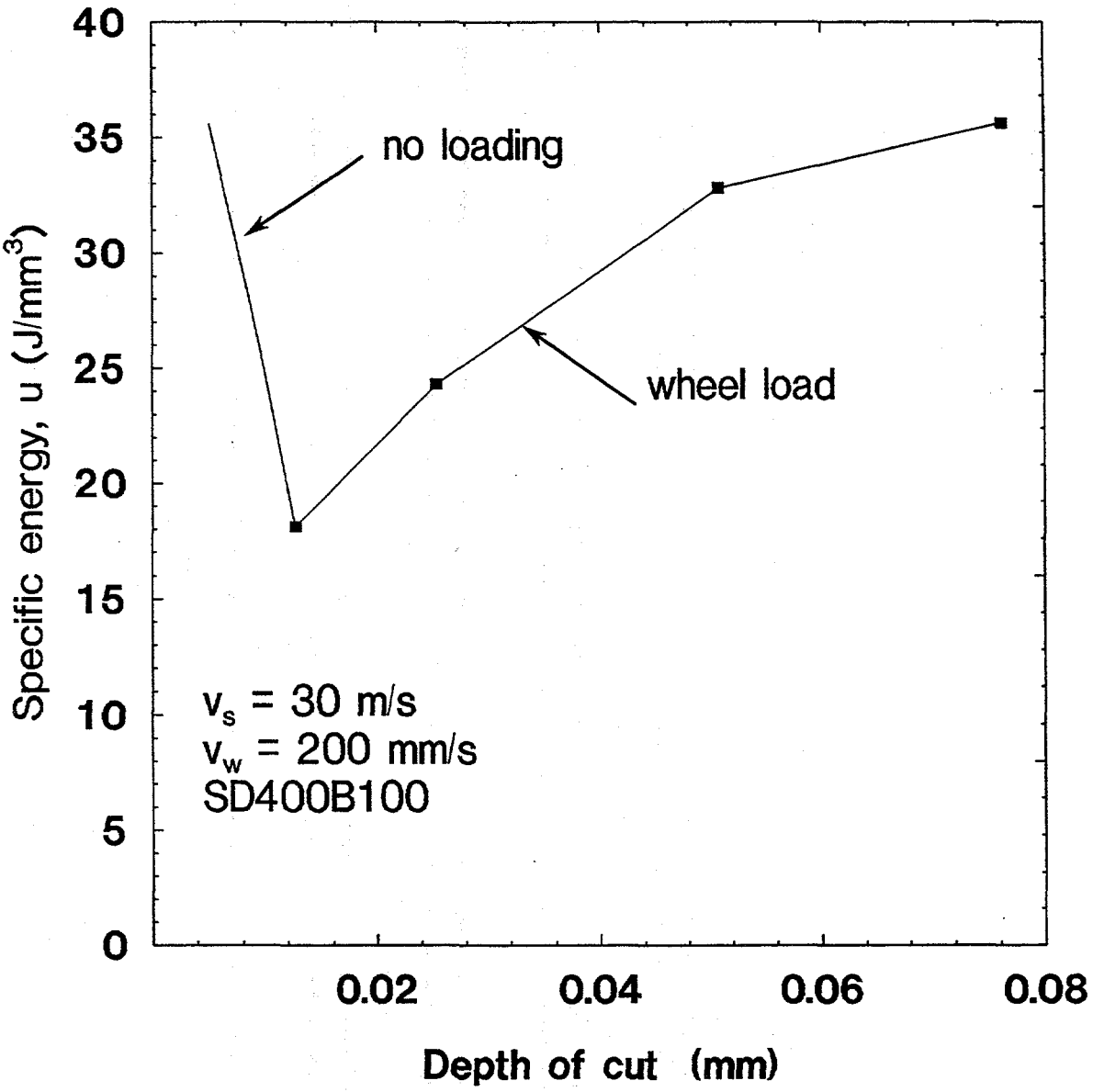

Figure 43. Specific energy versus depth of cut.

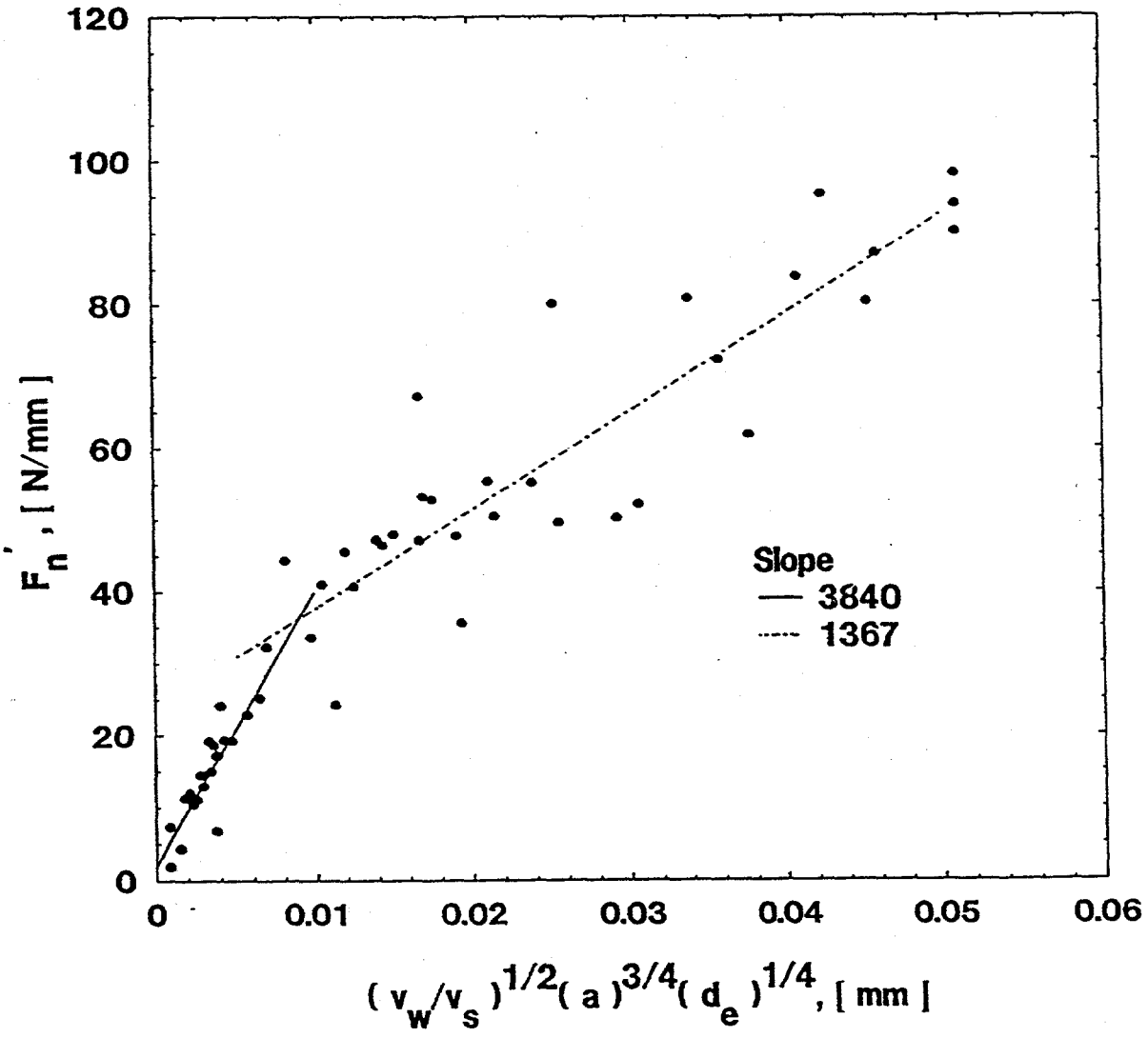

Figure 44. Normal force per unit width versus scratched surface parameter divided by wheel speed

$$p_d(c,w) = \frac{F_n - bh_d}{b(\frac{V_w}{V_s})^{1/2} a^{3/4} d_e^{1/4}} \tag{15}$$

$$p_b(c,w) = \frac{F_n - bh_b}{b(\frac{V_w}{V_s})^{1/2} a^{3/4} d_e^{1/4}} \tag{16}$$

For a specific diamond wheel and fluid application, parameters $p_d(c, w)$ and $p_b(c, w)$ should depend only on material property. Therefore, correlations between grindability G_c and parameters $p_d(c, w)$ and $p_b(c, w)$ exist. Experiments on one silicon nitride with a 400-grit diamond wheel (SD400B100, Coors) lead to the following results:

Table 8 Correlation results

Material	G_c (mm^{-4} mm^3/N m)	$p_d(c,w)$ (N/mm^2)	$p_b(c,w)$ (N/mm^2
1	22.5	3840	1367
2			
3			

With a few ceramics of different grindabilities being tested, the following correlations can be established:

$$p_d(c,w) = \frac{\beta_d}{G_c^{k_d}} \tag{17}$$

$$p_b(c,w) = \frac{\beta_b}{G_c^{k_b}} \tag{18}$$

Constants β_d, k_d, β_b, and k_b can be obtained using data in Table 8. Substituting those coefficients into equations (17) and (18), then into equations (15) and (16), and rearranging leads to:

$$(\frac{V_w}{V_s})^{1/2} a^{3/4} d_e^{1/4} = \frac{F_n - bh_d}{b} \frac{G_c^{k_d}}{\beta_d} \tag{19}$$

for ductile-dominant grinding and

$$(\frac{v_w}{v_s})^{1/2} a^{3/4} d_e^{1/4} = \frac{F_n - bh_b}{b} \frac{G_c^{k_b}}{\beta_b} \qquad (20)$$

for brittle-fracture-dominant grinding. Similar correlations can be established for any diamond wheels.

8.3 Application of the Correlation Formulation

After establishing the correlations between grinding parameters and grindability (equations (19) and (20)) for any diamond wheel, grinding parameters for grinding any ceramic of known grindability with this diamond wheel can be readily obtained from equations (19) and (20). The equivalent diameter d_e can be readily obtained from equation (14). Therefore, equations (19) and (20) can be rewritten as:

$$(\frac{v_w}{v_s})^{1/2} a^{3/4} = \frac{1}{\beta_d d_e^{1/4}} \frac{F_n - bh_d}{b} G_c^{k_d} \qquad (21)$$

for ductile-dominant grinding, and

$$(\frac{v_w}{v_s})^{1/2} a^{3/4} = \frac{1}{\beta_b d_e^{1/4}} \frac{F_n - bh_b}{b} G_c^{k_b} \qquad (22)$$

for brittle-fracture-dominant grinding. For any allowable normal grinding force per unit width of grinding, either equations (21) or (22) can be solved for $(v_w/v_s)^{1/2}a^{3/4}$. The larger value obtained should be used. The allowable grinding force depends on the diamond wheel used (too large force leads to wheel breakage and excessive wheel wear), the grinding machine used (too large force leads to excessive deflection), and the ceramic being ground (too large force may lead to workpiece breakage). The larger the allowable grinding force, the higher the achievable material removal rate will be.

9 Conclusions and Future Work

- A definition for ceramic grindability was developed which was based on the normalized removal rate under controlled force grinding. The defined grindability has the same unit as the specific wear rate.

- A cost-effective method for measuring ceramic grindability was developed based on the definition.

- A ceramic grindability test system (CGTS) was developed. It is a fully automatic test system for eliminating operators' influence. It uses diamond belts instead of diamond wheels for eliminating the influence of wheel dressing. It uses standard MOR bars as test specimen.

- Extensive grindability tests were conducted on 18 ceramic materials. Results indicate that ceramics have very different grindabilities even though their mechanical properties were similar.

- Preliminary correlation studies between grindability and some mechanical properties were conducted, which seemed to indicate that no simple correlations exist. More work is needed in this area.

- Understanding the correlation between grindability and microstructure is important for implementing 'design for grindability' in the development of new ceramics or improvement of existing ones.

- In order to produce ceramics of both the required mechanical properties and good grindability, grindability should be evaluated in addition to other mechanical properties, such as hardness, flexural strength, and fracture toughness.
- Grindability results do correlate with practical grinding practices in terms of grinding forces and specific energy. Ceramics of higher grindability could be ground faster than those of lower grindability. However, available spindle power, chip-storage capability of diamond wheels, and job requirement often limit the allowable material removal rate.

- Formulations correlating grindability and grinding parameters used in practical grinding were developed. Further funding is required to establish comprehensive correlations for various diamond wheels encountered in ceramic machining industry.

10 Acknowledgement

This research project was sponsored by the U.S. Department of Energy, Assistant Secretary for Conservation and Renewable Energy, Office of Transportation Technologies as part of the Ceramic Technology Project of the Materials Development Program under contract DE-AC05-84OR21400 with Lockheed Martin Energy Systems, Inc.

11 Publications

The following are lists of publications completed under this contract.

1. Guo, C., Chand, R.H., and Krishnan, N., "Cost-Effective Method for Determining Grindability of Ceramics," Proceedings for the 1994 Annual Automobile Technology Development Contractor's Coordination Meeting (ATD-CCM), October, 1994.

2. Guo, C., "Grinding of Ceramics," Presented at the *Advancements in the Application of Ceramics in Manufacturing*, SME, November, 1994, Golden, Colorado.

3. Guo, C. and Chand, R.H., 1995, "Grindability of Ceramics," *Proceeding of the 1st International Machining and Grinding Conference*, SME, MR95-168, Dearborn, MI, pp.123-136.

4. Guo, C. and Chand, R.H., 1995, "Characterization of Ceramics from the Machining View Point," *Proceedings of the International Symposium on Advanced Ceramics for Structural and Triobological Applications,* Vancouver, British Columbia, Canada, pp.413-424.

5. Guo, C. and Chand, R.H., 1996, "Precision Machining of Technical Ceramics," *Ceramic Technology International,* pp.49-52.

6. Guo, C. and Chand, R.H., "Grindability of Silicon Nitride Ceramics," *Proceedings of the International Symposium on Manufacturing Practices and Technologies,* New Orleans, 1995, to appear.

7. Guo, C. and Chand, R.H., "Grindability and Mechanical Property," *Proceedings of the International Symposium on Advanced Synthesis and Processing*, Cocoa Beach, 1996, to appear.

12 References

1. Guo, C. and Chand, R.H., 1995a, "Grindability of Ceramics," *Proceeding of the 1st International Machining and Grinding Conference*, SME, MR95-168, Dearborn, MI, pp.123-136.

2. Guo, C. and Chand, R.H., 1995b, "Characterization of Ceramic Materials from the Machining Point of View," *CIM International Symposium on Advanced Ceramics for Structural and Triobological Applications,* August 21-23, Vancouver, Canada.

3. Guo, C., Chand, R.H., and Krishnan, N., 1994, "Cost-Effective Method for Determining the Grindability of Ceramics,' *Proceedings of the Department of Energy Annual Automotive Technology Development Contractors' Coordination Meeting,* Dearborn, Michigan.

4. Hu, K.X. and Chandra, A., 1993,"A Fracture Mechanics Approach to Modeling Strength Degradation in Ceramic Grinding Processes," *ASME Journal of Engineering for Industry*, Vol.115, pp.73-84.

5. Kovach, J., et al, 1993, "Feasibility Investigation of High Speed, Low Damage Grinding for Advanced Ceramics," *Proceedings of the 5th International Grinding Conference*.

6. Kondo, Y., Tsukuda, A., Takada, A., and Okada, S., 1994, "Grinding Forces and Elastic Recovery in Ceramic Materials," *Journal of American Ceramic Society*,

Vol.77, pp.1654-1654.

7. Liao, T.W., Sathyanarayanan, G. and Buehler, W.L, 1990, "The Selection of Optimal Parameters for Minimum Damage in Creep Feed Grinding of Alumina," *SME Technical Paper,* MR90-540.

8. Malkin, S., Sunderland, J.E., Guo, C., Zhu, B., and Hwaung, T., "High Speed and Low Damage Grinding of Ceramics," Progress Report #8.

9. Moriwaki, T., Iwata, K., and Okuda, K., 1989,"Basic Study on Machinability of Zirconia Ceramics in Precision Diamond Cutting," ASME Winter Meeting, Production Engineering Division, pp.151-157.

10. Tonshoff, H.K., Seiner, H. and Wobker, G., 1989, "Residual Stress Measurements of Ceramic Materials after Grinding," ASME Winter Meeting, Production Engineering Division, pp.73-79.

11. Ota, M. and Miyahara, K., 1993, "A Study on Grinding Technology of Silicon Nitride for Application to Automobile Engine Parts," *Proceedings of the 5th International Grinding Conference*, SME.

12. Subramanian, K, 1985,"Parametric Study on Grindability of Structural and Electronic Ceramics - Part 1," *The Production Engineering Division, American Society of Mechanical Engineers*.

13. Zhu, B., Guo, C., Sunderland, J.E. and Malkin, S., 1995, "Energy Partition to the Workpiece for Grinding of Ceramics," *Annals of the CIRP*, Vol.44/1:267-271.

INTERNAL DISTRIBUTION

1. L. A. Abbatiello
2-11. P. J. Blau
12. R. A. Bradley
13. K. Breder
14. D. F. Craig
15. M. K. Ferber
16. C. L. Fitzpatrick
17-26. D. R. Johnson
27. F. W. Jones
28. W. K. Kahl
29. M. A. Karnitz
30. R. L. Martin
31. S. B. McSpadden
32. T. O. Morris
33. R. Ott
34. A. E. Pasto
35. L. Riester
36. A. C. Schaffhauser
37. D. P. Stinton
38. S. G. Winslow
39. J. M. Wyrick
40. E. S. Zanoria
41. R. E. Ziegler
42. Central Research Library
43. Document Reference Section
44-46. Laboratory Records
47. Laboratory Records-RC
48. ORNL Patent Section

EXTERNAL DISTRIBUTION

49. Marc Abouaf, Saint Gobain/Norton Industrial Ceramics, Goddard Road, Northboro, MA 01532-1545
50. Meryl D. W. Adler, Corning RD&E Div., SP PR 01 C21 PRC, Corning, NY 14831
51. Kenneth A. Anderson, Jr., WR Grace/Diamonite, 453 W. McConkey Street, Shreve, OH 44676
52. Patrick R. Annese, BMS, 334 Washington Street, Somerville, MA 02143
53. Bob Baker, Ceradyne, Inc., 3169 Redhill Avenue, Costa Mesa, CA 92626
54. Peter C. Balson, Diacraft Inc., 9033 General Drive, Plymouth, MI 48170
55. Richard Bandister, VERTEX Diamond Tool Company, 940 Cienega Ave., San Dimas, CA 91773
56. B. P. Bandyopadhyay, U. of North Dakota, Box 8359, Univ. Sta., Grand Forks, ND 58202-8359
57. Joe Basko, AlliedSignal, Inc., 401 N. Bendix Drive, P. O. Box 4001, South Bend, IN 46634
58. Giles Becket, Cincinnati Milacron, Products Division, 4701 Marburg Avenue, Cincinnati, OH 45209
59. Deepak Bhat, Valenite, Inc., 1711 Thunderbird Street, Troy, MI 48084
60. Chander P. Bhateja, Contemporary Technologies, P. O. Box 5533, Oak Ridge, TN 37830-5533
61. James R. Blackmore, AlliedSignal Ceramic Components, P. O. Box 2960, Torrance, CA 90509-2960
62. Ernst Borchert, S. E. Huffman Corporation, 1050 Huffman Way, Clover, SC 29710
63. Joseph F. Braza, Torrington/Advanced Technology, 59 Field Street, Torrington, CT 06790
64. Richard A. Brigham, Ferro Corporation, Diamonite Plant, 453 West McConkey Street, Shreve, OH 44676
65. John R. Bush, Abrasive Technology, Inc., 8400 Green Meadows Dr., Westerville, OH 43081
66. Bernard J. Busovne, AlliedSignal Inc., 2525 W. 190th Street, Torrance, CA 90509-2960
67. Alan C. Carius, GE Superabrasives, 6325 Huntley Road, Worthington,, OH 43085

68. Ronald H. Chand, Chand Kare Technical Ceramics, 2 Coppage Drive, Worcester, MA 01603-1252
69. J. Mark Chenoweth, Coors Technical Ceramics, 1100 Commerce Park Drive, Oak Ridge, TN 37830
70. William J. Chmura, Torrington Company, 59 Field Street, Torrington, CT 06790
71. Tom Collins, Nissan Motor Manufacturing Corp. U.S.A., 983 Nissan Drive, Smyrna, TN 37167
72. Keith P. Costello, Chand Kare Technical Ceramics, 2 Coppage Drive, Worcester, MA 01603-1262
73. Tom L. Davidson, Diacraft, P.O. Box 1135, Dickson, TN 37055
74. Frank G. Davis, Allied-Signal Aerospace Company, 7550 Lucerne Drive, #203, Middleburg Heights, OH 44130
75. Barry S. Draskovich, AlliedSignal Ceramic Components, 2525 West 190th Street, TOR 1/S-1-2700, Torrance, CA 90504
76. Ernest J. Duwell, 212 Elm Street, Hudson, WI 54016
77. Chuck J. Dziedzic, Nucermet, P. O. Box 667, Hendersonville, NC 28793
78. David Edwards, Cincinnati Milacron, P.O. Box 9013, Cincinnati, OH 45209
79. Tommy Ellenburg, Greenville, Weavexx, 3384 Blue Springs Parkway, Greeneville, TN 37743
80. William A. Ellingson, Argonne National Laboratory, 6700 S. Cass Avenue, ET Division, Bldg. 212, Argonne, IL 60439
81. David T. Ellis, Machined Ceramics, 629 N. Graham Street, Bowling Green, KY 42101
82. Bill English, GE Superabrasives, 6325 Huntley Road, P. O. Box 568, Worthington, OH 43085
83. Christopher J. Evans, NIST, Bldg. 220, Room A117, Precision Engineering Division, Gaithersburg, MD 20899
84. John R. Evans, Ferro Corporation/Diamonite Plant, Specialty Ceramics Division, 453 West McConkey Street, Shreve, OH 44676
85. Robert W. Evans, Jr., Abrasive Technology, 7062 Landsdonne Street, Worthington, OH 43085
86. Ron Felix, United Technologies Pratt & Whitney, 400 Main Street, MS:114-38, East Hartford, CT 06108
87. Michael E. Finn, I A M S, 111 Edison Drive, Cincinnati, OH 45069
88. Paul M. Fleischer, Mattison Machine Works, 545 Blackhawk Park Ave., Rockford, IL 61104-5135
89. James D. Flinchbaugh, Weldon Machine Tool, Inc., 1800 W. King Street, York, PA 17404
90. Robert Frech, Eonic, Inc., 464 E. Hollywood, Detroit, MI 48203-2099
91. David Fried, Xerox, 800 Phillips Road, Bldg. 6 208-06E, Webster, NY 14580
92. Roger Gary, Cincinnati Milacron, P. O. Box 9013, Cincinnati, OH 45209
93. J. Randall Gilmore, ExtrudeHone, 8075 Pennsylvania Avenue, Irwin, PA 15642
94. Leigh C. Girard, Gallmeyer & Livingston, 336 Straight Avenue S.W., Grand Rapids, MI 49504
95. Ed Gizonski, Eonic, Inc., 464 E. Hollywood, Detroit, MI 48203-2099
96. Brian H. Gold, STC Corp., P.O. Box 1028, St. Albans, VT 05478
97. Allan E. Goldman, U.S. Graphite, Inc., 907 West Outer Drive, Oak Ridge, TN 37830
98. Frank Gorman, Astro-Met Inc., 9974 Springfield Pike, Cincinnati, OH 45215
99. Bill Grant, Cummins Engine Co., 1900 McKinley Avenue (50183), Columbus, IN 47202-3005
100. Lance Groseclose, Allison Engine Company, P. O. Box 420, MS W-05, Indianapolis, IN 46206
101-110. Changsheng Guo, Chand Kare Technical Ceramics, 2 Coppage Drive, Worcester, MA 01603
111. H. Gupta, U. of CT-Grind Res Ct, 191 Auditorium Road, Storrs, CT 06269-3237
112. Robert A. Haines, INSACO, Inc., P.O. Box 9006, Quakertown, PA 18951-9006
113. Nabil S. Hakim, Detroit Diesel Corporation, 13400 Outer Drive West, Detroit, MI 48239-4001
114. Keith Hale, Deco-Group, Inc., 4850 Coolidge Hwy., Royal Oak, MI 48073-1023
115. Sim Hall, Process Forming Systems, 4545 McIntyre St., Golden, CO 80403
116. Marcel R. Hanard II., Caterpillar Technical Center., P.O. Box 1875, Peoria, IL 61656-1875
117. Tom Hannon, Moore Tool Company, 800 Union Avenue, Bridgeport, CT 06607-0088
118. Mark D. Hargis, Advanced Technology Projects, Williams International, 2280 West Maple Road, P. O. Box 200, Walled Lake, MI 48390-0200

119. Doug Harmon, Litton/Landis, 20 E. Sixth Street, Waynesboro, PA 17268-2050
120. Alan M. Hart, Dow Chemical Company, 1776 Building, Midland, MI 48674
121. Michael H. Haselkorn, Caterpillar Technical Center, Bldg. E, P.O. Box 1875, Peoria, IL 61656-1875
122. Debbie Haught, Department of Energy, 1000 Independence Avenue, S.W., Code EE-32, Washington, DC 20585
123. Norman L. Hecht, Univ. of Dayton Research Institute, 300 College Park, KL 165, Dayton, OH 45469-0172
124. Dave Herrala, Boride Products, Inc., 2879 Aero Park Drive, Traverse City, MI 49684
125. Patricia Hoffman, U.S. Department of Energy, EE-23 Forrestal Building, 1000 Independence Avenue, Washington, DC 20585
126. Gary A. Hollridge, EONIC, Inc., 464 E. Hollywood, Detroit, MI 48203-2099
127. Stephen M. Hsu, DOC/NIST, Bldg. 223, Room A256, Route 270 & Quince Orchard Road, Gaithersburg, MD 20899
128. Gary Huzinec, Cincinnati Milacron, P. O. Box 9013, Cincinnati, OH 45209
129. Lewis K. Ives, NIST, Quince Orchard & Clopper Road, Building 223, Room A256, Gaithersburg, MD 20899
130. Said Jahanmir, NIST, Bldg. 220, Rm. A-215, Gaithersburg, MD 20899
131. Jinmyun Jo, CTC, 1450 Scalp Ave., Johnstown, PA 15904
132. Yury Kalish, Detroit Diesel Corporation, 13400 Outer Drive, West, Detroit, MI 48239-4001
133. Ray Keefe, Eaton Corporation, Manufacturing Technologies Center, 32500 Chardon Road, Willoughby Hills, OH 44094
134. Richard Kegg, Cincinnati Milacron, P. O. Box 9013, Cincinnati, OH 45209
135. Ralph Kelly, Cincinnati Milacron, P.O. Box 9013, Cincinnati, OH 45209
136. Kristi Keyser, Machined Ceramics, Inc., 629 North Graham Street, Bowling Green, KY 42101
137. Michael P. King, Carborundum Company, P.O. Box 337, Niagara Falls, NY 14302
138. Robert N. Kopp, Norton Company, 105 Greystone Drive, Franklin, TN 37069-4301
139. Joseph Kovach, Eaton Corporation, 32500 Chardon Road, Willoughby Hills, OH 44094
140. Edwin Kraft, Kyocera Industrial Ceramics, 5713 E. Fourth Plain Blvd., Vancouver, WA 98661
141. Kishor M. Kulkarni, AMP, 12227 Crestwood Dr., Carmel, IN 46033-4322
142. K. V. Kumar, GE Superabrasives, 6325 Huntley Road, Worthington, OH 43085
143. Peter Kuo, Norton Company, 1 New Bond Street, Worcester, MA 01615
144. Vencel Lasic, Eaton Corporation, Engine Components Division, 824 Industrial Road, Marshall, MI 49068
145. Mike Laurich, Eaton Corporation, 32500 Chardon Road, Willoughby Hills, OH 44094
146. Robert H. Licht, Norton Company, Northboro R&D Center, Goddard Road, Northboro, MA 01532-1545
147. Mel Liebers, Professional Instrumenta Company, 7800 Powell Road, Hopkins, MNs 55343
148. Edward Lilley, Norton Company, Northboro Research Center, Northboro, MA 01532
149. Santosh Limaye, LoTEC, Inc., 1840 West Parkway Blvd., West Valley City, UT 84119
150. Jack F. Lininger, DU-CO Ceramics Co., 155 S. Rebecca Street, Saxonburg, PA 16056
151. Stephen J. Lombardo, Saint \-Gobain Industrial Ceramics, Northboro Research and Development Center, Goddard Road, Northboro, MA 01532-1545
152. Paul T. Louks, The Dow Chemical Company, Building 1776, Midland, MI 48674
153. Jay Lunzer, Lunzer Inc., Applied Technology, 330 W. 42nd Street, New York, NY 10036
154. William A. Mack, Carborundum Company, P.O. Box 337, Niagara Falls, NY 14302
155. Larry Mains, Deco Group, 4850 Coolidge Highway, Royal Oak, MI 48073-1023
156. Steven Malkin, U. of Massachusetts, Dept. of Mech. & Ind. Engineering, ELAB Building, Amherst, MA 01003-2210
157. John Mangels, Ceradyne, Inc., 3169 Redhill Avenue, Costa Mesa, CA 92626

158. Ken A. Marshall, Machined Ceramics, Inc., 629 North Graham Street, Bowling Green, KY 42101
159. Richard Marshall, Diacraft Inc., 9033 General Drive, Plymouth, MI 48170
160. Iaon D. Marinescu, Abrasive Micromachining Center, Kansas State University, 244 Durland Hall, Manhattan, KS 66506-5112
161. Newman Marsilius, Moore Tool Company, 800 Union Avenue, Bridgeport, CT 06607-0088
162. John E. Mayer, Jr., Texas A&M Univ., 117G Thompson Hall, College Station, TX 77843-3367
163. Martha McCrum, RayCham Corporation, 300 Constitution Drive, Menlo Park, CA 94025
164. Dale E. McCullum, Univ. of Dayton Research Institute, 300 College Park, KL 165, Dayton, OH 45469-0172
165. Brian McEntire, Norton Company, Goddard Road, Northboro, MA 01532-1545
166. John McGinnis, AlSiMag Technical Ceramics, Inc., Highway 14, Laurens, SC 29360
167. Donny McInturff, Coors Technical Ceramics Company, 1100 Commerce Park Drive, Oak Ridge, TN 37830
168. Nanu Menon, AlliedSignal Engines, MS 301-227, P. O. Box 52181, Phoenix, AZ 85072-2181
169. David Merrion, Detroit Diesel Corporation, 13400 Outer Drive, West, Detroit, MI 48239-4001
170. Clifford Michaud, United Technologies Pratt & Whitney, 400 Main Street, MS:115-78, East Hartford, CT 06108
171. Biljana Mikijelj, Ceradyne, Inc., 3169 Red Hill Avenue, Costa Mesa, CA 92626
172. Bradley J. Miller, Pakco, 55 Hillview Avenue, Latrobe, PA 15650
173. Mitch O. Miller, S. E. Huffman Corp., 1050 Huffman Way, Clover, SC 29710
174. Robert A. Miller, Materials Development, TAFA, 146 Pembroke Road, Concord, NH 03301
175. Sanjay Mishra, Chand Kare Technical Ceramics, 2 Coppage Drive, Worcester, MA 01603
176. Bob Nath, Quatro Corporation, 6100 Jefferson Street, N.E., Albuquerque, NM 87109
177. Bruce E. Nelson, Norton Company, 749 Cabot Drive, Knoxville, TN 37922
178. Devdas M. Pai, NC Agricultural & Technical State University, Dept. of Mech. Engr., Greensboro, NC 27411
179. Duane Parsons, Allison Engine Company, P. O. Box 420, MS 0-08, Indianapolis, IN 46206
180. Thomas E. Parsons, INSACO, Inc., 1365 Canary Road, P. O. Box 9006, Quakertown, PA 18951-9006
181. Thomas J. Parsons, Dow Chemical Company, 1616 Building, Midland, MI 48667
182. James W. Patten, Cummins Engine Company, Inc., Mail Code 50183, Box 3005, Columbus, IN 47203-3005
183. William W. Pflager, Litton Ind. Automat., 20 E. 6th Street, Waynesboro, PA 17268
184. Joseph Picone, Norton Company, 1 New Bond Street, Worcester, MA 01606
185. Ken Potter, Diesel Technology Company, P. O. Box 919, 2300 Burlingame Avenue, S.W., Wyoming, MI 49509-0919
186. Bob R. Powell, General Motors Corporation NAO, 30200 Mound Road, Warren, MI 48090-9055
187. Vimal K. Pujari, Norton Company, Goddard Road, Northboro, MA 01532-1545
188. Brad L. Rainey, Materials & Processes Engineering, Williams International, 2280 West Maple Road, P.O. Box 200, Walled Lake, MI 48390-0200
189. F. Rastegar, Cummins Engine Company, Inc., Piston Ring Division, 4500 Leeds AVenue, Suite 118, Charleston, SC 29405
190. Richard G. Rateick, Jr., Allied-Signal, 717 N. Bendix Drive, South Bend, IN 46620
191. Jerry Rearick, Electrofuel Industries, Inc., 2000 Ford Circle, Milford, OH 45150
192. Stephen G. Reder, Torrington Company, 59 Field Street, Torrington, CT 06790-4942
193. Patrick Redington, Norton Company, 1 New Bond Street, Bldg. 410, Worcester, MA 01606
194. Frank D. Reed, INSACO, Inc., P.O. Box 9006, Quakertown, PA 18951-9006
195. Jules Routbort, Argonne National Laboratory, ET Division, Bldg. 212, Argonne, IL 60439
196. Steven L. Sanner, Professional Instruments Co., 7800 Powell Road, Hopkins, MN 55343
197. Maryann V. Santos, Cal Poly Pomona, 220 S. Myrtlewood Street, West Covina, CA 91791

198. Maxine Savitz, AlliedSignal, Inc., 2525 West 190th Street, P. O. Box 1960, Torrance, CA 90509-2960
199. John Sayre, Manufacturing Program Development Department, Sandia National Laboratories, MS:0961, Albuquerque, NM 87185-5800
200. Ronald P. Scattergood, N.C. State University, Campus Box 7918, Raleigh, NC 27695-7918
201. Christopher Schilling, Iowa State University, 110 Engineering Annex, Ames, IA 50011-2070
202. Julie M. Schoenung, California State Polytechnic University, Department of Chemistry and Materials Engineering, Pomona, CA 91768-4069
203. Robert B. Schulz, U.S. Department of Energy, EE-33 Forrestal Building, Washington, DC 20585
204. Steve Schwegler, Radiac Abrasives Inc., 742A Bates Road, Lebanon, TN 37087
205. Terence Sheehan, Alpex Wheel Company, Tenafly, NJ 07670
206. Charles Shelly, INSACO, Inc., P. O. Box 9006, Quakertown, PA 18951-9006
207. George Shier, Dow Chemical Company, 1801 Building, Midland, MI 48674-1801
208. Albert J. Shih, Cummins Engine Company, P. O. Box 3005, 1460 National Road, MC 41618, Columbus, IN 47201
209. P. C. Smith, WESGO, 477 Harbor Blvd., Belmont, CA 94002
210. Russell G. Smith, Lanxide Corporation, 1300 Marrows Road, P. O. Box 6077, Newark, DE 19714-6077
211. Cors Smits, Cincinnati Milacron, P. O. Box 9013, Cincinnati, OH 45209
212. Anil Srivastava, IAMS, 1111 Edison Drive, Cincinnati, OH 45215-2265
213. Bill Stegmuller, Cincinnati Milacron, P. O. Box 9013, Cincinnati, OH 45209
214. Chris R. Stephens, Alsimag Technical Ceramics, One Technology Place, Hwy. 14, Laurens, SC 29360-0089
215. Robert Straub, Diesel Technology, 2300 Burlingame Avenue, S.W., Wyoming, MI 49509-0919
216. Dan Strong, Corning RD&E Div., SP PR 01 C34 PRC, Painted Post, NY 14870
217. Peter Strzepa, CarboMedics, 1300 East Anderson Lane, Austin, TX 78752
218. K. Subramanian, Norton Company, 1 New Bond Street, Worcester, MA 01615-0008
219. Jiangang Sun, Argonne National Laboratory, 9700 South Cass Avenue, ET/212, Argonne, IL 60439
220. Victor J. Tennery, 113 Newell Lane, Oak Ridge, TN 37830
221. Allen Thompson, Coors Technical Ceramics Co., 1100 Commerce Park Drive, Oak Ridge, TN 37830
222. Dennis M. Tracey, St. Gobain/Norton, Goddard Road, Northboro, MA 01532-1545
223. Clyde T. Treadwell, Sonic-Mill, 7500 Bluewater Road, Albuquerque, NM 87121
224. Marc Tricard, Norton Company, 1 New Bond Street, Box #15008, MS 413-201, Worcester, MA 01562-0008
225. Daniel Uffer, Saint-Gobain Industrial Ceramics, Advanced Ceramics Division, SE\epr - B.P.1, 84131 LE Pontet Cedex, France
226. Joseph B. Vincent, Norton Company, 4 Isham Lane, Savannah, GA 31411
227. Ron Walecki, AlliedSignal Inc., 2525 W. 190th Street, Torrance, CA 90509-2960
228. Stephen K. Weaver, INSACO, Inc., P. O. Box 9006, Quakertown, PA 18951-9006
229. John A. Webster, U. of Connecticut U-119, Storrs, CT 06269-5119
230. William H. Werst, Jr., U.S. Advanced Ceramic Association, 1600 Wilson Blvd., Suite 901, Arlington, VA 22209
231. Perry P. Yaney, University of Dayton, Department of Physics, Dayton, OH 45469-2314
232. Charles Yang, Cincinnati Milacron, Products Division, 4701 Marburg Avenue, Cincinnati, OH 45209

233. Thomas M. Yonushonis, Cummins Engine Company, Inc., MC 50183, 1900 McKinley Avenue, Columbus, IN 47201
234. Bi Zhang, Univ. of Connecticut, PMC, U-119, Longley Bldg., Rt. 44, Storrs, CT 06269-5119
235. Zhenqi Zhu, Univ. of Connecticut, PMC, U-119, Longley Bldg., Rt. 44, Storrs, CT 06269-5119
236-237. Office of Scientific & Technical Information, P. O. Box 62, Oak Ridge, TN 37831